ENERGY EFFICIENT RADIO RESOURCE MANAGEMENT FOR FUTURE MOBILE CELLULAR RADIO ACCESS NETWORKS

Charles Turyagyenda

MSc. Digital RF Wireless Communication
BSc. Electrical Engineering

Submitted in fulfilment of the requirements for the degree of

Doctor of Philosophy

Electronic and Electrical Engineering

Faculty of Engineering

The University of Sheffield

May 2014

ABSTRACT

Historically mobile Radio Access Networks (RANs) were optimised initially to maximise coverage and subsequently to improve capacity, user data rates and quality of service. However, the recent exponential growth in the volume of transmitted data coupled with the ever increasing energy costs has highlighted the need to optimise futuristic RANs from an energy efficiency perspective. This research study postulated the utilisation of radio resource management approaches to improve the energy efficiency of modern RANs, with a particular emphasis on the radio frequency energy performance.

The research study yielded the following major outcomes. First, there was notable positive correlation between user channel quality improvements and the energy efficiency of RANs. Second, channel quality aware packet schedulers were more energy efficient than channel quality ignorant packet schedulers. Third, energy aware scheduling metrics coupled with power control algorithms can be utilised to optimise and refine the energy efficiency performance of the rate adaptive frequency domain packet scheduling. Fourth, the dynamic temporal and spatial traffic load characteristics, in the radio access network, present energy saving opportunities through collaborative and cooperative Inter-Cell Interference (ICI) management among neighbouring base stations.

While the results presented in this thesis pertain to radio frequency and/or radio head energy consumption, the improved energy efficiency could be leveraged by increasing the inter site distance between base stations subsequently reducing the density of base stations in any given geographical area thus reducing the energy consumption of the RANs as a whole.

The benefits of energy efficient RANs are twofold, i.e. reduction in the amount of CO_2 emission and lower operating expenditure (OPEX).

TABLE OF CONTENTS

ACKNOWLEDGEMENTS

The work reported in this thesis has formed part of the Green Radio Core 5 Research Programme of the Virtual Centre of Excellence in Mobile & Personal Communications, Mobile VCE. Fully detailed technical reports on this research are available to industrial members of Mobile VCE. www.mobilevce.com.

I would like to express my gratitude to my supervisor, Professor Tim O'Farrell, for his invaluable support and guidance; not only regarding various technical issues but also with respect to the overall research approach.

I would also like to acknowledge the numerous Green Radio researchers and industrial partners for their insightful technical critiques of the research study.

DEDICATION

To my lovely wife Judith and daughter Eleanor Zita. Thank you for your precious support.

GLOSSARY OF ABBREVIATIONS

0G	Zero Generation
1G	First Generation
2G	Second Generation
3G	Third Generation
3GPP	Third Generation Partnership Project
AC	Admission Control
AF	Application Function
AM	Amplitude Modulation
AMTS	Advanced Mobile Telephone System
ARIB	Association of Radio Industries and Business
ARP	Allocation Retention Priority
ARQ	Automatic Repeat Request
ATIS	Alliance for Telecommunications Industry Solutions
BCCH	Broadcast Control Channel
BCH	Broadcast Channel
BEM	Bandwidth Expansion Mode
BLAST	Bell Laboratories Layered Space Time
BLER	Block Error Rate
BPF-ECR	Blind Proportional Fair Energy Consumption Ratio
BS	Base Station
CCCH	Common Control Channel
CCSA	China Communications Standards Association
CDF	Cumulative Distribution Function
CDMA	Code Division Multiple Access
CEPT	Conference of European Posts and Telecommunications
CO_2	Carbon Dioxide
CO_2~eq	Carbon Dioxide Equivalent
CQI	Channel Quality Information
C-RAN	Cloud infrastructure Radio Access Network
CSL	Candidate Selection List
dBs	Decibels
DCCH	Dedicated Control Channel

DL-SCH	Downlink Shared Channel
DSP	Digital Signal Processing
DTCH	Dedicated Traffic Channel
EARTH	Energy Aware Radio neTwork technologies
ECR	Energy Consumption Ratio
EDGE	Enhanced Data rates for GSM Evolution
E_{EM}	Embodied Energy
EGC	Equal Gain Combining
EMM	EPS Mobility Management
eNB	Evolved Node B
E_{OP}	Operational Energy
EPC	Evolved Packet Core
EPS	Evolved Packet System
ERG	Energy Reduction Gain
ESM	EPS Session Management
ETSI	European Telecommunications Standards Institute
E-UTRAN	Evolved UTRAN
FDD	Frequency Division Duplex
FD-PS	Frequency Domain Packet Scheduler
FEC	Forward Error Correction
FFR	Fractional Frequency Reuse
FM	Frequency Modulation
GBR	Guaranteed Bit Rate
GHG	Green House Gas
GHz	Giga Hertz
GPRS	General Packet Radio Service
GSM	Global System for Mobile communication
GTP	GPRS Tunnelling protocol
HARQ	Hybrid ARQ
HFR	Hard Frequency Reuse
HSDPA	High Speed Downlink Packet Access
HSPA	High Speed Packet Access
HSS	Home Subscriber Server

HSUPA	High Speed Uplink Packet Access
ICI	Inter-Cell Interference
ICT	Information and Communication Technology
IEEE	Institute of Electrical and Electronics Engineers
IET	Institute of Engineering and Technology
IMS	IP Multimedia Subsystem
IMT-2000	International Mobile Telecommunication 2000
IMTS	Improved Mobile Telephone Service
IP	Internet Protocol
ISD	Inter-Site Distance
ITU	International Telecommunications Union
KHz	Kilo Hertz
KW	Kilo Watt
LA	Link Adaptation
LOS	Line of Sight
LTE	Long-Term Evolution
MAC	Medium Access Control
MATLAB	MATrix LABoratory
Mbit/s	Mega Bits per Second
MBR	Maximum Bit Rate
MCCH	Multicast Control Channel
MCH	Multicast Channel
MCS	Modulation and Coding Scheme
MHz	Mega Hertz
MIMO	Multiple Input Multiple Output
MISO	Multiple Input Single Output
ML	Maximum Likelihood
MME	Mobility Management Entity
MMSE	Minimum Mean Square Error
MRC	Maximum Ratio Combining
MRRC	Maximum Ratio Receiver Combining
MRTS	Mobile Radio Telephone Systems
ms	Millisecond

MTCH	Multicast Traffic Channel
MTS	Mobile Telephone System
MVCE	Mobile Virtual Centre for Excellence
MWh	Mega Watt Hours
NAS	Non-Access Stratum
NBS	Nash Bargaining Solutions
NMT	Nordic Mobile Telephone
NTT	Nippon Telegraph and Telephone
OFDMA	Orthogonal Frequency Division Multiple Access
OH	Overhead
OPEX	Operating Expenditure
P2P	Peer to Peer
PA	Power Amplifier
PBCH	Physical Broadcast Channel
PCC	Policy Charging and Control
PCCH	Paging Control Channel
PCEF	Policy Charging and Enforcement Function
PCFICH	Physical Control Format Indicator Channel
PCH	Paging Channel
PCRF	Policy Charging and Rules Function
PDCCH	Physical Downlink Control Channel
PDCP	Packet Data Convergence protocol
PDSCH	Physical Downlink Shared Channel
PDU	Packet Data Units
PF-ECR	Proportional Fair Energy Consumption Ratio
P-GW	Packet Data Network Gate Way
PHY	Physical Layer
PMCH	Physical Multicast Channel
PRBs	Physical Resource Blocks
PSA	Player Status Assignment
PSU	Power Supply Unit
PTT	Push to Talk
PUCCH	Physical Uplink Control Channel

PUSCH	Physical Uplink Shared Channel
QAM	Quadrature Amplitude Modulation
QCI	QoS Class Identifier
QoS	Quality of Service
QPSK	Quadrature Phase Shift Keying
RF	Radio Frequency
RF-ECR	Radio Frequency Energy Consumption Ratio
RF-ERG	RF Energy Reduction Gains
RH	Radio Head
RH-ECR	Radio Head Energy Consumption Ratio
RH-ERG	Radio Head Energy Reduction Gains
RLC	Radio Link Control
RMS	Root Mean Square
RNC	Radio Network Controller
RR	Round Robin
RRC	Radio Resource Control
RRM	Radio Resource Management
SC	Selection Combining
SC-FDMA	Single Carrier Frequency Division Multiple Access
SDMA	Space Division Multiple Access
SDU	Service Data Units
SFBC	Space Frequency Block Code
SFR	Soft Frequency Reuse
SGC/RRM	Sequential Game Coordinated Radio Resource Management
S-GW	Serving Gateway
SIMO	Single Input Multiple Output
SINR	Signal to Interference Noise Ratio
SISO	Single Input Single Output
SOA	State-of-Art
SONs	Self-Organising Networks
STBC	Space Time Block Code
TACS	Total Access Cellular System
TCP	Transmission Control Protocol

TDD	Time-Division Duplex
TD-PF-Throughput	Time Domain Proportional Fair Throughput
TD-PS	Time Domain Packet Scheduler
TTA	Telecommunications Technology Association
TTC	Telecommunications Technology Committee
TTI	Transmission Time Interval
UE	User Equipment
UMTS	Universal Mobile Telecommunications Systems
USIM	Universal Subscriber Identity Module
UTRAN	UMTS Terrestrial Radio Access Network
VLSI	Very Large Scale Integration
W-CDMA	Wideband CDMA

LIST OF FIGURES

CHAPTER 1 **: INTRODUCTION**

1.1. Overview

The Information and Communication Technology (ICT) sector has experienced a prodigious growth in the number of mobile subscriptions over the last decade. Recent studies have shown that the number of global mobile subscriptions has increased exponentially from 500 million subscriptions in 2000 to 5 billion subscriptions in 2012 [1]. Furthermore, the total number of mobile subscriptions is expected to grow to about 6 billion in 2014 and tend to reach global penetration[1] of 100 percent after 2020. The exponential growth in the number of subscriptions, coupled with the fact that faster internet access and high data rate devices are constantly being utilised to access new digital services wirelessly, has resulted in the volume of transmitted data increasing by approximately a factor of 10 every five years [2]. In order to support the skyrocketing traffic volumes, data transmission rates have been increasing at approximately the same pace facilitated in part by the fact that the processing power and storage capabilities of mobile devices have doubled approximately every 18 months i.e. Moore's Law.

However, the increasing volume of transmitted data is sustained at the expense of a significant carbon footprint by the mobile communications industry. Three percent of the world-wide energy is consumed by the ICT infrastructure accounting for two percent of the global CO_2 emissions, which is comparable to the world-wide CO_2 emissions by aviation or one quarter of the global CO_2 emissions by cars, resulting in a global CO_2 equivalent (CO_2~eq) emission[2] of 1.3 percent [3-4]. The study in [1] estimates that mobile networks accounted for 0.2 and 0.4 percent of the global CO_2~eq emissions in 2007 and 2010,

[1] 100 percent global penetration means that the number of subscriptions equals the global population.
[2] CO_2~eq emission is the amount of CO_2 emission that would cause the same time-integrated radiactive forcing, over a given time horizon, as an emitted amount of a long lived Green House Gas (GHG) or a mixture of GHGs [5].

respectively and predicts that the footprint of mobile communications might triple by 2020 reaching more than one third of the present annual emissions of the entire United Kingdom.

Besides being environmentally benign, there is a strong economic incentive to reduce the energy consumption of mobile communication networks. The continuously rising energy consumption together with steadily increasing energy costs make it imperative to manage the energy bill if mobile operators are to remain competitive. From an operator's perspective, reducing the energy consumption is critical to lowering the operating expenditure (OPEX), and translates directly to an attractive bottom line.

1.2. Research Objective

The research study conducted for this doctorial thesis was one of several projects under the Green Radio Core 5 Research Programme of the Virtual Centre for Excellence in Mobile and Personal Communications, Mobile VCE. The ambition of the Green Radio project was to provide 100x operational energy reduction of the radio access networks [6-7]. This study was aligned to the overall objectives of the Green Radio project with a vision of providing a 3x energy reduction contribution to the overall 100-fold energy reduction aspiration of the Green Radio project, by addressing the following targeted innovations;

a) Improving the Quality of Service (QoS)/Radio Frequency (RF) power ratio-To develop techniques that will reduce the required RF output power required from base stations whilst still maintaining the required QoS.

b) Scaling of energy needs with traffic- To develop mechanisms that deliver substantial improvements in power consumption for base stations with no loads and techniques that allow power consumption to scale with load.

To this end this thesis carried out an in depth study of how radio resource allocation and management techniques can be utilised to deliver significant power reductions. The core objectives of the thesis were.

a) To develop Radio Resource Management (RRM) functionality for the Green Radio energy efficient architectures by exploiting Evolved Node B (eNB) cooperation, coordination and collaboration for the Universal Mobile Telecommunications Systems (UMTS) terrestrial radio access network (UTRAN) long-term evolution (LTE) system or the Evolved UTRAN (E-UTRAN). This objective focused on how connectivity between base stations in a cellular network can be used to shape interference and power consumption while maximising throughput. Interference is an important limiting factor to energy efficiency. Given a specified radio access technology, a requirement for performance in terms of throughput implies a required ratio of received signal level to received interference level at a receiver. Hence, if interference is increased by a given factor, the transmitted power level must be increased by that same factor in order to maintain the required performance, which of course has the effect of reducing energy efficiency for the system. Interference was therefore carefully examined in order to improve energy efficiency.

b) To investigate energy driven packet scheduling functionality for the E-UTRAN downlink. This objective was motivated by the multiuser diversity gain achievable in fast schedulers, such as used in LTE systems. It seeks to modify existing scheduling algorithms to minimise power consumption and ensure that QoS guarantees are met.

1.3. Methodology

This section describes the general research approach and how the scope of the work was bounded. In a mobile communications network, it is estimated that base stations contribute between 60-80% of the overall energy consumption [8-9]. The base station energy dissipation constitutes both load dependent (Radio Head and Radio Frequency energy) and load independent (Overhead energy) components. Radio Resource Management (RRM) techniques, such as packet scheduling, only affect the load dependent term. Whilst fixed overhead energy consumptions remain high, the potential to reduce overall energy consumption is small. Therefore, this work is positioned towards future systems where overhead energy consumption is envisioned to have been significantly reduced. This research focussed on the base station energy consumption with particular emphasis on Radio Frequency (RF) downlink transmissions. The research study was conducted in three phases.

First, a comprehensive energy efficiency characterisation of the state-of-the-art radio resource management techniques was conducted. This phase of the research focused on quantifying the energy performance and highlighting the salient features of the established packet schedulers.

Second, the research study explored the potential of improving the packet scheduler energy efficiency by utilising multiple transmit and receive antennas. This phase of the research focussed on applying diversity gain improving multiple antenna techniques to improve the energy efficiency.

Third, the research concentrated on the development and evaluation of novel radio resource management approaches designed to improve the energy efficiency. In addition to developing a new energy aware packet scheduling criteria this phase also developed an energy efficient interference management approach.

During the course of each phase, the performance evaluation of the radio resource management techniques was conducted using Monte-Carlo simulations developed in MATLAB.

1.4. Thesis Outline and Contributions

The thesis is structured as follows. Chapter 2 presents a background to wireless communication systems with specific emphasis placed on the Third Generation Partnership Project (3GPP) Long Term Evolution (LTE) radio access network. Chapter 3 presents a characterisation of the energy performance of common packet schedulers in a 3GPP LTE radio access network environment. Chapter 4 presents an energy efficiency comparison between Single Input Single Output (SISO) and multiple antenna systems particularly the Alamouti Space Frequency Block Code (SFBC) Multiple Input Multiple Output (MIMO) system. Chapter 5 introduces a novel time domain proportional fair energy policy coupled with an energy optimisation algorithm. Chapter 6 introduces a novel Inter-Cell Interference (ICI) management approach that improves the energy efficiency of the radio access network by mitigating the effects of ICI through a sequential game theory play off between cells in the radio access network. Finally, chapter 7 concludes the thesis with a highlight of the conclusions drawn and a proposal for potential future work. Each chapter contains a detailed literature review of the subject matter addressed therein. The key contributions of the thesis are summarised in the subsequent sub sections.

1.4.1. Chapter 3 – Energy efficiency comparison of common packet schedulers

In chapter 3 a characterisation and quantification of the energy performance of well-known packet schedulers is presented. The study demonstrated that channel quality aware packet scheduling improved the energy efficiency of the radio access network.

1.4.2. Chapter 4 – SFBC MIMO energy efficiency improvements of common packet Schedulers

In chapter 4 diversity gain improving multiple antenna techniques, particularly Alamouti SFBC, are shown to improve the user channel quality and hence the energy efficiency.

1.4.3. Chapter 5 – LTE downlink packet scheduling using a novel proportional fair energy policy

In chapter 5, a novel energy consumption aware packet scheduler is presented and evaluated. Furthermore, an energy optimisation algorithm is presented to supplement the packet scheduler. The study showed that the new composite energy aware packet scheduling criteria produced energy savings, without compromising the spectral efficiency performance and user QoS performance.

1.4.4. Chapter 6 – Energy efficient co-ordinated inter cell interference avoidance

In chapter 6, the dependence of energy efficiency on the availability of good channel conditions, developed in chapters 3 and 4, is explored further. A novel dynamic Inter-Cell Interference (ICI) management technique is presented; and shown to yield user channel quality improvements. The channel quality improvements translated into significant energy savings both at low and high offered loads.

1.5. List of Publications

This thesis is partly based on the following publications.

- C. Turyagyenda, T. O'Farrell, and W. Guo, "Energy efficient coordinated radio resource management: a two player sequential game modelling for the long-term evolution downlink," IET Journal on Communications, vol. 6, Iss. 14, pp. 2239-2249, November 2012.
- C. Turyagyenda, T. O'Farrell, J. He, and P. Loskot, "SFBC MIMO Energy Efficiency Improvements of Common Packet Schedulers for the Long Term Evolution Downlink," in Proceedings of the IEEE Vehicular Technology Conference, pp. 1-5, May 2011.
- C. Turyagyenda, T. O'Farrell, and W. Guo, "Long Term Evolution Downlink Packet Scheduling using A Novel Proportional-Fair-Energy Policy," in Proceedings of the IEEE Vehicular Technology Conference, pp. 1-5, May 2012.
- S. Wang, C. Turyagyenda, and T. O'Farrell, "Energy Efficiency and Spectral Efficiency Trade-Off of a Novel Interference Avoidance Approach for LTE-Femtocell Networks," in Proceedings of the IEEE Vehicular Technology Conference, pp. 1-5, May 2012.
- W. Guo, C. Turyagyenda, H. Hamdoun, S. Wang, P. Loskot, T. O'Farrell " Towards a Low Energy LTE Cellular Network: Architectures," EURASIP European Signal Processing Conference, pp. 879-883, Aug 2011.
- W. Guo, S. Wang, C. Turyagyenda, and T. O'Farrell, "Integrated cross-layer energy savings in a smart and flexible cellular network," in Proceedings of the IEEE International Conference on Communication in China, pp. 79-84, August 2012.

CHAPTER 2 **: BACKGROUND**

Historically mobile Radio Access Networks (RANs) were optimised initially to maximise coverage and subsequently to improve capacity, user data rates and quality of service. However, the recent exponential growth in the volume of transmitted data coupled with the ever increasing energy costs has highlighted the need to optimise futuristic RANs from an energy efficiency perspective.

The early 20th century witnessed the advent of the first Mobile Radio Telephone Systems (MRTS) such as, Push to Talk (PTT), Mobile Telephone System (MTS), Advanced Mobile Telephone System (AMTS), and Improved Mobile Telephone Service (IMTS) [10-12]. These early wireless communication systems are commonly referred to as pre cellular systems i.e. communication systems utilised before the advent of the cellular concept. The major drawback associated with pre cellular systems was their limited capacity.

In the 1970s the cellular concept was born that addressed the limited capacity problem by reducing the transmit power and re-using the frequencies at base stations that were sufficiently far away from each other [13]. The cellular concept triggered the first generation (1G) evolution with the first commercial cellular network launched by Nippon Telegraph and Telephone (NTT) in Japan in 1979. In Europe a number of 1G systems were launched in the early 1980s with several countries having their own systems and frequency allocations. For instance, Germany launched the C-450 system, the Nordic countries launched the Nordic Mobile Telephone (NMT) system and the United Kingdom launched the Total Access Cellular System (TACS) [14]. All the 1G systems were invariably analogue and utilised Frequency Modulation (FM) on the air-interface. The various 1G systems restricted the operation of mobile equipment to boundaries of each country.

To overcome the 1G constraints, the Conference of European Posts and Telecommunications (CEPT[3]) formed the Global System for Mobile communication (GSM) tasked with developing a pan-European mobile cellular radio system. Unlike the existing cellular systems, GSM was developed using digital technology; and in 1991, the first commercial GSM service was launched. GSM is commonly referred to as a second generation (2G) system. GSM supports high quality voice and circuit switched data services at up to 9.6 Kbit/s. The General Packet Radio Service (GPRS[4]) added packet switched functionality to GSM resulting in a theoretical downlink data rate of 171 Kbit/s. The Enhanced Data rates for GSM Evolution (EDGE[5]) further increased the GSM downlink data rates to 384 Kbit/s with evolved EDGE having data rates of up to 1.3Mbit/s in the downlink and 653 Kbit/s in the uplink [15].

In 1999, the International Telecommunications Union (ITU) defined a family of third generation (3G) mobile communications technologies also known as the International Mobile Telecommunication 2000 (IMT-2000) technologies. Among the IMT-2000 technologies, is the IMT-2000 Code Division Multiple Access (CDMA) Direct Spread commonly known as Wideband CDMA (W-CDMA); proposed by the Universal Mobile Telecommunications Systems (UMTS[6]) Third Generation Partnership Project (3GPP) as the evolution of GSM systems. WCDMA has typical downlink data rates of 384 Kbit/s. High Speed Uplink Packet Access (HSUPA) and High Speed Downlink Packet Access (HSDPA) increased the WCDMA data rates to between 7.2Mbit/s and 14.4Mbit/s. The evolution of High Speed Packet Access (HSPA), also known as HSPA+, further increased the data rate to between 21Mbit/s and 42Mbit/s; paving the way for the 3GPP Long Term Evolution (LTE) Standard [16].

[3]In 1989, the responsibility of the GSM specification was passed from CEPT to the European Telecommunications Standards Institute (ETSI).
[4] GPRS is commonly referred to as a 2.5G system
[5] EDGE is commonly referred to as a 2.75G system
[6] UMTS is the umbrella term for 3G technologies developed within 3GPP.

The rest of the chapter is structured as follows; Section 2.1 presents an overview of the Third Generation Partnership Project (3GPP) Long Term Evolution (LTE). Section 2.2 presents the base station power consumption model. Section 2.3 concludes the chapter with an introduction to energy metrics.

2.1. Third Generation Partnership Project (3GPP) Long Term Evolution (LTE)

3GPP is a consortium of six telecommunications standards development organisations, namely: European Telecommunications Standards Institute (ETSI), Association of Radio Industries and Business (ARIB), Alliance for Telecommunications Industry Solutions (ATIS), China Communications Standards Association (CCSA), Telecommunications Technology Association (TTA) and Telecommunications Technology Committee (TTC). Work on the 3GPP LTE standard commenced in 2004 with a definition of targets benchmarked against the High Speed Packet Access (HSPA) release 6 standard [17]. The main LTE performance targets are highlighted below:

- Spectral efficiency two to four times more than HSPA release 6.
- Peak data rates of 100Mbit/s for the downlink and 50Mbit/s for the uplink.
- Round trip time less than 10ms.
- Packet switched optimised.
- Optimised terminal power efficiency.
- Frequency flexibility from 1.5MHz to 20MHz allocations.

In order to realise the stipulated performance targets, the 3GPP LTE standard incorporates the following enabling technologies:

- Orthogonal Frequency Division Multiple Access (OFDMA) for downlink multiple access.
- Single Carrier Frequency Division Multiple Access (SC-FDMA) for uplink multiple access.

- Link Adaptive Modulation and Coding with a turbo code channel encoder and the following modulation schemes: Quadrature Phase Shift Keying (QPSK), 16 Quadrature Amplitude Modulation (QAM) and 64 QAM.
- Multiple Input Multiple Output (MIMO) transmission modes such as: transmit diversity, spatial multiplexing, and multi-user MIMO.

3GPP LTE also supports both Time-Division Duplex (TDD) and Frequency Division Duplex (FDD). Table 2.1 and 2.2 present the LTE frequency band specification for unpaired and paired bands respectively. The focus of this study was the 3GPP LTE downlink with FDD operating in band 1 with frequencies between 2110 and 2170 MHz.

Table 2.1. 3GPP LTE Unpaired Frequency Bands

Operating Band	3GPP Name	Uplink and Downlink (MHz)
Band 33	UMTS TDD 1	1900-1920
Band 34	UMTS TDD 2	2010-2025
Band 35	US 1900 UL	1850-1910
Band 36	US 1900 DL	1930-1990
Band 37	US 1900	1910-1930
Band 38	2600	2570-2620
Band 39	UMTS TDD	1880-1920
Band 40	2300	2300-2400

Table 2.2. 3GPP LTE Paired Frequency Bands			
Operating Band	3GPP Name	Uplink (MHz)	Downlink (MHz)
Band 1	2100	1920-1980	2110-2170
Band 2	1900	1850-1910	1930-1990
Band 3	1800	1710-1785	1805-1880
Band 4	1700/2100	1710-1755	2110-2155
Band 5	850	824-849	869-894
Band 6	800	830-840	875-885
Band 7	2600	2500-2570	2620-2690
Band 8	900	880-915	925-960
Band 9	1700	1750-1785	1845-1880
Band 10	1700/2100	1710-1770	2110-2170
Band 11	1500	1427.9-1452.9	1475.9-1500.9
Band 12	US700	698-716	728-746
Band 13	US700	777-787	746-756
Band 14	US700	788-798	758-768
Band 17	US700	704-716	734-746
Band 18	Japan800	815-830	860-875
Band 19	Japan800	830-845	875-890

2.1.1. Evolved Packet System (EPS)

The 3GPP LTE EPS is an Internet Protocol (IP) connectivity layer constituting: the User Equipment (UE), E-UTRAN[7] and Evolved Packet Core (EPC) [18].

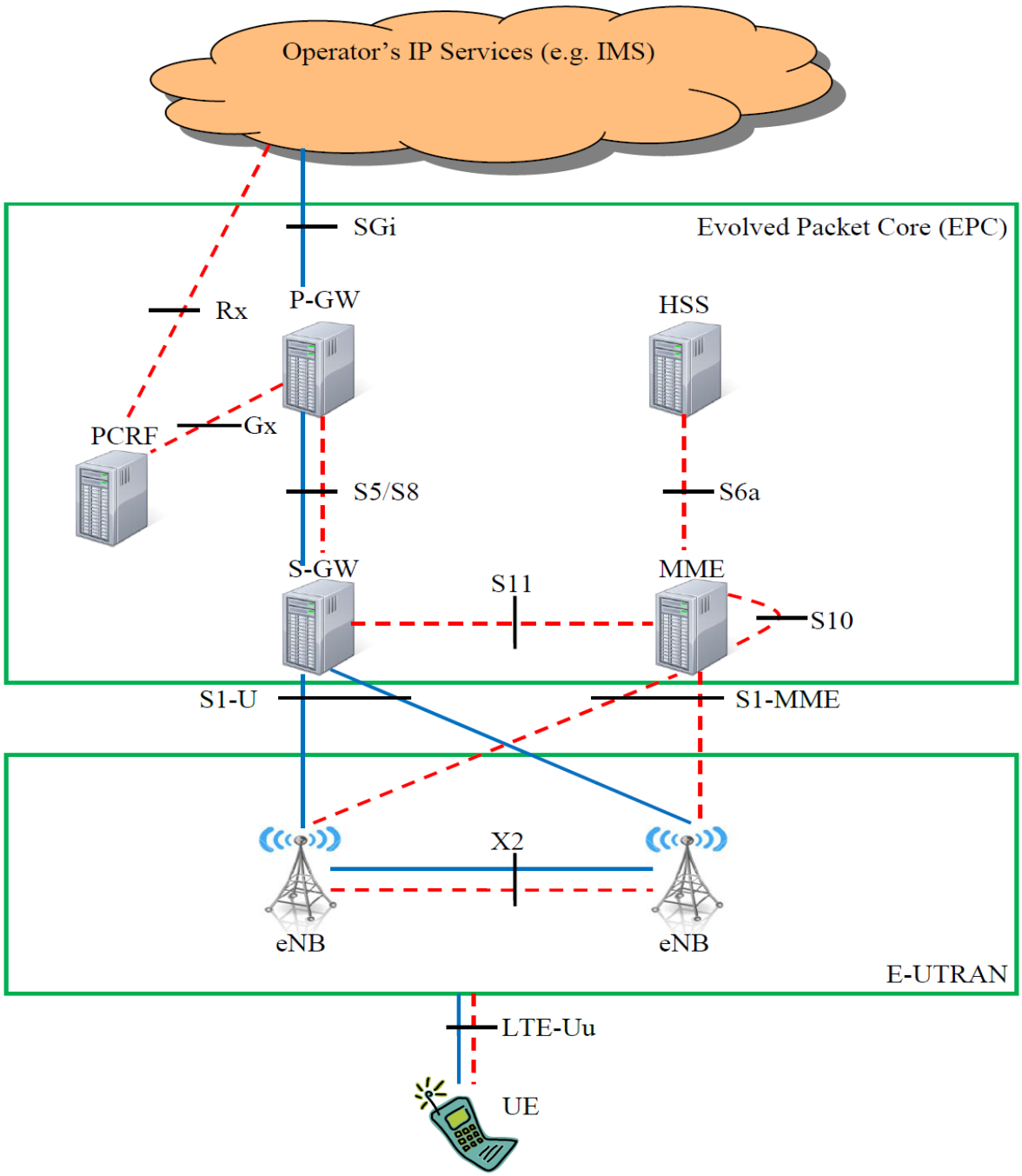

Figure 2. 1. 3GPP LTE Evolved Packet System

[7] Evolved Universal Mobile Telecommunications Systems (UMTS) terrestrial radio access network (UTRAN)

2.1.1.1. User Equipment (UE)

The UE is a communication device used by the end user e.g. a smart phone. The UE contains a Universal Subscriber Identity Module (USIM) used for authentication and generating security keys to ensure secure radio interface transmissions. The main functions of the UE include providing communication applications such as IMS clients and location reporting used for mobility management.

2.1.1.2. The E-UTRAN

The E-UTRAN is made up of a number of evolved NodeBs[8] (eNBs) distributed throughout the network's coverage area [19]. The eNBs are interconnected by the X2 interface. The eNB provides layer 2 connectivity between the UE and the EPC. The eNB is connected to the UE and EPC via the LTE-Uu and the S1 interfaces, respectively. The main functions of the eNB include [19] allocation of resources to UEs in both uplink and downlink (i.e. scheduling), and routing of User Plane data towards Serving Gateway (S-GW).

2.1.1.3. Mobility Management Entity (MME)

The MME is the main control element in the EPC. The MME connects to the eNB, Serving Gateway (S-GW), Home Subscriber Server (HSS) and other MMEs via the S1-MME, S11, S6a, and S10interfaces, respectively. The main functions of the MME include [18] authentication and authorisation, P-GW and S-GW selection and lawful interception of signalling traffic.

[8] evolved NodeB is the LTE terminology for a base station.

2.1.1.4. Serving Gateway (S-GW)

The S-GW connects to the eNB, MME and P-GW via the S1-U, S11 and S5/S8 interfaces, respectively. The main functions of the S-GW include [18] packet routing or forwarding, mobility anchor point for inter-eNB handover, monitor and collect data in the tunnels for accounting, user charging and lawful inspection.

2.1.1.5. Packet Data Network Gateway (P-GW)

The P-GW is the edge router between the EPS and other packet data networks. The P-GW connects to the S-GW, Policy Charging and Rules Function (PCRF) and other packet data networks via the S5/S8, Gx, and SGi interfaces, respectively. The main functions of the P-GW include [18] highest-level mobility anchor, assigns an IP address to the UE, packet filtering, performs Policy Charging and Enforcement Function (PCEF), set up bearers on request and monitor and collect data in the tunnels for accounting, user charging and lawful inspection.

2.1.1.6. Policy Charging and Rules Function (PCRF)

The PCRF is responsible for Policy Charging and Control (PCC). The PCRF connects to the P-GW and the IP Multimedia Subsystem (IMS) via the Gx and Rx interfaces, respectively. The main function of the PCRF is to set the Quality of Service (QoS) parameters for IP flows and provide this information to the PCEF in the P-GW so that appropriate bearers can be set up [20].

2.1.1.7. Home Subscriber Server (HSS)

The HSS is the database for all permanent user data. The HSS is connected to the MME via the S6a interface. The HSS records user specific details such as: subscriber profile, visited networks, permanent key used to compute authentication vectors, and serving MME [18].

The focus of this study was the 3GPP LTE E-UTRAN downlink operating on the LTE-Uu interface.

2.1.2. 3GPP LTE Radio Protocols

The 3GPP LTE standard defines a number of radio protocols tasked with: setting up, reconfiguring and releasing radio bearers. The radio protocol architecture can be separated into a user plane protocol stack (Figure 2.2) and a control plane protocol stack (Figure 2.3) [19]. The main functions of the radio protocols are highlighted below:

- Non-Access Stratum: The highest layer of the control plane between the UE and MME [21]. The main functions include; support for mobility of the UE commonly referred to as EPS Mobility Management (EMM) and support of session management procedures commonly referred to as EPS Session Management (ESM).
- Radio Resource Control (RRC): The main functions include; broadcasting of system information, RRC connection control (i.e. establishment, maintenance and release) between UE and E-UTAN, network controlled mobility, and measurement and configuration reporting [19].
- Packet Data Convergence protocol (PDCP): The main functions include; transfer of user and control plane data, header compression, and ciphering and integrity protection [22].

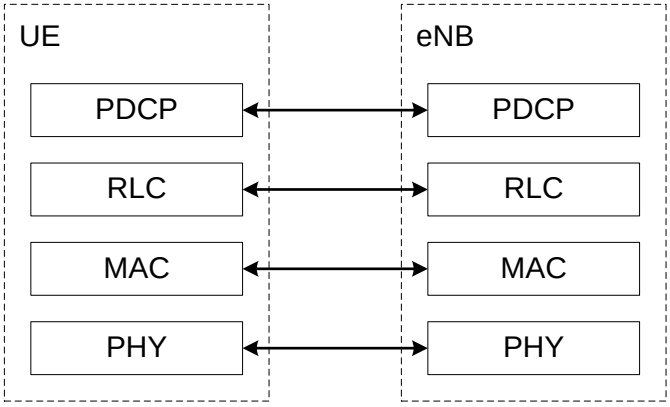

Figure 2. 2. User Plane Protocol Stack [19]

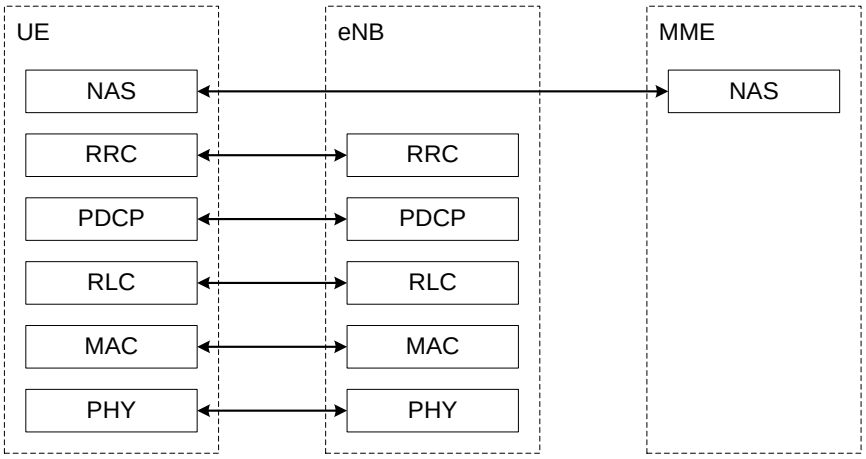

Figure 2. 3. Control Plane Protocol Stack [19]

• Radio Link Control (RLC): The main functions include; concatenation, segmentation and re-assembly of RLC Service Data Units (SDU), duplicate detection, and Automatic repeat request (ARQ) error correction [23].

• Medium Access Control (MAC): The MAC is responsible for; mapping between logical channels and transport channels, dynamic scheduling, scheduling information reporting and error correction through Hybrid ARQ (HARQ) [24].

• Physical Layer (PHY): The main functions include mapping of transport channels to physical channels, radio characteristics measurements and reporting to higher layers, Forward Error Correction (FEC) encoding and decoding, modulation and demodulation of physical

channels, frequency and time synchronisation, multiple antenna processing, and Radio Frequency (RF) processing [25].

Figure 2.4 presents the mapping sequence of radio bearers to logical channels to transport channels and finally to the physical channels [19]. Logical channels define “what type” of data is transmitted e.g. traffic, control and broadcast. Transport channels define “How is” the data transmitted e.g. what type of modulation and coding to be used. Physical channels define “where is” the data transmitted e.g. which OFDM symbols in the downlink frame.

2.1.3. Radio Resource Management (RRM)

The primary objective of radio resource management is to control the utilisation of the radio resources in order to ensure.

- The fulfilment of user Quality of Service (QoS) requirements.
- The minimisation of the overall radio resource usage on a system level.

Figure 2.5 presents an overview of the eNB user-plane and control-plane protocol architecture and the mapping of the primary RRM functions to the different layers.

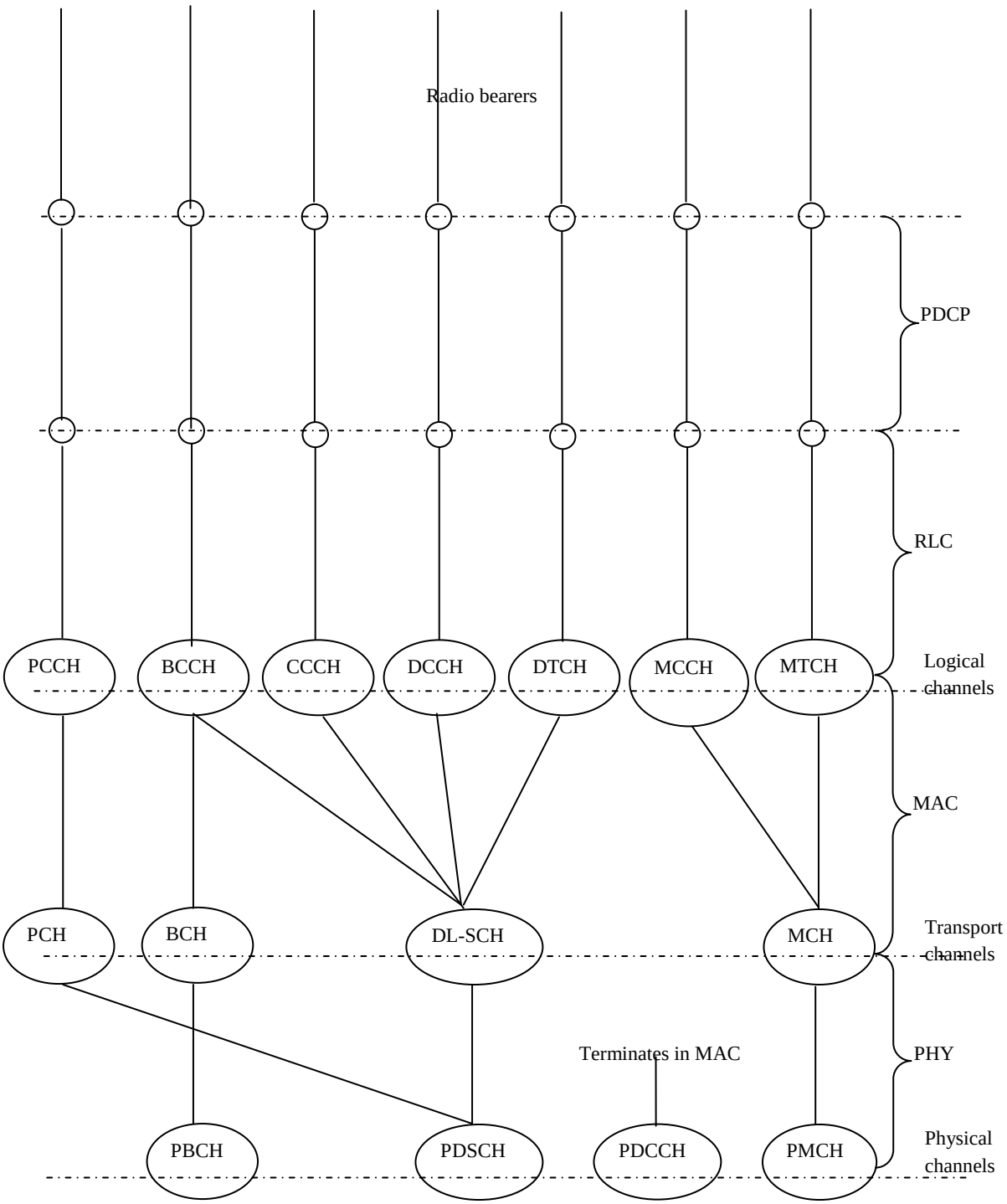

Figure 2. 4. Radio Bearer Mapping at various Protocols

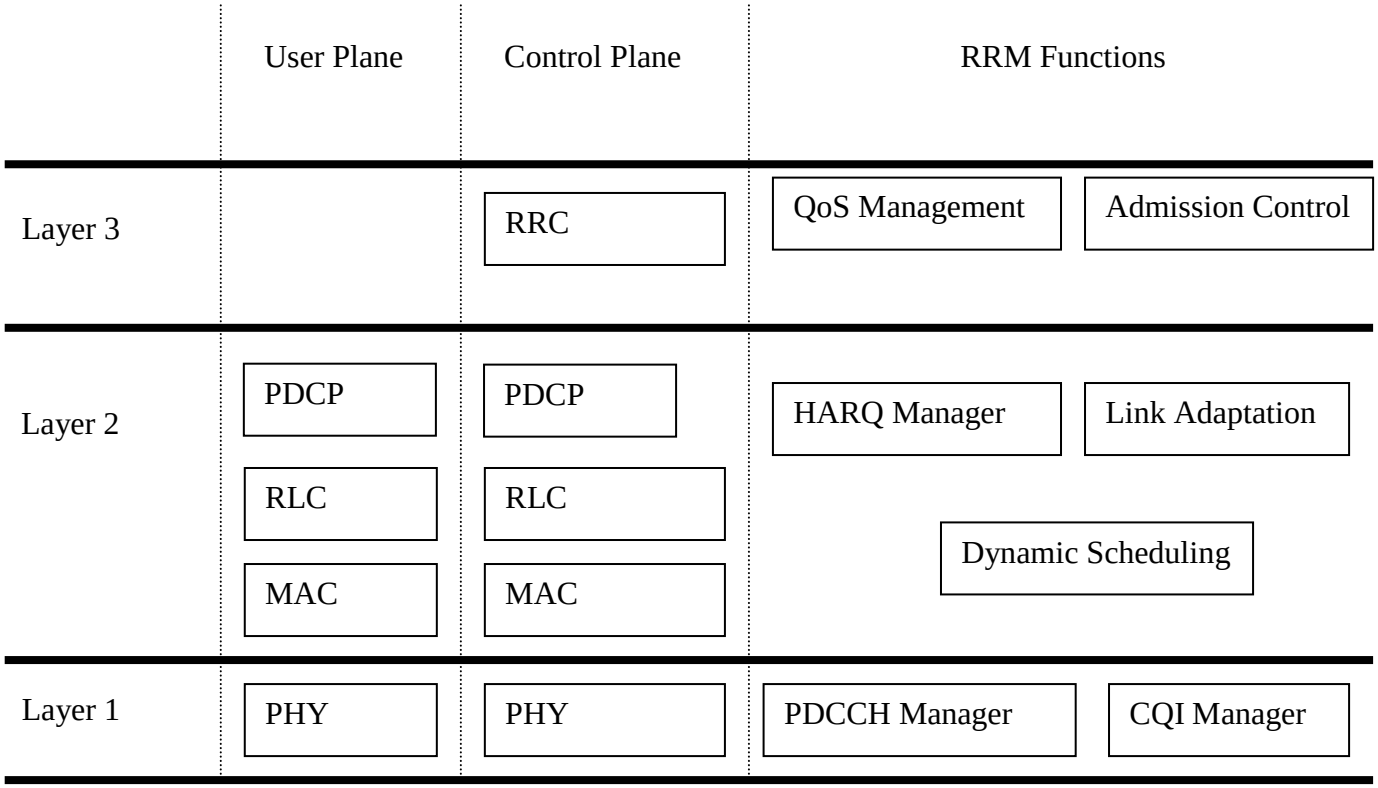

Figure 2. 5. RRM Functions at different layers

The RRM functions at layer 3 are characterised as semi-dynamic because they are mainly executed during the setup of new data flows while the RRM functions at layers 1 and 2 are very dynamic with new decisions made every Transmission Time Interval (TTI) [17] [26]. A brief description of the RRM functions is presented below.

- QoS Management: Each LTE EPS bearer is characterised by a QoS profile consisting of the following parameters [20]: QoS Class Identifier (QCI), Allocation Retention Priority (ARP), Guaranteed Bit Rate (GBR), and Maximum Bit Rate (MBR). The GBR parameter is only specified for GBR bearers while the MBR parameter is specified for non-GBR bearers. The ARP parameter defines the importance of a resource request. The QCI parameter is a reference to the following specific parameters: resource type (GBR or non-GBR), priority, packet delay budget (between UE and P-GW), and packet error loss rate.
- Admission Control: Responsible for granting or rejecting requests for new Evolved Packet System (EPS) bearers.

- Hybrid Automatic Repeat Request (HARQ) Manager: Responsible for error detection and correction by performing physical layer retransmission combining.
- Channel Quality Indicator (CQI) Manager: Responsible for handling the CQI reports from system users. The study utilised CQI reports derived from the prevailing channel conditions, i.e. measurements of the Signal to Interference Noise Ratio (SINR) on a resource block and/or sub-carrier level, as perceived by the UE.
- Link Adaptation: Link adaption provides information to the dynamic packet scheduler about the supported modulation and coding scheme (MCS) for each user based on the user's CQI measurement. This study utilised a number of link adaptation tables specified at a Block Error Rate (BLER) of 10^{-1} (Appendix A).
- Dynamic Scheduling: The dynamic packet scheduler is responsible for allocating Physical Resource Blocks (PRBs) and assigning the modulation and coding scheme (MCS) to active users. This study executed the packet scheduling process every Transmission Time Interval of 1ms.
- Physical Downlink Control Channel (PDCCH) Manager: The allocated PRBs and the assigned MCS are signalled to the active UEs on the (PDCCH). This study utilised the first three OFDM symbols in each Time Interval for control signalling.

2.1.3.1. 3GPP LTE Radio Resources

The Universal Mobile Telecommunications Systems (UMTS) terrestrial radio access network (UTRAN) long-term evolution (LTE) system or the Evolved UTRAN (E-UTRAN) employs Orthogonal Frequency Division Multiple Access (OFDMA) as the multiple access scheme for downlink transmissions. This translates to a time-frequency grid of available physical resource blocks (PRBs) depicted in Figure 2.6. In addition to time and frequency, the 3GPP LTE standard supports the exploitation of the spatial domain with multiple antenna techniques. The total number of physical resource blocks depends on the system bandwidth.

This study only considered a system bandwidth of 20 MHz with 100 physical resource blocks. A physical resource block spans 12 subcarriers each with a subcarrier bandwidth of 15 KHz over a 0.5ms time slot, each time slot consists seven OFDM symbols. Resource allocation is performed at intervals of 1ms in the time domain called the transmission time interval (TTI). Thus, one TTI is made up of 100 resource blocks in the frequency domain and 14 OFDM symbols in the time domain. The first three OFDM symbols of every TTI are reserved for transmission of related downlink control channels e.g. the physical downlink control channel (PDCCH) and the physical control format indicator channel (PCFICH) while the remaining eleven OFDM symbols constitute the physical downlink shared channel (PDSCH) used for transmission of user data.

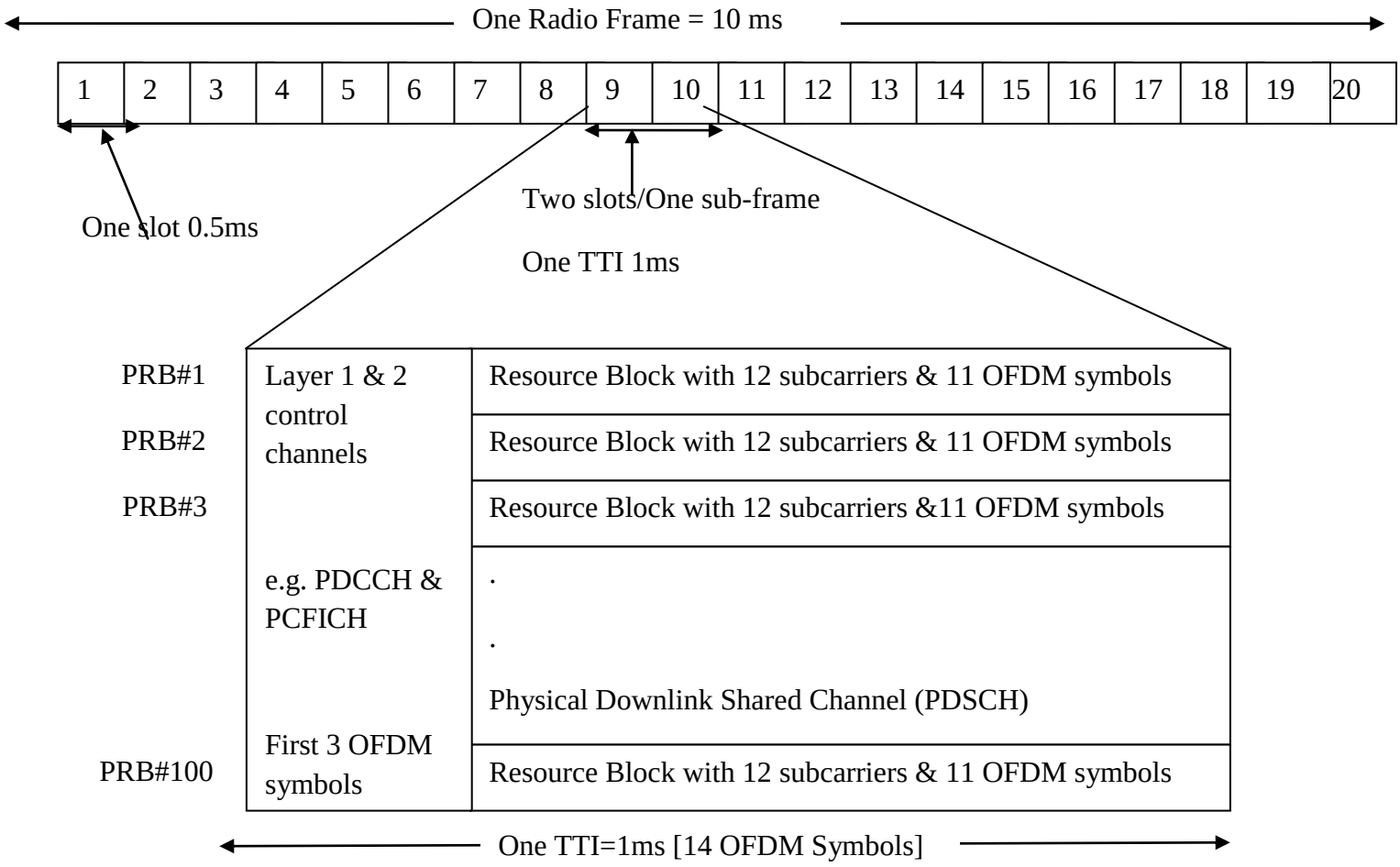

Figure 2. 6. 3GPP LTE FDD Downlink Radio Frame structure

2.2. Base Station Power Consumption Model

The authors in [27] presented a macro cell base station architecture (Figure 2.7) constituting the following: a Power Supply Unit (PSU), cooling system, baseband component, radio component, Power Amplifier (PA), Switch/duplexer and an antenna. The base station power consumption has been modelled as a linear relationship by a number of research groups, for example; the Energy Aware Radio neTwork tecHnologies (EARTH) project [28] [29], and the Mobile Virtual Centre for Excellence (MVCE) Green Radio project [30].

The base station power consumption is defined as the sum of the Radio Head (RH) power and the Overhead (OH) power. The Overhead (OH) power is not load dependent and is the power consumed by elements such as the cooling system and the base band processing unit while the Radio Head (RH) power is load dependent and is the power consumed by RH elements such as the power amplifier and the duplexer. The base station cell site may constitute one or more cell sectors. This study considered both cell sites with a single sector (omni directional) and cell sites with three sectors (directional).

The RH power, $P_{RH} = {P_{RF}}/{\mu_{\varepsilon}}$, where μ_{ε} is the aggregate efficiency of the RH components and

P_{RF} is the Radio Frequency (RF) transmit power. The base station operational power is therefore described by equation (2.1)

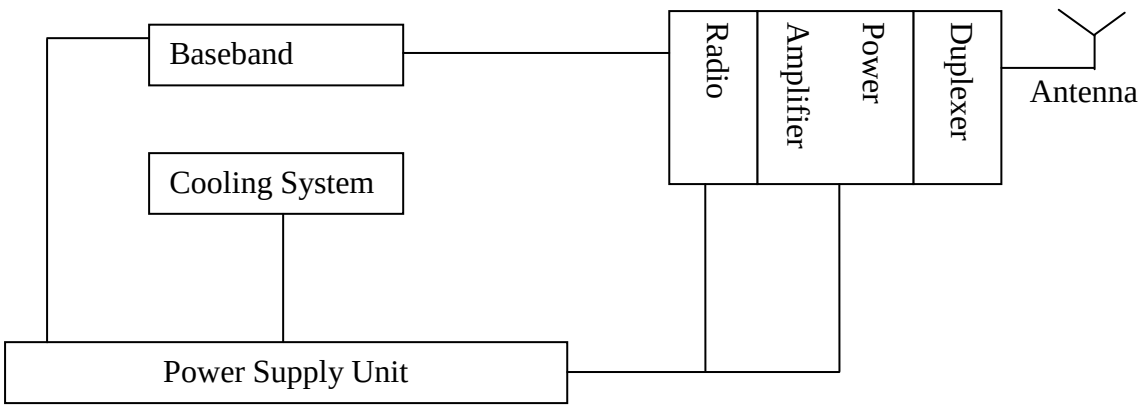

Figure 2. 7. Base Station Architecture

$$P_{BS}^{OP} = \sum_{i=1}^{N_c} N_{tx} \left(\frac{P_i^{RF}}{\mu_\varepsilon} + P_i^{OH} \right), \quad (2.1)$$

Where P_{BS}^{OP} is the BS operational power, N_c is the number of cells sectors per BS site, N_{tx} is the number of transmit antennas for cell sector i, and P_i^{OH} is the Overhead (OH) power consumption of cell sector i.

It is worth noting that radio resource management techniques can only impact the RF transmit power. Consequently these techniques have substantially greater impact on the energy performance in a Cloud infrastructure Radio Access Network (C-RAN) deployment [31] (i.e. where the radio head power is greater than the overhead power) compared to the traditional BS deployment (where the overhead power is greater than the radio head power).

Furthermore RF energy performance improvements could be leveraged by increasing the inter site distance between base stations subsequently reducing the density of base stations in any given geographical area thus reducing the energy consumption of the RANs as a whole.

2.3. Energy Metrics

Energy metrics are required to accurately quantify and evaluate the energy efficiency performance of; different radio access networks, different configurations of a radio access network and existing and future "green" techniques and methods.

The total system wide energy should include embodied energy (E_{EM}) as well as operational energy (E_{OP}) for services delivery, equation (2.2) [32] [33]. The embodied energy is the energy dissipated over the equipment's total lifetime while the operational energy is a function of the radio access architecture. Thus the operational energy constitutes the radio head (RH) Energy and the overhead (OH) energy.

$$E_{Total} = E_{EM} + E_{OP}, \quad (2.2)$$

Energy metrics can be broadly grouped into two categories, namely metrics that relate network power consumption to coverage area (i.e. watts/m^2) and metrics that relate the

energy consumption, during a given time period, to the total number of bits transmitted (i.e. Joules/Bit). This study adopted the latter energy metric, because radio resource management techniques have a greater impact on the number of transmitted bits than on network coverage. A framework for measuring the energy efficiency of a telecommunications network and equipment found in [34] where the power consumption to throughput ratio was proposed as an energy consumption ratio (ECR) metric, equation (2.3).

$$ECR = \frac{E}{M} = \frac{PT}{M} = \frac{P}{D}, \tag{2.3}$$

The ECR is defined as the energy per delivered application bit (Joules/Bit), where E is the energy required to deliver M application bits over time T, $D = {}^{M}/_{T}$ is the data rate in bits per second and P is the power.

This study also utilised a variant of the ECR metrics namely, the percentage Energy Reduction Gain (ERG) defined by equation (2.4).

$$ERG = \frac{ECR_1 - ECR_2}{ECR_1} \times 100\%, \tag{2.4}$$

The 3GPP LTE, base station model and energy metrics frameworks presented in this chapter provide the fundamental understanding required for the energy efficient radio resource management analyses and discussions presented in the subsequent chapters.

CHAPTER 3 **: ENERGY EFFICIENCY COMPARISON OF COMMON PACKET SCHEDULERS**

Since their inception, radio access networks have been continuously optimized to achieve enhanced throughput and coverage performance. However, the energy performance has received less consideration despite the inefficiency of the base stations associated to the radio access networks. For example, in cellular networks each base station can require up to 2.7KW of electrical power, which can lead to an energy consumption of tens of mega watt hours (MWh) per annum for wide area networks [35]. This chapter presents a characterisation of the energy performance of common and well-known packet schedulers in a multi-cell multi-user radio access network environment. The energy characterisation presented in this chapter is intended to provide a benchmark from which the energy efficiency performance of the techniques presented in the proceeding chapters can be evaluated.

The chapter is structured as follows; Section 3.1 presents a brief review of some research activity pertaining to packet scheduling. Section 3.2 discusses the packet-scheduling model. Section 3.3 describes the system model. Section 3.4 presents the performance results and analysis. Section 3.5 concludes the chapter with a summary of the key results.

3.1. Review of Packet Scheduling Research

The spectral efficiency, fairness and throughput performance of dynamic packet scheduling protocols in the UTRAN Long Term Evolution (LTE) has been studied extensively e.g. in [36-41], however, the energy consumption performance has received less consideration. [36] Presents a decoupled time and frequency domain scheduling framework and evaluates the throughput and fairness performance of different packet scheduling algorithms for the LTE downlink. In [37] it was shown that the frequency domain packet scheduler utilising frequency domain channel reports achieved average system capacity and cell-edge data rate

gains of over 40% compared to the frequency-blind but time opportunistic scheduling. [38] Presented the spectral efficiency of four basic antenna configurations for the LTE downlink, namely: Single Input Single Output (SISO), 1×2 Single Input Multiple Output (SIMO), 2×2 space frequency block coding (SFC) and 2×2 BLAST. In [39] the LTE spectrum efficiency, user throughput and peak data rate performance was compared against that of High-Speed Downlink Packet Access (HSDPA). In [40] it was shown that a decoupled time and frequency domain packet scheduler could be effectively used to control fairness among the users and achieve a throughput and coverage gain of 35% over the time-domain only scheduler. In [41] it was shown that fairness among the users could be controlled by frequency domain metric weighting or time domain priority setting depending on the number of users. It was also shown that metric decoupling between the time and frequency domain schedulers is fundamental for maximising throughput control.

3.2. Packet Scheduling Model

As previously stated in section 2.1.3.1, the Universal Mobile Telecommunications Systems (UMTS) terrestrial radio access network (UTRAN) long-term evolution (LTE) system or the Evolved UTRAN (E-UTRAN) employs Orthogonal Frequency Division Multiple Access (OFDMA) as the multiple access scheme for downlink transmissions. This translates to a time-frequency grid of available physical resource blocks (PRBs) depicted in Figure 3.1. The minimum resolution for packet scheduling is the 180 KHz physical resource block bandwidth in the frequency domain and 1ms Transmission Time Interval (TTI) in the time domain.

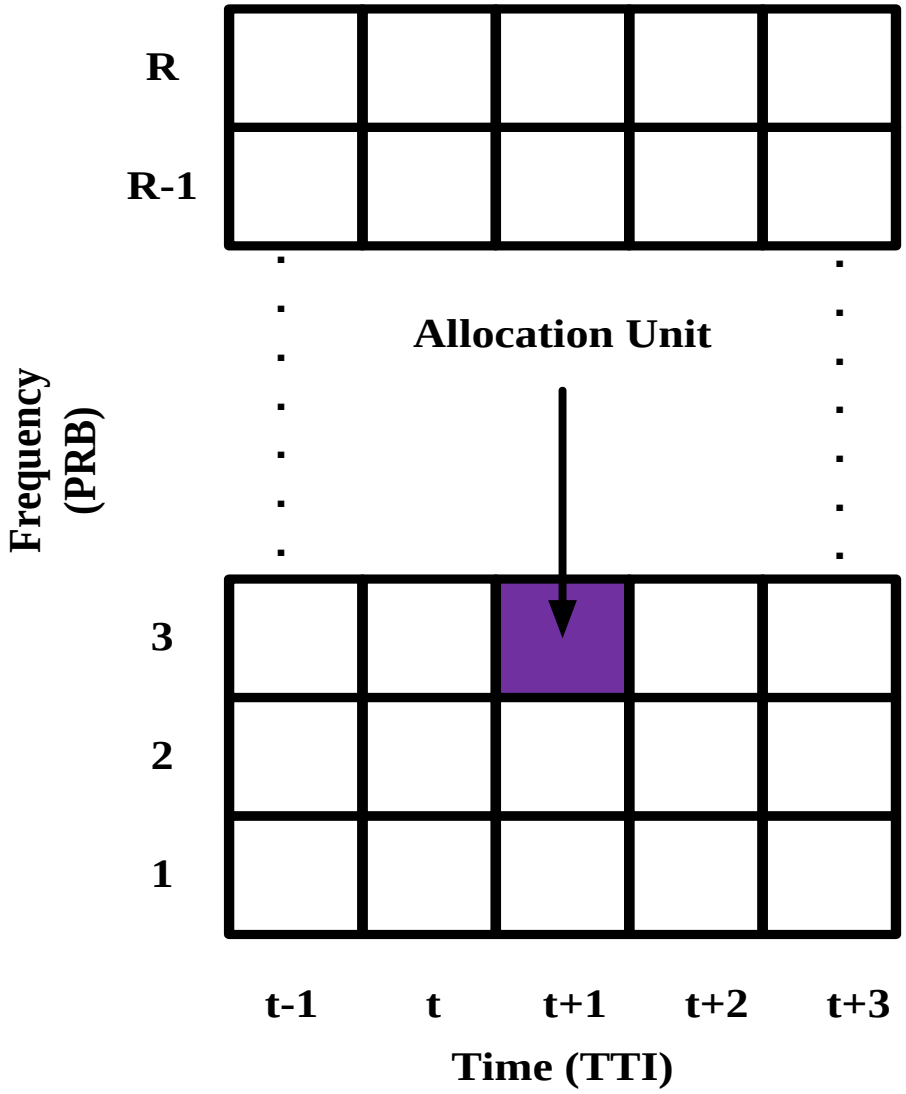

Figure 3. 1. Physical Resources in a Time-Frequency Grid for OFDMA

The packet scheduler was decoupled into two stages with the Time Domain Packet Scheduler (TD-PS) as the first stage and the Frequency Domain Packet Scheduler (FD-PS) as the second stage. Figure 3.2 illustrates the two-step packet scheduling implementation proposed in [36-37] and [40]. The Time Domain Packet Scheduler (TD-PS) selects users to be scheduled in the next Transmission Time Interval (TTI) and passes the candidate selection list (CSL) to the Frequency Domain Packet Scheduler (FD-PS). The Frequency Domain Packet Scheduler (FD-PS) allocates physical resource blocks (PRB) to users in the candidate selection list (CSL) provided by the Time Domain Packet Scheduler (TD-PS).

The separation of packet scheduling into time domain and frequency domain scheduling is advantageous for the following reasons:

- Improved scheduling flexibility since both time and frequency domains can be configured independently;
- Decreased complexity of the Frequency Domain Packet Scheduling (FD-PS) structure since only a sub-set of users are considered for multiplexing on the physical resource blocks.

Packet scheduling in both the time and frequency domains was carried out using specific scheduling priority metrics. A packet scheduling priority metric serves the purpose of enforcing a particular characteristic(s) of the scheduling algorithm. These characteristics are often a trade-off between the two major performance requirements i.e. maximising the system throughput and promoting fairness among users. Most packet scheduling metrics can be used for both time and frequency domain packet scheduling.

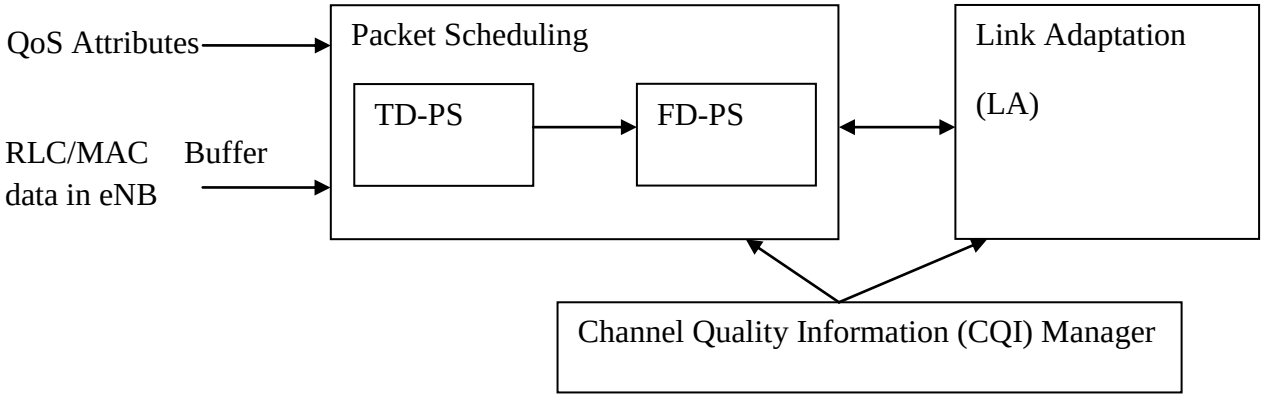

Figure 3. 2. Packet Scheduling Framework

The packet scheduler interacts closely with the Channel Quality Information (CQI) manager, Link Adaptation (LA) and the RLC/MAC buffer manager. CQI measurements provide a feedback report to the eNB characterising the channel quality. The channel quality is estimated by the UE based on downlink transmission of reference signals and reported to the eNB using the PUCCH or PUSCH [17]. Uncompressed CQI feedback or different CQI compression techniques such as, Best-M average CQI and wideband CQI can be utilised. In

this study, uncompressed CQI feedback was utilised. Link Adaptation (LA) provides information to the packet scheduler of the supported Modulation and Coding Scheme (MCS) based on the channel quality measurements feedback from the users. The buffer stores the data to be transmitted to the users. In this study, a full buffer[9] was assumed.

3.2.1. Time Domain Packet Scheduler (TD-PS)

The Time Domain Packet Scheduler (TD-PS) selects a subset of users form all the users requesting transmission resources. The Time Domain Packet Scheduler (TD-PS) only selects users who:

- Have pending data for transmission;
- Configured for scheduling in the next Transmission Time Interval (TTI).

The Time Domain Packet Scheduler (TD-PS) assigns a precedence measure to each of the selected users based on the time domain priority metric.

Additionally, the Time Domain Packet Scheduler (TD-PS) amends the number of selected users based on a control channel check [17]. The control channel check is performed to determine whether there are sufficient resources within the PDCCH for each of the selected users. The selected users are appended to the candidate selection list (CSL) which is passed to the Frequency Domain Packet Scheduler (FD-PS).

3.2.2. Frequency Domain Packet Scheduler (FD-PS)

The purpose of the Frequency Domain Packet Scheduler (FD-PS) is to allocate physical resource blocks (PRB) to users in the candidate selection list (CSL) provided by the Time Domain Packet Scheduler (TD-PS). Frequency domain packet scheduling aims to improve the system throughput by exploiting the varied frequency selective fading experienced by

[9] Full buffer is defined as condition whereby each user persistently demands transmission data in every transmission time interval.

different users on different physical resource blocks. Multiple physical resource blocks can be allocated to a user, and the PRBs need not be consecutive. LTE supports both localised and distributed transmission modes. Under the localised transmission mode, all the sub-carriers with in a physical resource block are allocated to the same user while under the distributed transmission mode one physical resource block can be shared among multiple users [26]. In this study, the localised transmission mode was the preferred. The frequency domain packet scheduler can be operated in two modes, namely [36]:

- ByUser- Physical resource blocks are allocated to each user in turn until the user is satisfied;
- ByPRB- For each physical resource block, the user with the best PRB specific priority metric is selected.

In this study, the "ByUser" mode of operation was chosen. The physical resource block allocation together with the modulation and coding assignment is finally forwarded to layer one of the eNB.

3.2.3. Packet Scheduling Metrics

3.2.3.1. Maximum Signal to Interference Noise Ratio (SINR)

The maximum Signal to Interference Noise Ratio (SINR) metric has the property of maximising the system throughput. This metric prioritises users with high SINR channel quality measurements over users with low SINR channel quality measurements. From link adaptation, higher channel quality values lead to more spectrally efficient modulation and coding schemes. Therefore, the maximum Signal to Noise Ratio (SINR) metric assigns a greater rank measure to the users that can support high instantaneous data rates. The obvious benefit of this metric is the maximisation of both system throughput and spectral efficiency; however, this comes at the cost of fairness since users with low SINR channel quality

measurements will receive less of the available radio resources. The maximum SINR metric $M[n]$ for user n is given by equation (3.1).

$$M[n] = SINR[n], \tag{3.1}$$

3.2.3.2. Proportional Fair (PF)

The proportional fair metric introduces some degree of fairness to the maximum SINR metric by considering both the instantaneous supportable data rate and the historic data rates supported by the user. The proportional fair metric $M[n]$ for user n is given by equation (3.2).

$$M[n] = \frac{D[n]}{R[n]}, \tag{3.2}$$

$D[n]$ is the wideband instantaneous throughput estimated by link adaptation and $R[n]$is the past average throughput of user *n* calculated with exponential average filtering as defined in [42].

3.2.3.3. Round Robin (RR)

The Round Robin (RR) metric has the property of allocating resources fairly to all the users. This metric assigns resources to users in closed loop circular manner according to the last scheduled time without regard to the users' channel state information. Therefore, the round robin metric assigns a greater rank measure to the users that have been in the queue the longest. The round robin metric $M[n]$ for user n is given by equation (3.3).

$$M[n] = \mathrm{T}[n], \tag{3.3}$$

$\mathrm{T}[n]$ is the last scheduled time.

3.3. System Model

An LTE system level simulator was developed in MATLAB to evaluate the E-UTRAN downlink Radio Frequency Energy Consumption Ratio (RF-ECR) for various packet schedulers in a multi-cell, multi-user system environment.

Downlink transmission between the eNB and the user equipments (UEs) was based on the Single Input Single Output (SISO) principle. The location coordinates of the UEs were randomly assigned following a uniform distribution while the location coordinates of the eNBs were pre-assigned and fixed. In addition, each UE experienced Inter-Cell Interference (ICI) from all the neighbouring cells in the radio access network (Figure 3.3). The main simulation parameters are detailed in Table 3.1.

Table 3.1. Simulation Parameters and Model Assumptions	
Parameter	Setting
System Bandwidth	20 MHz
Cellular Layout	Hexagonal grid, 19 Cells
Cell Radius	0.5 Km
Maximum Transmit Power	40 W
Number of Users (UEs)	10,20,30,40,50,60,70,80,90 100 UEs per Cell
Downlink Transmission Band	2.11-2.17 GHz
Number of Resource Blocks	100
Path Loss Model	COST 231 HATA Model
Multipath Fading Model	ITU Pedestrian A
eNB Height	20m
UE Height	1.5 m
UE Antenna Gain	0 dB
Channel Estimation	Perfect
CQI delay	1 ms
Modulation and coding schemes	QPSK ½, 16QAM ½ , ¾ & 64QAM ¾
EPS[10] Bearer data amounts per TTI	1 Kbit

[10] EPS Bearer is the LTE terminology for a data flow

3.3.1. Path Loss Model

The path loss was computed from the standard COST 231 HATA model [43] defined by equations (3.4) and (3.5).

$$L_{dB} = 46.3 + 33.9\log_{10} f_c - 13.82\log_{10} h_b - a(h_m) + (44.9 - 6.55\log_{10} \mathrm{h_b})\log_{10} \mathrm{d} + \mathrm{C}, \quad (3.4)$$

$$a(h_m) = (1.1\log_{10} 0.7f_c)h_m - (1.56\log_{10} f_c - 0.8), \quad (3.5)$$

L_{dB} Path loss in decibels.

f_c Operating frequency in MHz

h_b Height of eNB in metres.

h_m Height of UE metres.

d Distance between eNB and UE in kilometres.

C Correction factor of 3dBs for metropolitan centres and 0dB for medium cities and suburban centres.

$a(h_m)$ UE correction factor.

3.3.2. Multipath Model

The multipath fading was computed based on the ITU Pedestrian A model [44] [45] with a Root Mean Square (RMS) delay spread of 0.045 μs. From equation (3.6), a 0.045 μs RMS delay spread results in a 90% coherence bandwidth of approximately 444 KHz. This implies that any two successive physical resource blocks will experience uncorrelated multipath channel gains.

$$Bandwidth_{90\%\, correlation} \approx \frac{1}{50 \times RMS_{delay\ spread}}, \quad (3.6)$$

3.3.3. Signal to Interference Noise Ratio (SINR)

The SINR for SISO was computed for each UE on every physical resource block from equation (3.7).

$$SINR = \frac{|h_p|^2 P_{r_{AVG}}}{\sum_{j=1, j\neq p}^{Z} |h_j|^2 P_{j_{AVG}} + w}, \quad (3.7)$$

p and j are the serving and interfering cell indices respectively. h is the multipath channel gain modelled as a circular symmetric Gaussian random variable of zero mean and variance of 1. $P_{r_{AVG}}$ is the average received signal power, $P_{j_{AVG}}$ is the average received power from the j^{th} interfering cell and the noise power $w = KTB$, where K is the Boltzmann constant, T is the thermal temperature of 290K and B is the resource block bandwidth of 180 KHz.

3.3.4. Link Adaptation

Link Adaptation (LA) provides information to the packet scheduler of the supported Modulation and Coding Scheme (MCS) based on the channel quality measurements feedback from the users. Table 3.2 presents the LA look up table utilised for this study [17].

Table 3.2. Modulation and Coding Lookup Table

MCS Level	SINR Range (dB)	Rate (Mbit/s)
QPSK, ½	-8 to 6	16.8
16QAM, ½	6 to 8	33.6
16QAM, ¾	8 to10	50.4
16QAM	10 to 12	67.2
64QAM, ¾	12 to 15	75.6
64QAM	>15	100.8

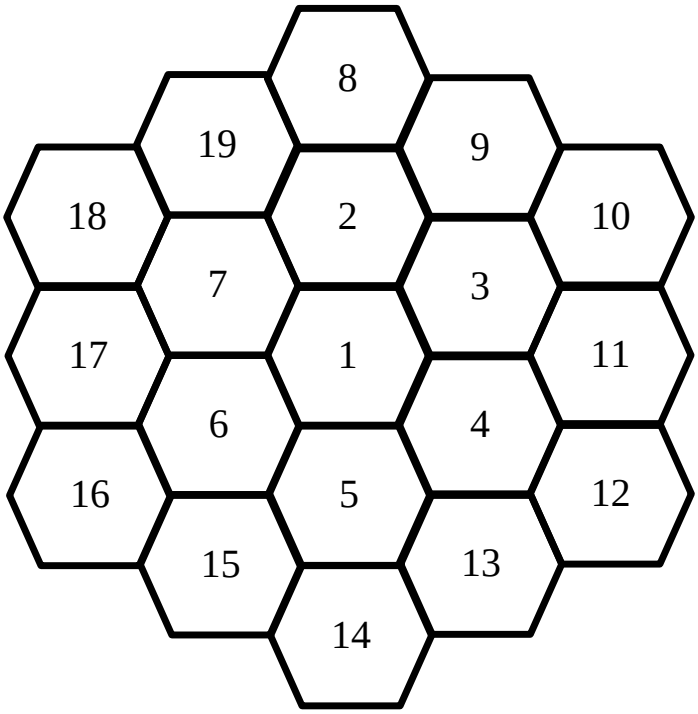

Figure 3. 3. E-UTRAN Layout

3.4. Results and Analysis

The Radio Frequency (RF) energy performance of the packet schedulers was evaluated using the RF Energy Consumption Ratio (RF-ECR) metric. In order to characterise the impact of the various packet scheduler components, the following experiments were setup. First the energy performance of the FD-PS was explored by varying the frequency domain priority metric while keeping the time domain metric constant. Second, the energy performance of the TD-PS was explored by varying the time domain priority metric while keeping the frequency domain metric constant.

3.4.1. FD-PS Energy Performance

Figure 3.4 presents the RF Energy Consumption Ratio (RF-ECR) of the frequency domain packet schedulers with a constant maximum SINR metric as the time domain metric.

Figure 3.5 presents the RF Energy Consumption Ratio (RF-ECR) of the frequency domain packet schedulers with a constant round robin metric as the time domain metric.

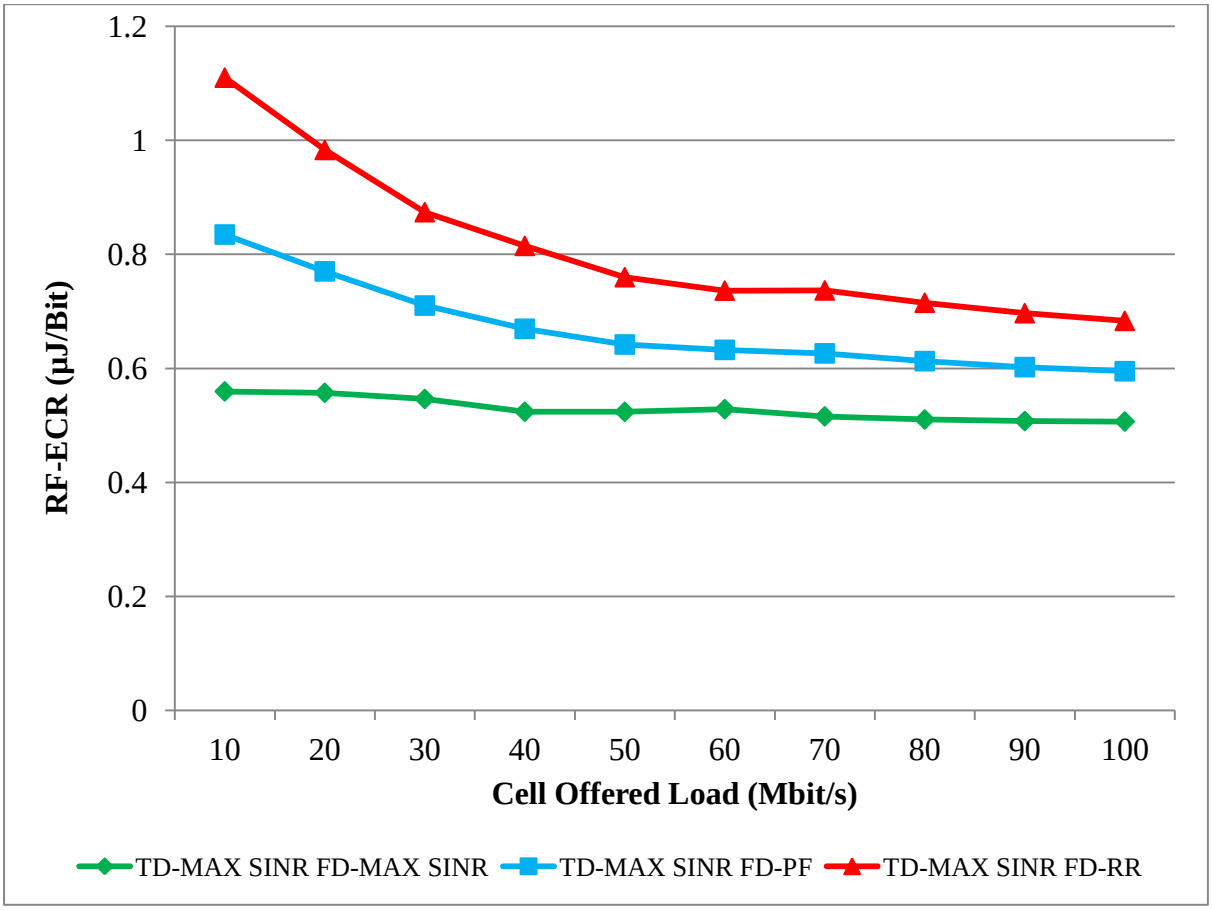

Figure 3. 4. RF-ECR Vs Offered Load (Fixed TD-MAX SINR Scheduler)

From Figure 3.4, the frequency domain maximum SINR packet scheduler produced RF Energy Reduction Gains (RF-ERG) ranging from 25% to 49% over the frequency domain round robin packet scheduler.

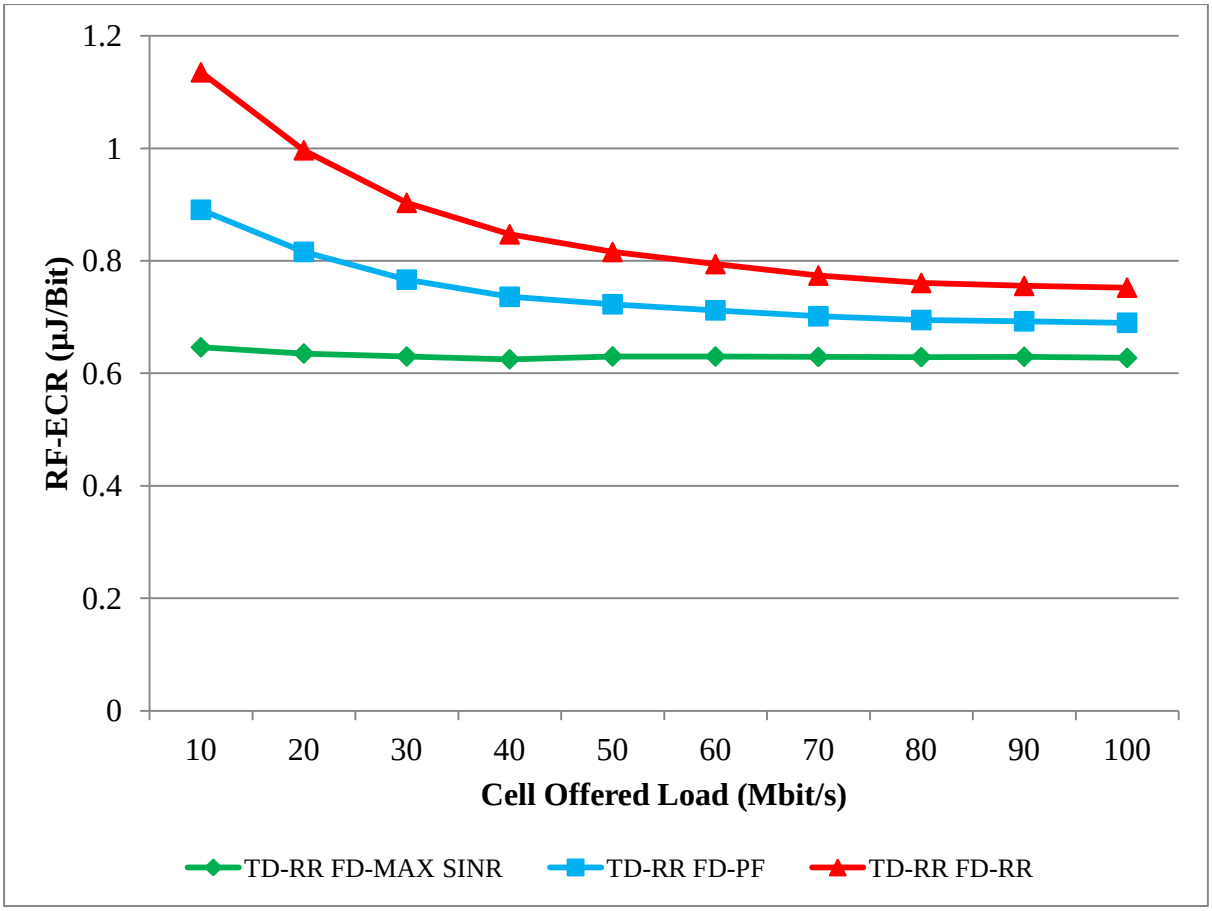

Figure 3. 5. RF-ECR Vs Offered Load (Fixed TD-RR Scheduler)

From Figure 3.5, the frequency domain maximum SINR packet scheduler produced RF Energy Reduction Gains (RF-ERG) ranging from 16% to 43% over the frequency domain round robin packet scheduler.

The results in both Figure 3.4 and Figure 3.5, exhibited the following key features of interest:

• The energy performance of the frequency domain maximum SINR packet scheduler was largely independent of the offered load. This is because the maximum SINR metric better exploits the frequency diversity, experienced by the users, and allocates the physical resource blocks with good channel conditions.

• The energy performance of the frequency domain round robin packet scheduler improved with increasing offered load. The round robin physical resource block allocation does not

consider the user channel state information. However, as the number of users in the system increases, the likelihood of users with good channel conditions also increases; hence the energy performance improvement at higher loads.

- The frequency domain maximum SINR packet scheduler is more energy efficient than the frequency domain round robin packet scheduler. Assigning good channel quality physical resource blocks translates to more transmitted data and hence lower energy consumption ratio values.

3.4.2. TD-PS Energy performance

Figure 3.6 presents the RF Energy Consumption Ratio (RF-ECR) of the time domain packet schedulers with a constant round robin metric as the frequency domain metric.

Figure 3.7 presents the RF Energy Consumption Ratio (RF-ECR) of the time domain packet schedulers with a constant maximum SINR metric as the frequency domain metric.

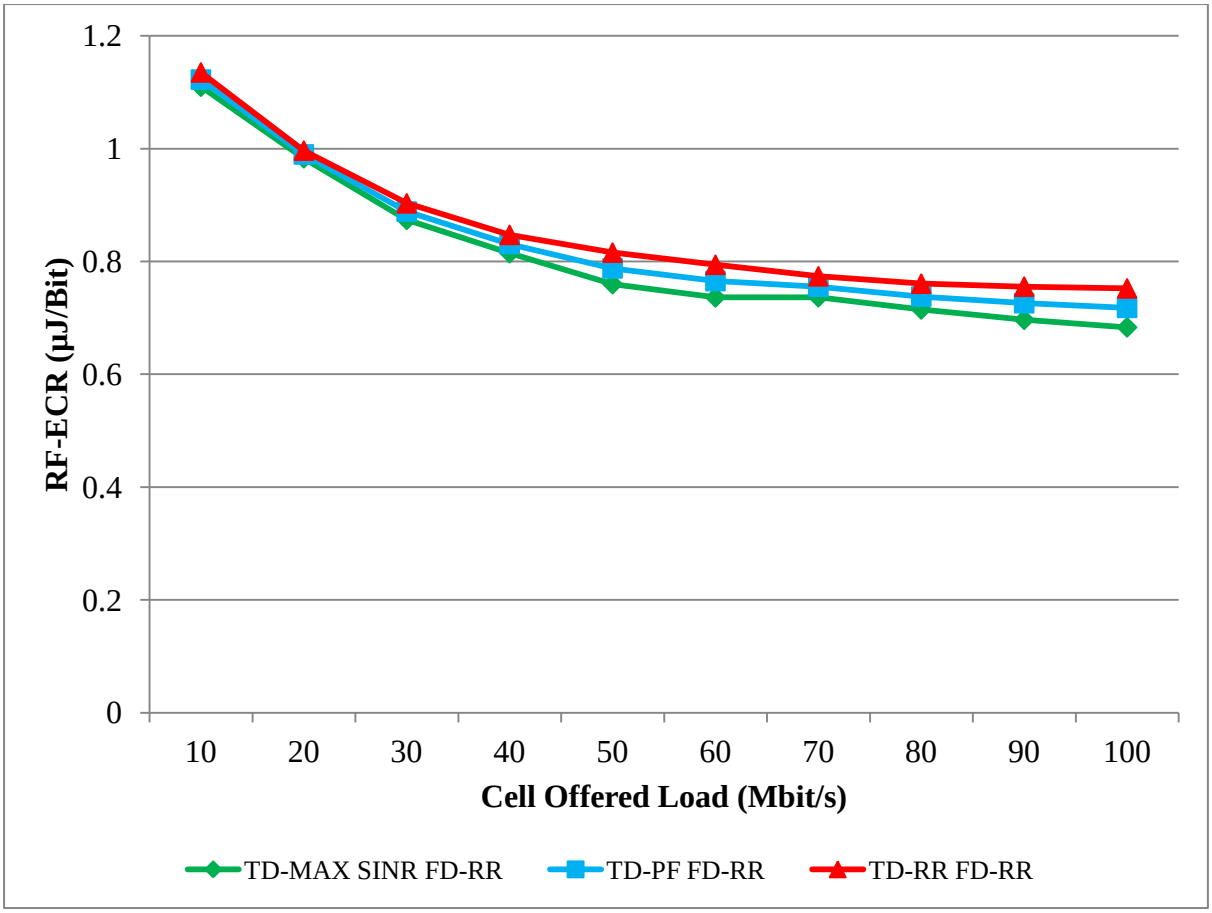

Figure 3. 6. RF-ECR Vs Offered Load (Fixed FD-RR Scheduler)

From Figure 3.6, the time domain maximum SINR packet scheduler produced RF Energy Reduction Gains (RF-ERG) ranging from 2% to 9% over the time domain round robin packet scheduler.

From Figure 3.7, the time domain maximum SINR packet scheduler produced RF Energy Reduction Gains (RF-ERG) ranging from 13% to 18% over the time domain round robin packet scheduler.

The time domain maximum SINR packet scheduler is more energy efficient than the time domain round robin packet scheduler. This is because the time domain maximum SINR metric produces a candidate selection list of users sorted in descending order from highest to lowest channel quality. Consequently, users with good channel quality will get the first pick of the available physical resource blocks. Since the frequency domain packet scheduler is

operated in the “ByUser” mode, more data is transmitted and hence improved energy efficiency.

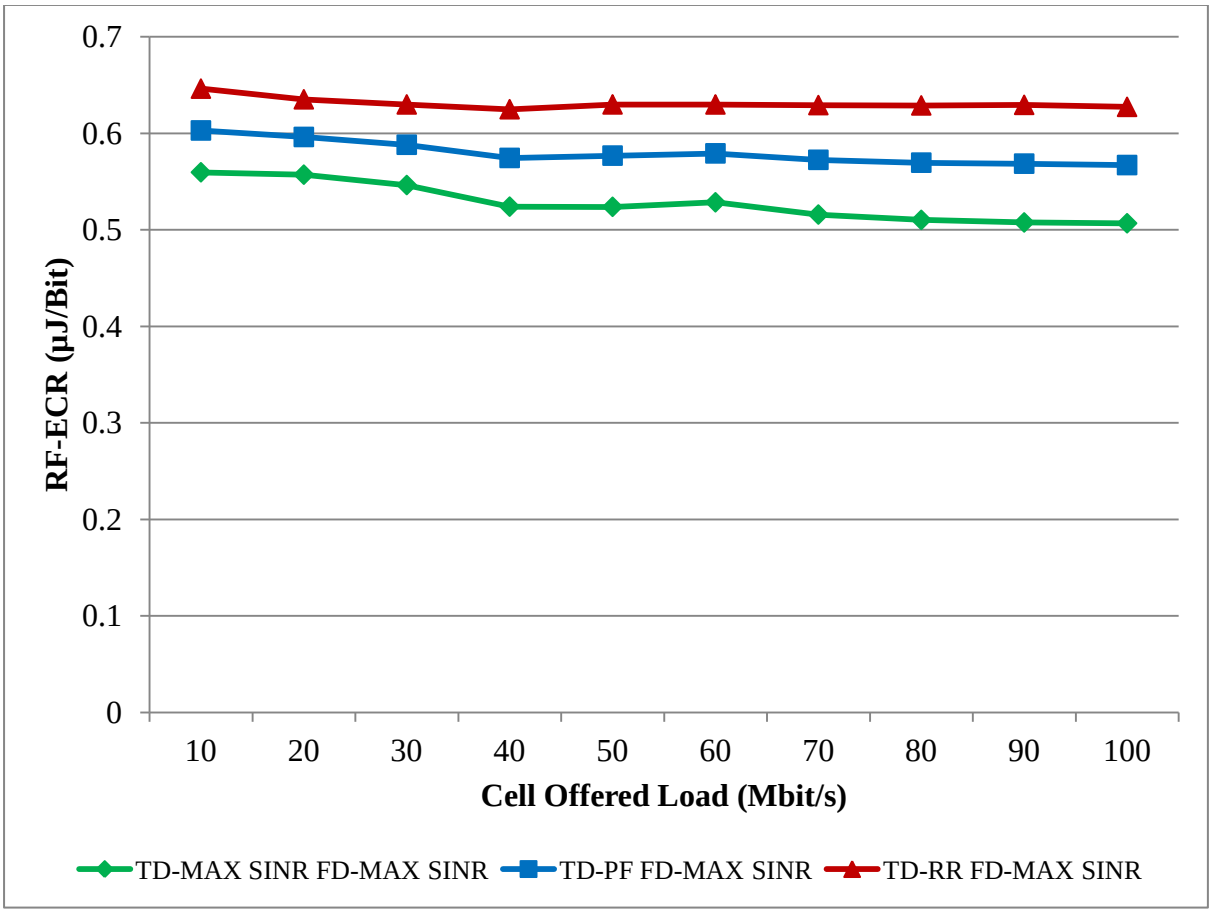

Figure 3. 7. RF-ECR Vs Offered Load (Fixed FD-MAX SINR Scheduler)

3.5. Summary of Results

This chapter presented a characterisation of the energy performance of common and well-known packet schedulers in a multi-cell multi-user UTRAN long-term evolution (LTE) system.

First, it was shown that the maximum SINR metric is more energy efficient than the round robin metric for both time and frequency domain packet scheduling. However, the energy efficiency of the maximum SINR metric is achieved at the following costs:

- Accurate channel quality measurements;
- Fairness to users with low SINR channel quality measurements

Second, it was shown that frequency domain packet scheduling had a greater impact on the energy efficiency of the system than time domain packet scheduling; i.e. RF Energy Reduction Gains (RF-ERG) ranging from 16% to 49% and 2% to 18% respectively.

In this chapter, channel quality aware packet scheduling was shown to improve the energy efficiency of the UTRAN long-term evolution (LTE) system. The next chapter investigates the energy efficiency derived from Multiple Input Multiple Output (MIMO) antenna techniques.

CHAPTER 4 **: SFBC MIMO ENERGY EFFICIENCY IMPROVEMENTS OF COMMON PACKET SCHEDULERS**

Multiple antenna systems, commonly referred to as Multiple Input Multiple Output (MIMO) systems, use multiple antennas to increase system throughput and immunity to fading, interference and noise. The benefits often associated with MIMO are: multiplexing gain, diversity gain, and antenna gain; however, the energy efficiency potential of MIMO is relatively unexplored. This chapter investigates the following research question. Does MIMO with its two radio heads but better SINR (diversity gain) or better throughput (multiplexing gain) end up being more energy efficient than Single Input Single Output (SISO)? This chapter presents an RF energy efficiency comparison between SISO systems and MIMO with the 2×2 Alamouti Space Frequency Block Code (SFBC) chosen for this case study.

The chapter is structured as follows; Section 4.1 presents a brief review of some research activities pertaining to MIMO systems. Section 4.2 discusses spatial diversity. Section 4.3 describes the system model. Section 4.4 presents the performance results and analysis. Section 4.5 concludes the chapter with a summary of the key results.

4.1. Review of Multiple Input Multiple Output Research

Research into MIMO wireless communication systems commenced in the late 1990s and gained an unprecedented interest from both academia and industry. Consequently the field evolved rapidly resulting in a number of MIMO techniques being embedded in major third-generation (3G) and fourth-generation (4G) standards, such as: Long Term Evolution (LTE) [46], IEEE 802.11n [47], and Code Division Multiple Access (CDMA) systems [48].

The authors in [49] and [50] derived mathematical models for the theoretical capacity of MIMO systems under the following assumptions: channel parameters can be estimated at the receiver, independent multipath gains between different antenna pairs, and frequency flat channels. The authors further demonstrated that the ergodic capacity of MIMO flat fading

wireless links grows roughly proportionally with the minimum of the number of transmit or receive antennas thus promising significantly larger data rates than SISO.

In a bid to realise the predicted high bit rates, the authors in [51] invented a layered space-time architecture with an equal number of transmit and receive antennas. This architecture demonstrated that capacity increased linearly with half the minimum of the number of transmit or receive antennas.

In [52], a ground breaking elegantly simple two-branch transmit diversity scheme was proposed. This scheme, commonly known as Alamouti transmit diversity boasts the following advantages: no channel state information feedback from the receiver, produces the same diversity gain as maximum ratio receiver combining (MRRC) and simple maximum likelihood (ML) detection due to the orthogonality property.

The authors in [53] proposed a new family of space-time codes called space-time trellis codes and argued that these codes could be readily implemented in digital signal processing (DSP) and very large scale integration (VLSI).

A comprehensive literature survey on multiple antennas techniques can be found in [54] and references therein. The authors provide an overview of the major topics of interest pertaining to multiple antennas research and development such as:

- Transmitter and receiver structures for spatial multiplexing and spatial diversity.
- Co-located and distributed MIMO systems
- Single user and multiuser MIMO schemes
- Open-loop and closed-loop techniques
- Space Division Multiple Access (SDMA)
- Smart antenna techniques

Figure 4.1 summarises the key benefits of multiple antennas techniques.

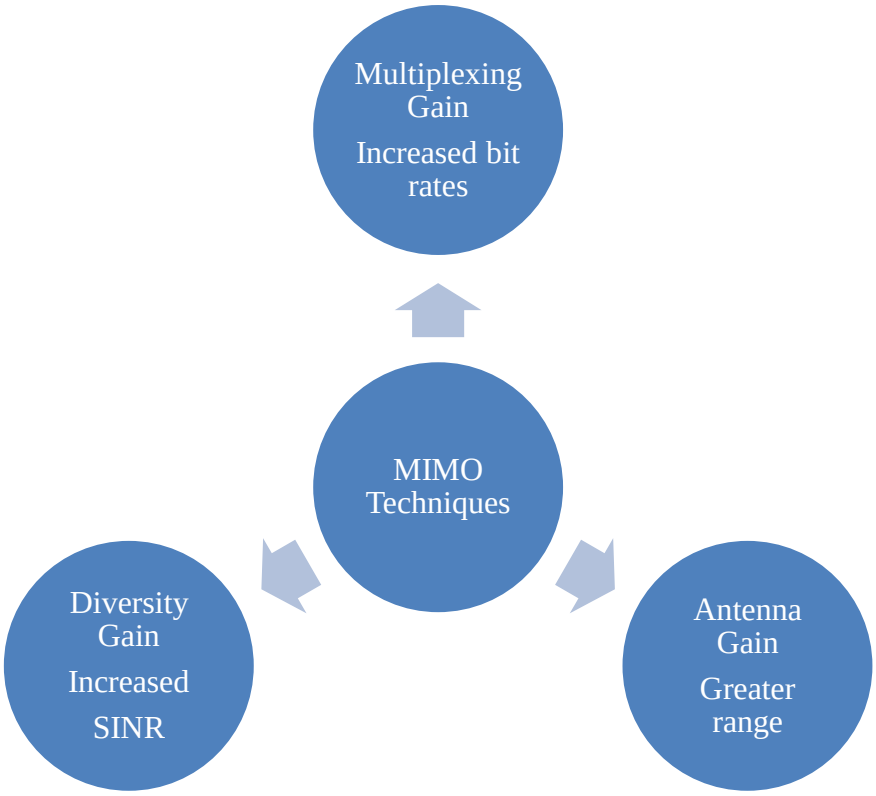

Figure 4. 1. Advantages attributed to MIMO Techniques

4.2. Multiple Antenna Model

Multiple antenna techniques are broadly grouped into three major categories, namely: multiplexing techniques, diversity techniques and smart antenna techniques. There are an abundant number of implementations proposed, for each of the MIMO categories, in the public domain literature.

Spatial multiplexing techniques increase the transmission data rate by transmitting independent streams of symbols across the transmit antennas. However, since the channel matrix is not orthogonal, maximum likelihood (ML) detection of the transmitted symbols grows exponentially with the number of transmit antennas. This results in the following undesirable drawbacks: increased detector complexity, processing power and time. These drawbacks are particularly magnified when the transmitted symbols are drawn from large

symbol sets such as 64 QAM[11]; one of the modulation techniques proposed for LTE to achieve high data rates. The following suboptimal detectors have been proposed to address the ML detector complexity problem: zero forcing detector and minimum mean square error (MMSE) detector.

Beam forming techniques employ multiple transmit antennas to produce larger antenna gains and signal strength in a desired direction thus improving the channel quality of the users in the chosen direction. However, this is achieved at the expense of reduced signal strength in other directions and in extreme cases may result in a total loss of signal power i.e. null regions. Users in regions of weak signal strength experience poor channel conditions and hence exhibit a poor energy performance that detrimentally affects the energy performance of the overall radio access network.

Spatial diversity techniques improve the SINR by transmitting and receiving the same symbols across multiple antennas. This improves the bit error rate performance and hence the reliability of signal detection at the receiver. Spatial diversity techniques are further subdivided into two categories, namely: receive diversity also known as Single Input Multiple Output (SIMO) and transmit diversity also known as Multiple Input Single Output (MISO).

Receive diversity techniques, such as maximum ratio combining (MRC), equal gain combining (EGC) and selection combining (SC), employ multiple receive antennas to obtain multiple copies of the same transmitted symbol and apply linear processing to improve the power and hence SINR of the received symbol. The diversity gain is maximised if the channels, to each receive antenna, are independent. The necessary condition for independent channels is that the receive antennas should be at least six wavelengths apart. However, given

[11] Quadrature Amplitude Modulation

the ever decreasing size of popular mobile handsets, the receive diversity gain and the energy efficiency improvements derived there from are not fully exploited.

Transmit diversity techniques, such as beam forming, employ multiple transmit antennas and apply linear processing prior to transmitting the same symbols in order to improve the power and hence SINR of the received symbol. Transmit diversity requires the knowledge of channel state information at the transmitter prior to transmission i.e. an informed transmitter. However, in many applications the channel state information cannot be accurately known at the transmitter. A solution to the informed transmitter problem is the Alamouti space time block code (STBC) [52].

In this case study, a variant of the Alamouti STBC namely, the Alamouti space frequency block code (SFBC) was chosen as the multiple antenna technique.

4.2.1. 2x2 Alamouti SFBC MIMO

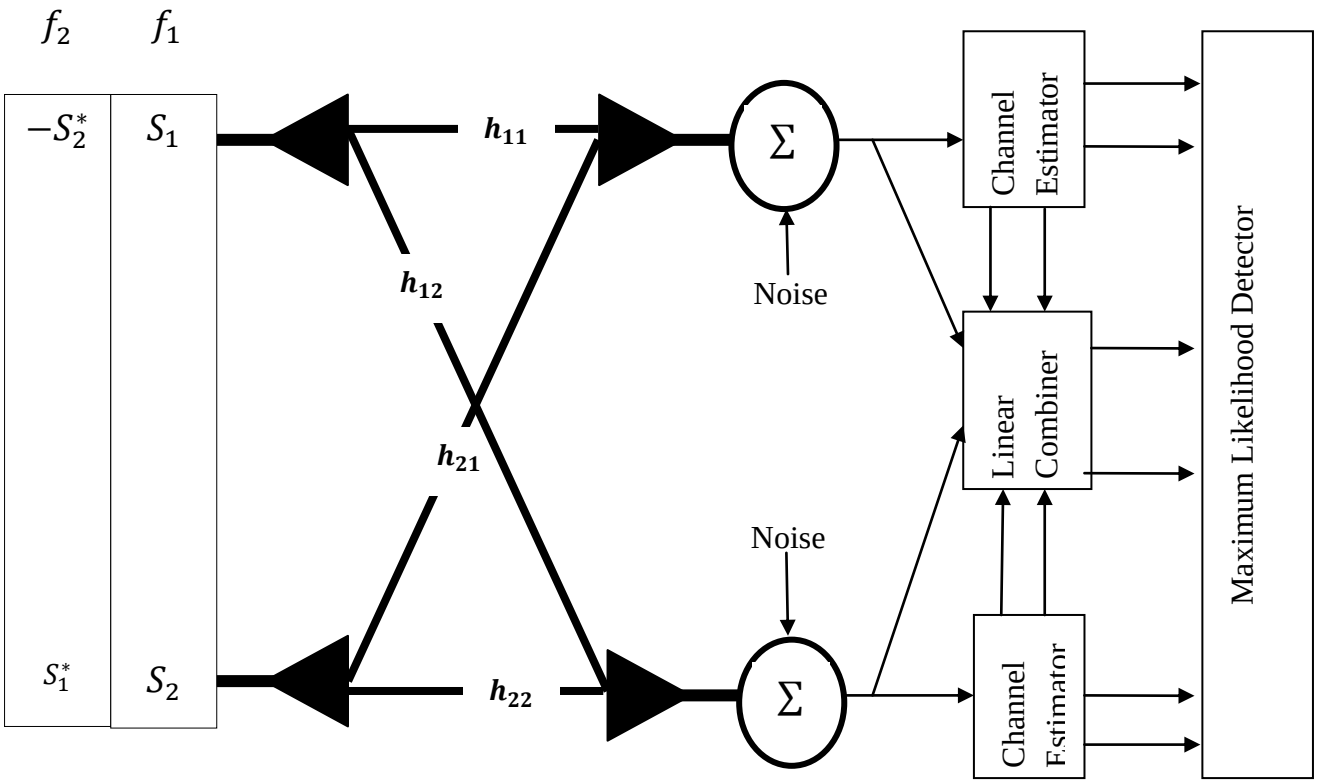

Figure 4. 2. 2x2 Alamouti SFBC MIMO Architecture

Two symbols S_1 and S_2 are transmitted from antennas 1 and 2, respectively on frequency f_1. Within the same transmission time slot, symbols $-S_2^*$ and S_1^* are transmitted from antennas 1 and 2, respectively on frequency f_2.

The received symbol on antenna 1 on frequency f_1 is.

$$y_1 = h_{11}S_1 + h_{21}S_2 + n_1, \tag{4.1}$$

The received symbol on antenna 2 on frequency f_1 is.

$$y_3 = h_{12}S_1 + h_{22}S_2 + n_3, \tag{4.2}$$

The received symbol on antenna 1 on frequency f_2 is.

$$y_2 = -h_{11}S_2^* + h_{21}S_1^* + n_2, \tag{4.3}$$

The received symbol on antenna 2 on frequency f_2 is.

$$y_2 = -h_{12}S_2^* + h_{22}S_1^* + n_4, \tag{4.4}$$

Equations 4.1, 4.2, 4.3 and 4.4 can be combined as,

$$\begin{bmatrix} y_1 \\ y_3 \\ y_2^* \\ y_4^* \end{bmatrix} = \begin{bmatrix} h_{11} & h_{21} \\ h_{12} & h_{22} \\ h_{21}^* & -h_{11}^* \\ h_{22}^* & -h_{12}^* \end{bmatrix} \begin{pmatrix} S_1 \\ S_2 \end{pmatrix} + \begin{bmatrix} n_1 \\ n_3 \\ n_2^* \\ n_4^* \end{bmatrix}, \tag{4.5}$$

The channel matrix is defined as,

$$H = \begin{bmatrix} h_{11} & h_{21} \\ h_{12} & h_{22} \\ h_{21}^* & -h_{11}^* \\ h_{22}^* & -h_{12}^* \end{bmatrix}, \tag{4.6}$$

Since

$$H^H H = \begin{bmatrix} |h_{11}|^2 + |h_{12}|^2 + |h_{21}|^2 + |h_{22}|^2 & 0 \\ 0 & |h_{11}|^2 + |h_{12}|^2 + |h_{21}|^2 + |h_{22}|^2 \end{bmatrix}$$

Symbol detection can be decoupled, thus the estimated transmitted symbols are:

$$\begin{bmatrix} \widehat{S_1} \\ \widehat{S_2} \end{bmatrix} = (H^H H)^{-1} H^H \begin{bmatrix} y_1 \\ y_3 \\ y_2^* \\ y_4^* \end{bmatrix}, \quad (4.7)$$

4.3. System Model

An LTE system level simulator was developed in MATLAB to evaluate the E-UTRAN downlink Radio Frequency Energy Consumption Ratio (RF-ECR) spectral efficiency and user QoS for various packet schedulers in a multi-cell multi-user system model.

Downlink transmission between the eNB and the user equipments (UEs) was based on two criteria, namely: the single input single output (SISO) transmission mode with a uniform transmit power allocation and the 2×2 SFBC Alamouti multiple input multiple output (MIMO) transmission mode also with a uniform transmit power allocation. The power per antenna in the 2×2 SFBC MIMO mode is half the power per antenna in the SISO mode.

The location coordinates of the UEs were randomly assigned following a uniform distribution while the location coordinates of the eNBs were pre-assigned and fixed. In addition, each UE experienced Inter-Cell Interference (ICI) from all the neighbouring cells in the radio access network (Figure 3.3). The main simulation parameters are detailed in Table 4.1.

4.3.1. Path Loss Model

The path loss was computed from the WINNER II Urban Micro and Urban Macro channel models [55].

4.3.1.1. Path Loss Urban Micro

In order to compute the path loss the following the following parameters were calculated: the breakpoint distance (equation 4.8), and the line of sight (LOS) probability (equation 4.9).

$$d_{BP} = \frac{4h_b h_m f_c}{c}, \quad (4.8)$$

f_c Operating frequency in Hz

d_{BP} Breakpoint distance in metres.

h_b Height of eNB in metres.

h_m Height of UE metres.

$$P_{LOS} = \min(18/d, 1).\left(1 - exp^{-d/36}\right) + exp^{-d/36} \quad (4.9)$$

P_{LOS} LOS probability

d Distance between eNB and UE in metres.

If the LOS probability was less than 0.5, the path loss was computed from equation (4.10). However if the LOS probability was greater than 0.5, the path loss computation was dependant on the UE distance relative to the breakpoint distance. If the UE distance was greater than the breakpoint distance, the path loss was computed from equation (4.11); if the UE distance was less than the breakpoint distance, the path loss was computed from equation (4.12).

$$L_{dB} = 36.7 \log_{10} d + 22.7 + 26 \log_{10} f_c, \quad (4.10)$$

$$L_{dB} = 40 \log_{10} d + 7.8 - 18 \log_{10} h_b - 18 \log_{10} h_m + 2 \log_{10} f_c\,, \quad (4.11)$$

$$L_{dB} = 22 \log_{10} d + 28 + 20 \log_{10} f_c, \quad (4.12)$$

4.3.1.2. Path Loss Urban Macro

The LOS probability was computed from equation 4.13.

$$P_{LOS} = \min(18/d, 1).\left(1 - exp^{-d/63}\right) + exp^{-d/63} \quad (4.13)$$

If the LOS probability was less than 0.5, the path loss was computed from equation (4.14). However if the LOS probability was greater than 0.5, the path loss computation was dependant on the UE distance relative to the breakpoint distance. If the UE distance was greater than the breakpoint distance, the path loss was computed from equation (4.15); if the

UE distance was less than the breakpoint distance, the path loss was computed from equation (4.16).

$$L_{dB} = (44.9 - 6.55\log_{10} h_b)\log_{10} d + 34.46 + 5.83\log_{10} h_b \ + 23\log_{10} {}^{f_c}/_{5}, \quad (4.14)$$

$$L_{dB} = 40\log_{10} d + 13.7 - 14\log_{10} h_b - 14\log_{10} h_m \ + 6\log_{10} {}^{f_c}/_{5}, \quad (4.15)$$

$$L_{dB} = 26\log_{10} d + 39 + 20\log_{10} {}^{f_c}/_{5}, \quad (4.16)$$

4.3.2. Multipath Model

The multipath fading effect was modelled based on the urban micro and urban macro power delay profiles presented in [55].

Table 4.1. Simulation Parameters and Model Assumptions	
Parameter	Setting
System Bandwidth	20 MHz
Cellular Layout	Hexagonal grid, 19 Cells
Cell Site Radius	150m Micro cell and 1000m Macro cell
Maximum Transmit Power	SISO 20 Watts, MIMO 10 Watts per antenna
Number of Users (UEs)	25 UEs per Cell
Downlink Transmission Band	2.11-2.17 GHz
Number of Resource Blocks	100
Path Loss Model	WINNER II Channel model (Urban Micro and Urban Macro)
Multipath Fading Model	WINNER II Channel model (Urban Micro and Urban Macro)
eNB Height	10m (Urban Micro) and 25m (Urban Macro)
UE Height	1.5 m
UE Antenna Gain	0 dB
Channel Estimation	Perfect
CQI delay	1 ms
Modulation and coding schemes	QPSK 1/3, 1/2, 3/4 & 16QAM 1/3, 1/2, 3/4 & 64QAM 3/5, 3/4, 6/7
EPS Bearer data amounts per TTI	1 Kbit

4.3.3. Link Adaptation

Tables A1, A2, A3, and A4 of appendix A present the link adaptation tables utilised for this study. The tables were obtained from link level simulations of WINNER II multipath and path loss channel models at a Block Error Rate (BLER) of 10^{-1} by the authors in [89].

4.4. Results and Analysis

The performance of the frequency domain packet schedulers was evaluated using the following measurands: RF Energy Consumption Ratio (ECR), spectral efficiency and User Quality of Service (QoS). The following experiments were setup. First the energy, spectral efficiency and user QoS performance of the frequency domain packet schedulers was explored by varying the frequency domain priority metric while keeping the time domain metric constant in an urban micro environment. Second the energy, spectral efficiency and user QoS performance of the frequency domain packet schedulers was explored by varying the frequency domain priority metric while keeping the time domain metric constant in an urban macro environment.

4.4.1. Energy Performance Results

Figure 4.3 and Figure 4.4 present the energy consumption ratio cumulative distribution function (CDF) plots of the various frequency domain packet schedulers for the Urban Micro and Urban Macro network scenarios respectively.

From Figure 4.3, SFBC MIMO in an urban micro deployment produces 75% quartile RF energy reduction gains (RF-ERG) of 31%, 32% and 14% for the Max SINR, Proportional Fair and Round Robin frequency domain packet schedulers respectively over SISO.

From Figure 4.4, SFBC MIMO in an urban macro deployment produces 75% quartile RF energy reduction gains (RF-ERG) of 40%, 39% and 49% for the Max SINR, Proportional Fair and Round Robin schedulers respectively over SISO.

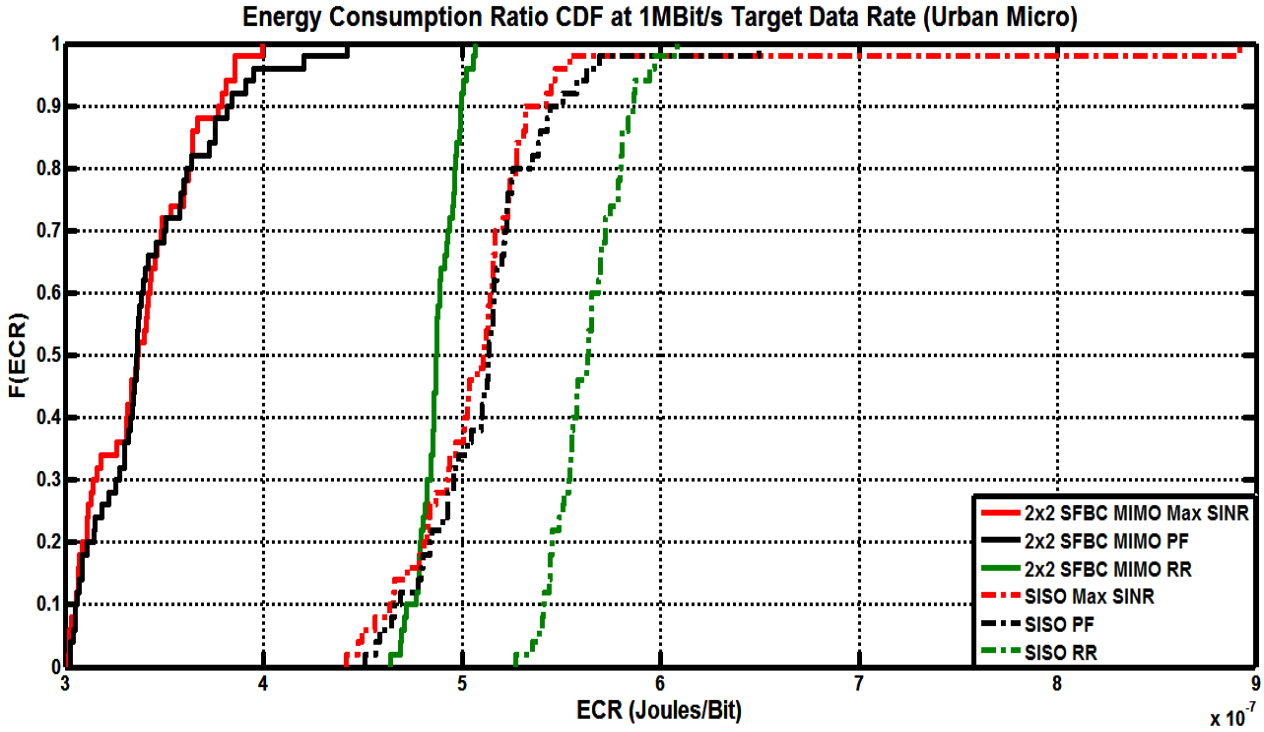

Figure 4. 3. Energy Consumption Ratio CDF **(Urban Micro)**

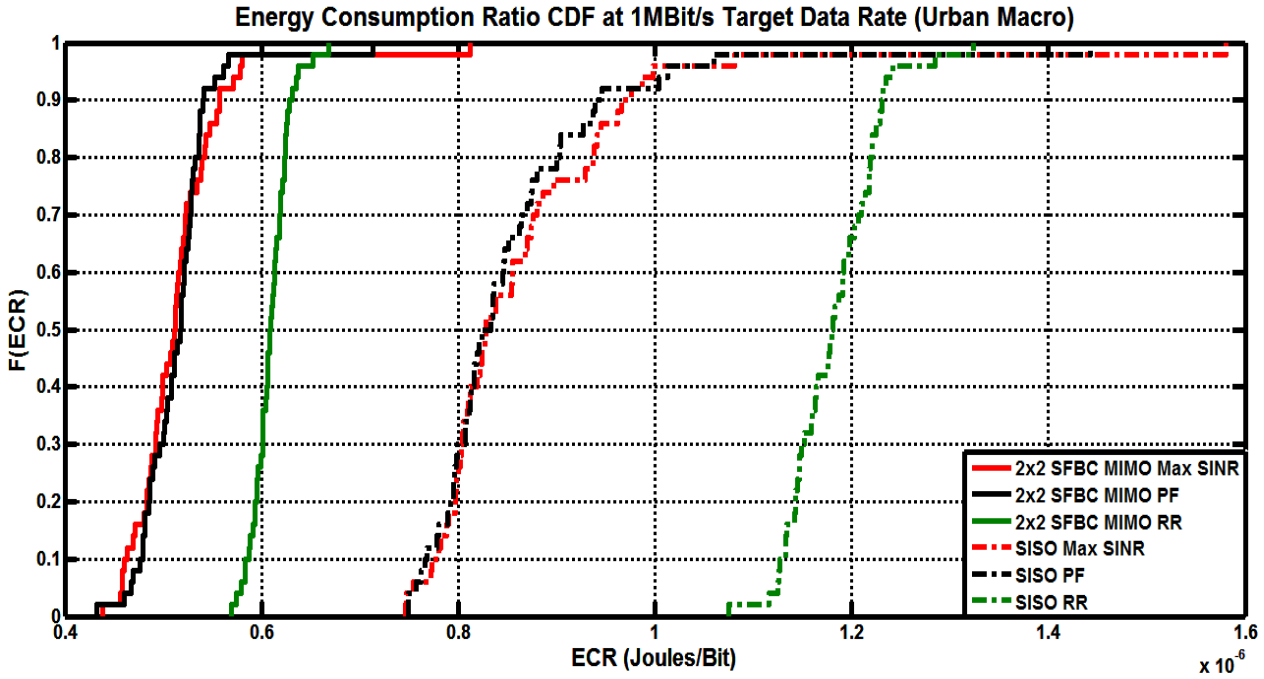

Figure 4. 4. Energy Consumption Ratio CDF **(Urban Macro)**

The results in both Figure 4.3 and Figure 4.4, exhibited the following features of interest:

- SFBC MIMO improved the RF energy efficiency performance of all the frequency domain packet schedulers both in the urban micro and urban macro scenarios. The improved energy performance is attributed to the fact that SFBC MIMO improves the user SINR. Improved SINR values enable link adaptation to select higher order modulation and coding schemes hence more bits can be loaded onto the physical resource blocks. Since the ECR metric is inversely proportional to the number of transmitted bits, improved SINR values yield smaller ECR measurements.
- The RF energy efficiency performance improvements of SFBC MIMO over SISO were more pronounced in the urban macro cell environment. This is attributed to fact that users in a macro cell are more susceptible to experiencing poor channel conditions resulting from comparably larger propagation distances than those characteristic of micro cells. Consequently the much needed channel quality improvements in a macro cell environment yield more transmission data rate improvements and hence more energy efficiency improvements than in a micro cell environment.

4.4.2. User QoS Results

Figure 4.5 and Figure 4.6 present the user QoS performance of the frequency domain packet schedulers for the Urban Micro and Urban Macro network scenarios respectively. In this study user QoS performance of the packet schedulers was measured as a percentage of scheduled users together with their associated realised user data rates.

From Figure 4.5 for SFBC MIMO, the Max SINR, Proportional Fair and Round Robin schedulers scheduled 98%, 98% and 99% of the users at data rates of 1, 1 and 0.89Mbit/s, respectively. For SISO, the Max SINR, Proportional Fair and Round Robin schedulers scheduled 92%, 91% and 99% of the users at data rates of 1, 1 and 0.75Mbit/s, respectively.

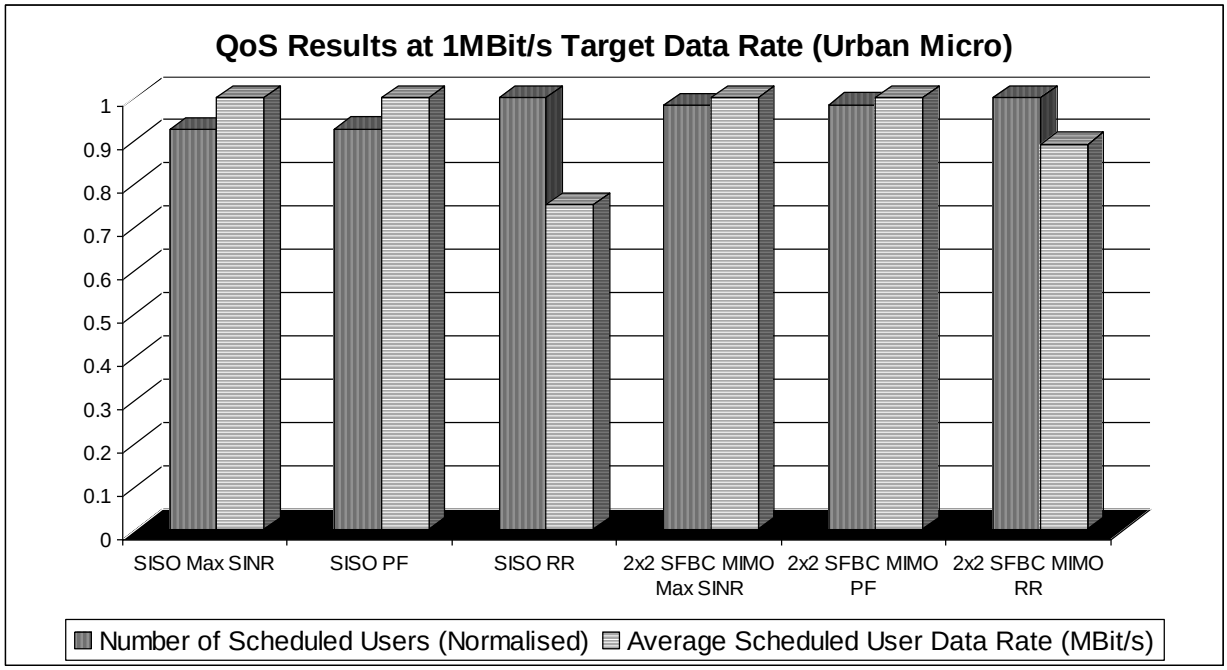

Figure 4. 5. User Quality of Service (Urban Micro)

From Figure 4.6 for SFBC MIMO, the Max SINR, Proportional Fair and Round Robin schedulers scheduled 90%, 91% and 99% of the users at data rates of 0.98, 0.98 and 0.74Mbit/s, respectively. For SISO, the Max SINR, Proportional Fair and Round Robin schedulers scheduled 63%, 65% and 99% of the users at data rates of 0.98, 0.98 and 0.52Mbit/s, respectively.

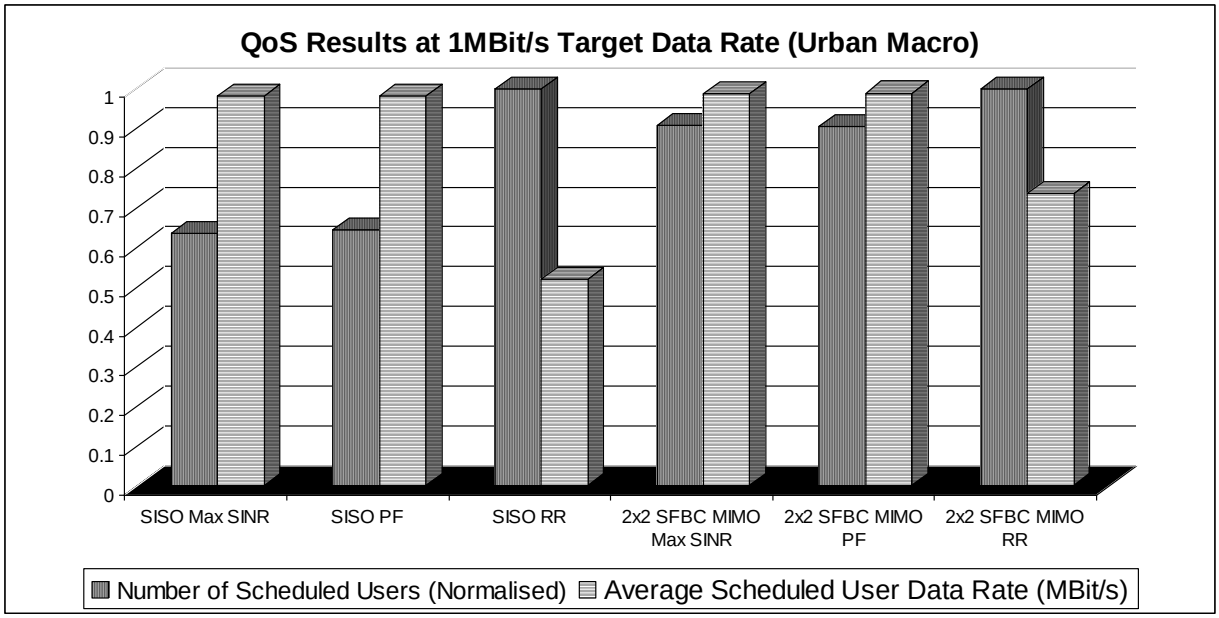

Figure 4. 6. User Quality of Service (Urban Macro)

SFBC MIMO improved the user QoS performance of all the frequency domain packet schedulers both in the urban micro and urban macro scenarios. The SFBC MIMO user QoS performance improvements are due to the efficient utilisation of the available physical resource blocks resulting from the improved SINR performance.

From Shannon's capacity formula , the improved user channel quality derived from SFBC MMIO translates into increased data rates and hence the packet scheduler can schedule more users thus improving their quality of service experience.

4.4.3. Spectral Efficiency Results

Figure 4.7 and Figure 4.8 present the spectral efficiency performance of the frequency domain packet schedulers for the Urban Micro and Urban Macro network scenarios respectively.

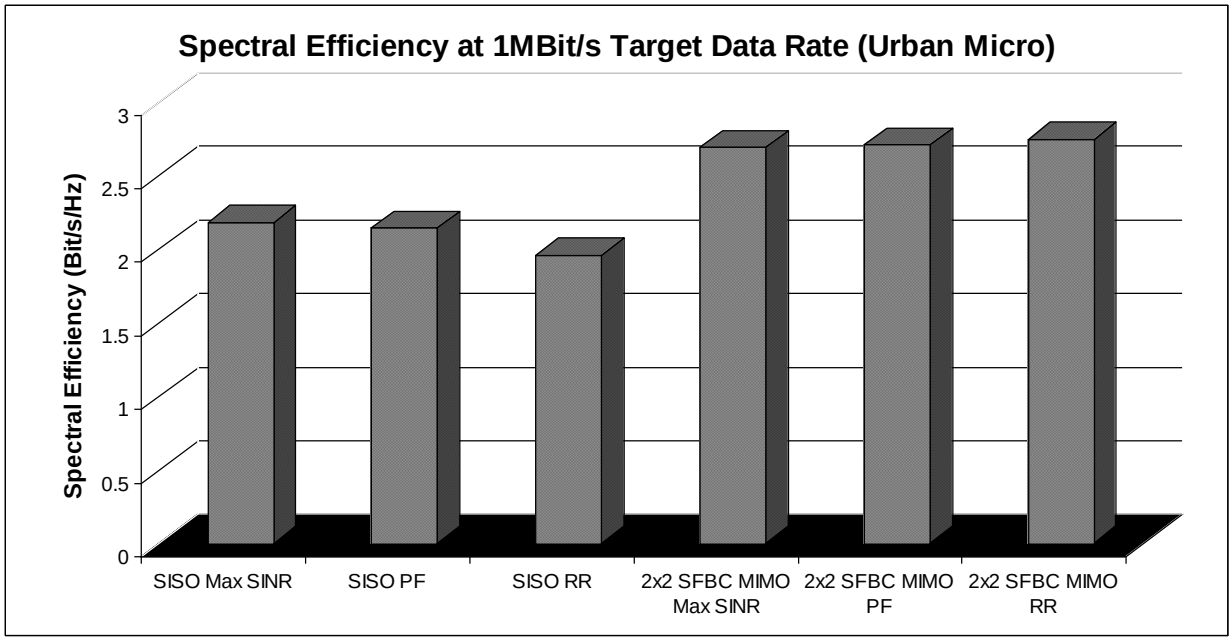

Figure 4. 7. Spectral Efficiency (Urban Micro)

SFBC MIMO improved the spectral efficiency performance of all the frequency domain packet schedulers both in the urban micro and urban macro scenarios. The SFBC MIMO spectral efficiency performance improvements are due to the improved user channel quality.

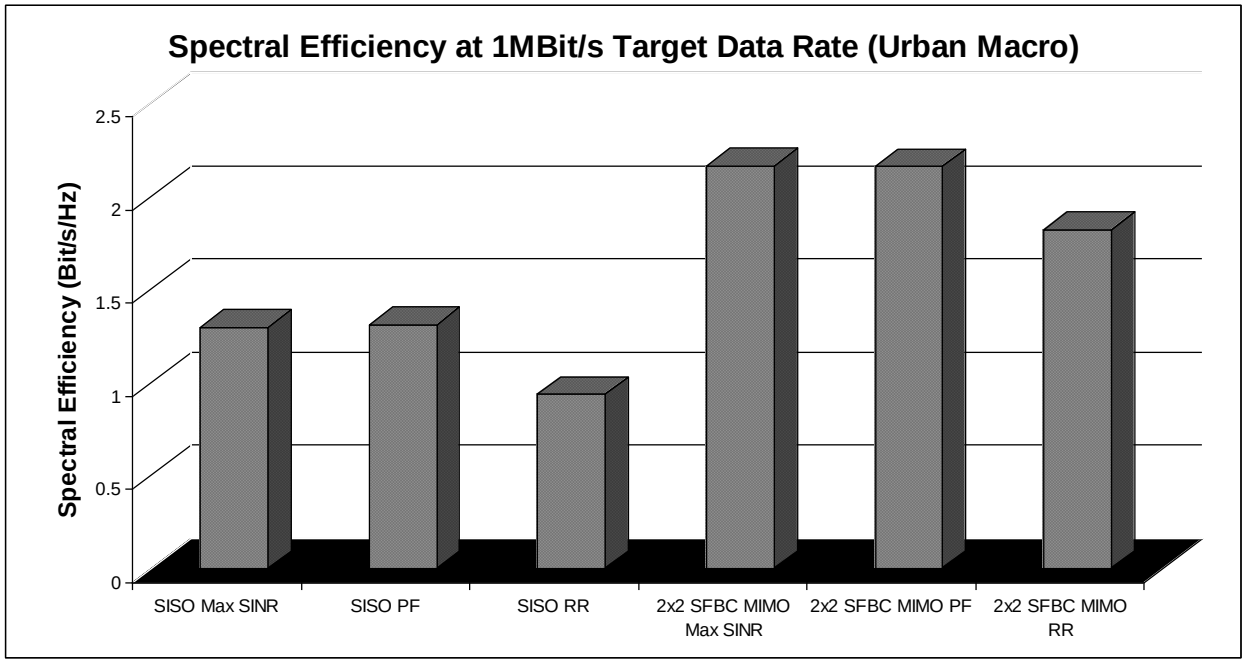

Figure 4. 8. Spectral Efficiency (Urban Macro)

4.5. Summary of Results

This chapter presented an RF energy efficiency, spectral efficiency and user QoS performance comparison between SISO and 2x2 Alamouti SFBC in an Urban Macro and an Urban Micro environment.

First, it was shown that SFBC MIMO improved the RF energy efficiency performance of all the frequency domain packet schedulers in both the urban micro and urban macro scenarios. However, the RF energy efficiency of SFBC MIMO is achieved at the cost of installing multiple antennas at both the eNB and the UE.

Second, it was shown that SFBC MIMO improved the user QoS and spectral efficiency performance of all the frequency domain packet schedulers in both the urban micro and urban macro scenarios.

The SFBC MIMO performance improvements are derived from the fact that SFBC MIMO improves the user SINR. Improved SINR values enable link adaptation to select higher order modulation and coding schemes hence more bits can be loaded onto the physical resource blocks.

It is worth noting that despite the MIMO RF energy efficiency improvements, the overhead energy consumption attributed to multiple radio heads makes MIMO less attractive as an energy efficient solution. However, one could argue that MIMO improves the user channel quality and hence the data rates, ECR and QoS performance at the RF level. This improved performance could be leveraged by increasing the inter site distance between base stations consequently reducing the density of base stations in any given geographical area thus reducing the energy consumption of the radio access network as a whole.

CHAPTER 5 **: LTE DOWNLINK PACKET SCHEDULING USING A NOVEL PROPORTIONAL FAIR ENERGY POLICY**

Chapters 3 and 4 revealed a dependency of packet scheduler energy efficiency on the channel quality experienced by the users in the system. For instance, chapter 3 demonstrated that packet schedulers such as the maximum Signal to Interference Noise Ratio (SINR) scheduler, that utilised the user channel quality, were more energy efficient than channel quality ignorant packet schedulers such as the round robin scheduler. Furthermore, chapter 4 demonstrated that multiple antennas techniques, that improved the user channel quality, also improved the RF energy efficiency performance of the packet schedulers.

This chapter addresses the challenge of producing energy efficiency improvements in a radio access network when the channel quality cannot be improved. To this end, the following approach was proposed and evaluated.

First, a new energy consumption aware Time Domain Packet Scheduling policy, that incorporates the temporal dynamic user energy performance in its prioritization metric, was presented. The proposed Proportional Fair Energy Consumption Ratio (PF-ECR) scheduler utilizes the users' cumulative past average ECR and/or the users' instantaneous ECR to assign different scheduling priorities to the users. The proposed PF-ECR metric strives to maintain a balance between two competing interests, namely; prioritizing inner cell users results in less PRBs being allocated and hence less RF power and energy expended however, this comes at the expense of cell edge user service experience. On the other hand prioritizing cell edge users improves their service experience at the expense of energy efficiency in that more PRBs are utilized thus more RF power and energy is expended. The proposed PF-ECR scheduler is equally applicable at both low and high offered loads conditions.

Second, an RF energy optimization algorithm was introduced to complement the Time Domain Packet Scheduler. The algorithm exploits the sub-carrier domain to enhance the PF-

ECR Scheduler energy performance. The energy optimization algorithm is based on the concept of a variable power allocation for each assigned sub-carrier and constitutes two stages, namely: a Lower Order Modulation Assignment stage and a Power Reduction stage.

The new energy aware packet scheduling criteria is compared against the established throughput based proportional fair scheduler with uniform power allocation and is shown to produce 20% Energy Reduction Gains (ERG) without compromising the spectral efficiency and QoS performance.

The chapter is structured as follows; Section 5.1 presents a brief review of some research activity pertaining to energy aware packet schedulers. Section 5.2 discusses the proposed packet-scheduling model. Section 5.3 describes the system model. Section 5.4 presents the performance results and analysis. Section 5.5 concludes the chapter with a summary of the key results.

5.1. Review of Energy Efficient Packet Scheduling

The energy efficiency of packet schedulers for the LTE downlink has not been investigated comprehensively with only a few works on the subject found in the public domain literature. The authors in [56] proposed the introduction of small delays in LTE uplink transmissions and showed that the power savings achieved could enhance the battery life of mobile devices. The authors in [57] and [58] presented an energy performance evaluation of the state-of-the-art packet scheduling protocols for the LTE downlink. In [59] it was shown that multiple antenna techniques, particularly Space Frequency Block Coding (SFBC), mitigated the effects of Inter-Cell Interference thus improving the LTE downlink energy performance of the packet schedulers. However, the studies [56-59] fail to address the issue of how packet scheduling could be exploited to improve energy efficiency. The most popular solution proposed for energy efficient scheduling is the discontinuous reception and/or transmission approach also

referred to as the sleep mode operation. The numerous variants of the sleep mode operation [60-63] generally involve deferring transmission and/ or reception for a given time, particularly under low load conditions, in order to achieve a power or energy saving. However, the energy saving is achieved at the expense of the inherent introduction of additional delay to some traffic flows. In [64] a Bandwidth Expansion Mode (BEM) technique was proposed that allocates more low power physical resource blocks (PRBs) to users under low load conditions hence reducing the energy consumption of the E-UTRAN. It should be noted that both the sleep mode operation approach and the BEM technique fail to produce energy savings under high load conditions.

5.2. Packet Scheduling Model

The packet scheduler was decoupled into three independent stages with the Time Domain Packet Scheduler (TD-PS) as the first stage, the Frequency Domain Packet Scheduler (FD-PS) as the second stage and the new sub-carrier energy optimisation algorithm as the third stage as depicted in Figure 5.1.

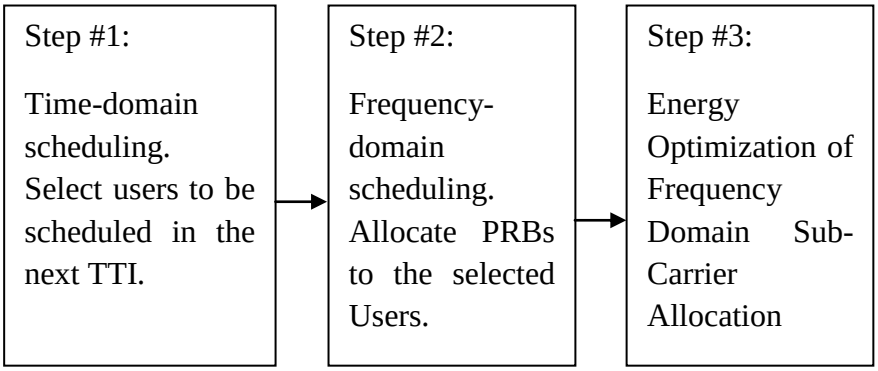

Figure 5. 1. Decoupled TD-PS, FD-PS and Energy Optimisation

5.2.1. Time Domain Packet Scheduler (TD-PS)

The TD-PS selects users to be scheduled in the next Transmission Time Interval (TTI) and passes the candidate selection list (CSL) to the FD-PS. The CSL is obtained by ranking all the users according to the TD-PS policy. The following TD-PS metrics were considered.

5.2.1.1. Proportional Fair Energy Consumption Ratio (PF-ECR)

$$M[n] = \frac{ECR[n]}{\overline{ECR[n]}}, \tag{5.1}$$

$M[n]$is the time domain scheduling priority metric for user *n*. $ECR[n]$is the wideband RF ECR estimated by link adaptation under the assumption that a user is allocated all the resource blocks. $\overline{ECR[n]}$ is the cumulative past average wideband RF ECR of user *n*.

5.2.1.2. Blind Proportional Fair Energy Consumption Ratio (BPF-ECR)

$$M[n] = \frac{1}{\overline{ECR[n]}}, \tag{5.2}$$

$M[n]$is the time domain scheduling priority metric for user *n*. $\overline{ECR[n]}$is the cumulative past average wideband RF ECR of user *n*. It is worth noting that the TD-BPF-ECR scheduler does not require instantaneous user energy consumption information and is thus simpler to implement compared to the TD-PF-ECR scheduler.

5.2.1.3. Time Domain Proportional Fair Throughput (TD-PF-Throughput)

$$M[n] = \frac{D[n]}{R[n]}, \tag{5.3}$$

$M[n]$ is the time domain scheduling priority metric for user *n*, $D[n]$is the wideband throughput estimated by link adaptation and $R[n]$is the past average throughput of user *n*

calculated with exponential average filtering. In this study, the TD-PF Throughput scheduler was used as the benchmark for packet scheduler comparison.

5.2.2. Frequency Domain Packet Scheduler (FD-PS)

The FD-PS allocates PRBs to users in the CSL provided by the TD-PS. The PRB allocation is carried out based on the concept of localized resource allocation whereby an entire PRB is assigned to a single user. In order to fully exploit the good channels, this study only considered the maximum Signal to Interference Noise Ratio (SINR) scheduler for the frequency domain.

5.2.3. Energy Optimisation of Subcarrier Allocation

The RF energy optimisation of the sub-carrier allocation can be broken down into two stages, namely: a Lower Order Modulation Assignment stage and a Power Reduction stage.

- Lower Order Modulation Assignment

  It is well known that lower order modulation and coding schemes (MCSs) require less transmit power compared to higher order MCSs. The lower order modulation assignment stage takes the PRB allocation performed by the FD-PS and re-distributes the MCS assignment per sub-carrier with a bias towards lower order MCSs without compromising the amount of data that should be carried by the PRB. Equation 5.4 provides the necessary condition for the lower order modulation assignment stage to be energy efficient.

$$\beta = \frac{D_i}{C_i} < 1, \tag{5.4}$$

  Where D_i is the amount of data to be transmitted on PRB i at a particular TTI instant and C_i is the data capacity of PRB i at a particular TTI instant. If this condition is not fulfilled the lower order modulation assignment stage will allocate the same MCS levels to the sub-carriers as the FD-PS.

for $i = 1$ to Number of RBs (N)
if PRB_i is not assigned by the FD-PS
continue;
else
Initialise: $D_i = I_{i,n}$
Initialise: $N_i = 0$
Initialise: $\Phi = 0$
while $N_i < D_i$
for $j = 1$ to Number of Sub-Carriers (12)
$\Phi_{i,j} = 0$
if $MAX\_\Phi_{i,j} \geq \Phi$
$\Phi_{i,j} = \Phi$
else
$\Phi_{i,j} = MAX\_\Phi_{i,j}$
end if
$N_i = N_i + f(\Phi_{i,j})$
end for
if $N_i \geq D_i$
break
else
$\Phi = \Phi + 1$
$N_i = 0$
end if
end while
end if
end for

Figure 5. 2. Algorithm for the Lower Order Modulation Assignment

Figure 5.2 presents the Lower Order Modulation Assignment algorithm. Where PRB_i is PRB i, D_i is the amount of data to be transmitted on PRB i, $I_{i,n}$ is the bits of user n that is assigned to PRB i by the FD-PS, N_i is the new data computation based on the new PRB sub-subcarrier

MCS level assignment, Φ is the MCS level as defined in Table 5.1 with $\Phi = 0$ representing QPSK 1/3 and $\Phi = 26$ representing 64 QAM 6/7. $\Phi_{i,j}$ is the MCS level assignment for sub-carrier j of PRB i and $MAX\_\Phi_{i,j}$ is the highest MCS level that sub-carrier j on PRB i can support at a particular TTI instant. The Lower Order Modulation Assignment algorithm is broken down into the following steps.

Step 1: Initialise the new PRB sub-subcarrier MCS level assignment to the lowest MCS level $\Phi = 0$.Step 2: For each sub-carrier check if the new PRB sub-subcarrier MCS level can be supported by the sub-carrier. If the sub-carrier cannot support the new PRB sub-subcarrier MCS level then the sub-carrier is assigned the highest MCS level it can support. If the sub-carrier can support the new PRB sub-subcarrier MCS level then the sub-carrier is assigned the new PRB sub-subcarrier MCS level. Step 3: Using all the sub-carriers within a PRB compute the new data that can be transmitted on the PRB given the new PRB sub-subcarrier MCS level assignment. If the new data is less than the user data that should be transmitted on that PRB, then the new PRB sub-subcarrier MCS level is increased by 1 and steps 2 and 3 are repeated. If the new data is greater than or equal to the user data that should be transmitted on that PRB, then the current PRB sub-subcarrier MCS level assignment is maintained.Step 4: Repeat steps 1, 2, and 3 for all PRB allocated by the FD-PS.

Power Reduction StageOnce the MCS level assignment for every allocated sub-carrier is finalised, the power reduction stage reduces the transmit power to the lowest permissible transmit power that can support the assigned MCS. For each allocated sub-carrier the transmit power per sub-carrier is reduced by a factor α.

$$\alpha = \frac{\gamma_2}{\gamma_1}, \tag{5.5}$$

γ_1 is the realised SINR in the prevailing channel conditions and γ_2 the minimum SINR required to support the particular MCS. The power reduction and hence, the energy reduction can be represented as.

$$Enery\ Reduction = P \times T \times \left(\sum_{i=1}^{Q} \sum_{j=1}^{M} \propto_{i,j} \right), \tag{5.6}$$

where j is the sub-carrier index and M is the number of sub-carriers per PRB. i is the PRB index and Q is the number of allocated PRBs which is a subset of the total number of system PRBs. P is the transmit power per sub-carrier and T=1ms is the duration of one TTI.

Table 5.1. Modulation and Coding Lookup Table 20 MHz (Urban Macro SISO)			
MCS	SINR values	Rate (Mbit/s)	**MCS Level(Φ)**
QPSK, 1/3	-4.06	0.35	0
	-2.06	1.98	1
	-0.06	5.60	2
	1.94	9.21	3
	3.70	10.81	4
QPSK, 1/2	4.70	13.00	5
	5.70	15.10	6
16QAM, 1/3	6.95	18.70	7
	8.95	21.63	8
16QAM, 1/2	10.71	29.06	9
	12.71	32.71	10
	13.65	33.10	11
16QAM, 3/4	14.47	33.88	12
	15.07	41.20	13
64QAM, 3/5	15.26	43.09	14
	17.26	55.70	15
	19.26	59.84	16
	20.10	60.40	17
64QAM, 3/4	22.23	71.82	18
	24.23	74.66	19
	26.23	75.60	20
	27.60	75.60	21
64QAM, 6/7	28.81	79.49	22
	30.81	83.33	23
	32.81	85.23	24
	34.81	85.67	25
	36.81	86.40	26

5.3. System Model

An LTE simulator was developed in MATLAB to evaluate the E-UTRAN downlink Radio Head Energy Consumption Ratio (RH-ECR), spectral efficiency and user QoS for various packet schedulers in a multi-cell multi-user system model. Communication between the evolved Node B (eNB) and the user equipments (UEs) was based on the single input single output (SISO) criteria.

The location coordinates of the UEs were randomly assigned following a uniform distribution while the location coordinates of the eNBs were fixed. In addition, each UE experienced Inter-Cell Interference (ICI) from the neighbouring cells. The path loss and the multipath fading were computed from the WINNER II Urban Macro channel models.

The packet scheduler interacts with the Admission Control (AC), Channel Quality Indication Manager (CQI), and Link Adaptation (LA). CQI calculates the average Signal to Interference Noise Ratio (SINR) of each user on every sub-carrier. LA selects the MCS based on the SINR (see Table 5.1). AC selects the users to be passed to the packet scheduler. The main simulation parameters are detailed in Table 5.2.

5.3.1. Energy Metrics

Equation (5.7), computes the RH-ECR for one eNB, where E^{RH} is the RH energy required to deliver M application bits, P_j^{RF} is the RF transmit power on sub-carrier j and Z is the total number of utilised sub-carriers, T is the TTI and $f(SINR[n,j])$ is the LA function (of Table 5.1) which determines the MCS and hence the number of bits that can be transmitted on sub-carrier j by scheduled user n.

$$ECR^{RH} = \frac{E^{RH}}{M} = \frac{\frac{T}{\mu_\epsilon}\sum_{j=1}^{Z} P_j^{RF}}{\sum_{j=1}^{Z} f(SINR[n,j])}, \tag{5.7}$$

Table 5.2. Simulation Parameters and Model Assumptions	
Parameter	**Setting**
System Bandwidth	20 MHz
Cellular Layout	Hexagonal grid, 19 Cells
Cell Site Radius	1000m Macro cell
Maximum Transmit Power	20 Watts
Number of Users (UEs)	25 UEs per Cell
Downlink Transmission Band	2.11-2.17 GHz
Number of Resource Blocks	100
Path Loss Model	WINNER II Channel model (Urban Macro)
Multipath Fading Model	WINNER II Channel model (Urban Macro)
eNB Height	25m
UE Height	1.5 m
UE Antenna Gain	0 dB
Channel Estimation	Perfect
CQI delay	1 ms
Modulation and coding schemes	QPSK 1/3, 1/2, 3/4 & 16QAM 1/3, 1/2, 3/4 & 64QAM 3/5, 3/4, 6/7
EPS Bearer data amounts per TTI	1 Kbit[12]
μ_ϵ	0.25

[12] 1 Kbit per TTI translates to 1 MBit/s which is considered the acceptable minimum data rate required by a number of multimedia services.

5.4. Results and Analysis

The performance of the time domain packet schedulers was evaluated using the following measurands: Radio Head Energy Consumption Ratio (RH-ECR), spectral efficiency and User Quality of Service (QoS). The energy, spectral efficiency and user QoS performance of the time domain packet schedulers was explored by varying the time domain priority metric while keeping the frequency domain metric constant in an urban macro environment.

The eNB energy efficiency (ECR) is made up of the energy efficiency (ECR) of individual user transmissions at any TTI instant. The PF-Throughput criteria aims to schedule users such that on average each UE achieves the same throughput performance, however this implies that UEs that have poor channel conditions (cell edge UEs) may be prioritized in order to improve their throughput thus resulting in the eNB utilizing more PRBs hence higher RF transmit power and RH ECR. The eNB RH ECR will constitute both low and high RH ECR values resulting in a high average eNB RH ECR due to the skew resulting from high RH ECR values. The PF-ECR criteria aims to schedule UEs such that on average each UE exhibits the same ECR performance therefore the eNB RH ECR will constitute RH ECR values that are almost equal. This results in a lower average eNB RH ECR as there is no skew from high RH ECR values. In order to capture this effect this study divided the E-UTRAN into five regions as show by table 5.3.

Figure 5.3 presents the eNB RH-ECR variance/spread at different regions within the cell. From Figure 5.3, it was observed that the PF-Throughput scheduler had a higher RH-ECR variance compared to the PF-ECR scheduler particularly at the cell edge. This is due to the skew resulting from high RH ECR values. The PF-ECR scheduler 'smoothens' out these high RH ECR values by incorporating the temporal dynamic user ECR in its prioritization metric.

Table 5.3. Macro Cell Regions	
Region Index	Radius Range from Base Station
Region 1	0 metres and 200 metres
Region 2	200 metres and 400 metres
Region 3	400 metres and 600 metres
Region 4	600 metres and 800 metres
Region 5	800 metres and 1000 metres

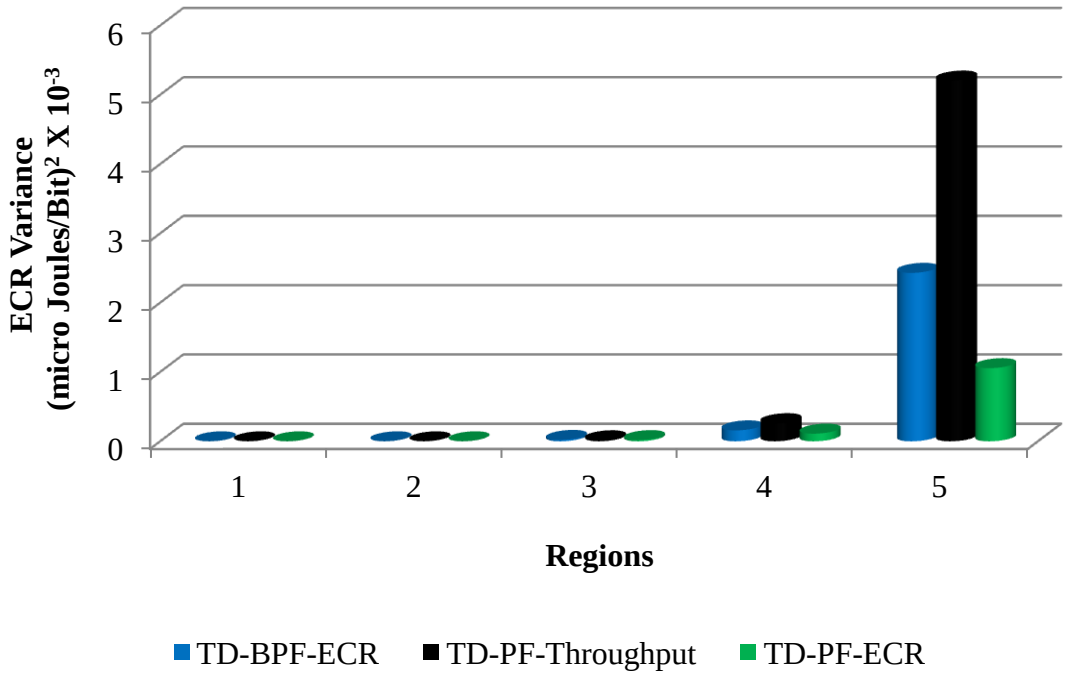

Figure 5. 3. ECR Variance for different cell regions

5.4.1. Energy Performance Results

Figure 5.4 presents the E-UTRAN RH-ECR comparison of the baseline TD-PF Throughput scheduler with uniform power allocation against the new TD-PF ECR and TD-BPF ECR scheduler with sub-carrier energy optimisation.

For each TTI, the E-UTRAN RH-ECR for the packet schedulers was computed as the average RH-ECR over all eNBs in the E-UTRAN. The energy comparison was performed using RH-ECR Cumulative Distribution Function (CDF) plots drawn from 10000 TTIs with the TD-PF-Throughput scheduler as the baseline. The new TD-PF ECR and TD-BPF ECR schedulers with sub-carrier energy optimisation produced median energy reduction gains of 20% and 18% respectively over the TD-PF Throughput scheduler with uniform power allocation. It is worth noting that the RH energy efficiency of the TD-BPF ECR scheduler is very close to that of the TD-PF ECR scheduler and yet it has lower implementation complexity, as the instantaneous user ECR is not required.

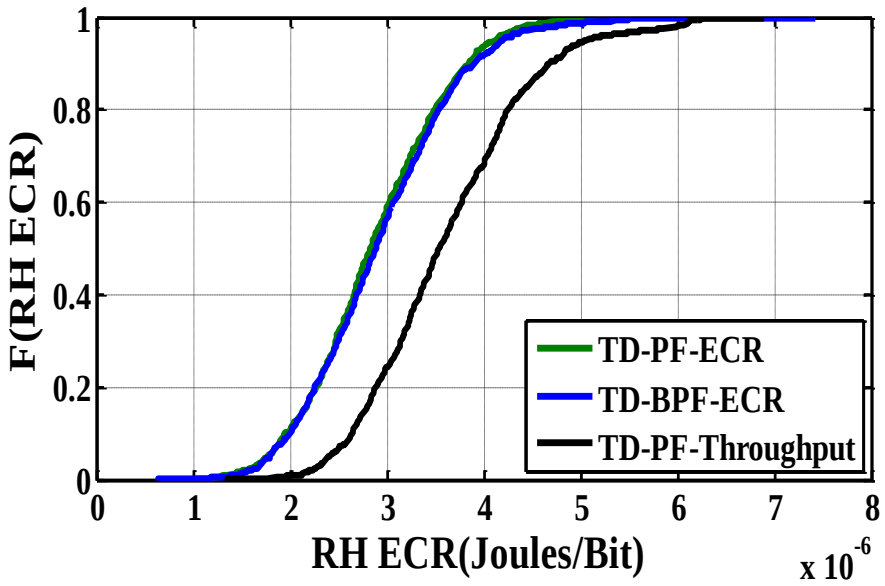

Figure 5. 4. RH-ECR CDF Comparing TD-PF Throughput against TD-PF ECR and TD-BPF ECR Schedulers

5.4.2. User QoS Results

The user QoS was defined as the average proportion users scheduled in a TTI and the achieved user data rate. Figure 5.5 presents the user QoS performance of the packet schedulers. It was observed that both the TD-BPF ECR and the TD-PF ECR schedulers with sub-carrier power/energy optimization achieved a user QoS performance similar to the baseline TD-PF Throughput scheduler with uniform power allocation of 0.2 $watts$ per PRB. i.e. all the users were scheduled and every user achieved the target data rate of 1Mbit/s.

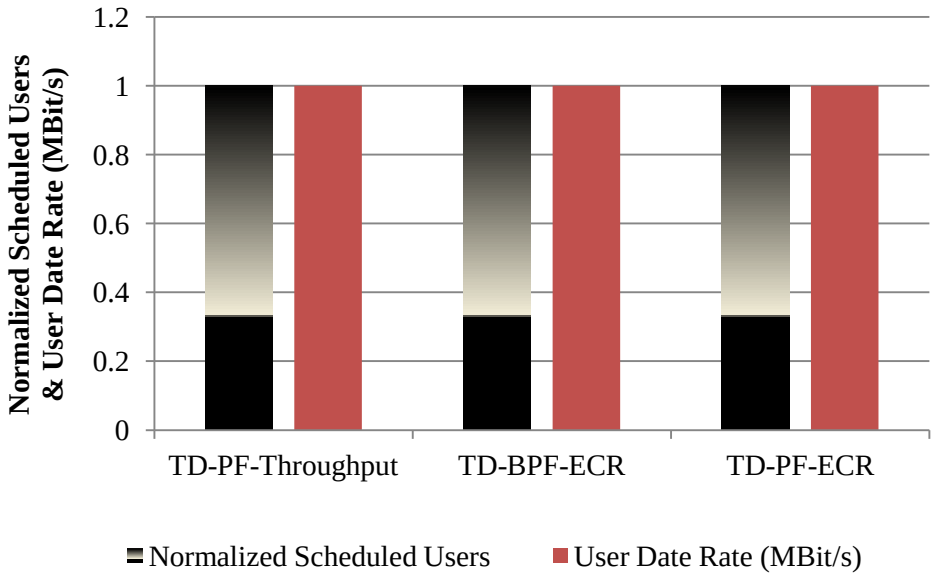

Figure 5. 5. User QoS Results

5.4.3. Spectral Efficiency Results

Both the TD-BPF ECR and the TD-PF ECR schedulers with sub-carrier energy optimization achieved a 95% percentile spectral efficiency, of 1.25 Bit/s/Hz, similar to the baseline TD-PF Throughput scheduler with uniform power allocation of 0.2 $watts$ per PRB.

5.5. Summary of Results

This chapter presented and evaluated a novel energy consumption aware Time Domain Packet Scheduler that incorporates the temporal dynamic user energy performance in its prioritization metric. The proposed Proportional Fair Energy Consumption Ratio (PF-ECR) scheduler utilizes the users' cumulative past average ECR and/or the users' instantaneous ECR to assign different scheduling priorities to the users. The PF-ECR criteria schedules users such that on average each user exhibits the same ECR performance therefore the eNB RH-ECR will constitute RH-ECR values that are almost equal. This results in a low average eNB RH-ECR as there is no skew from high RH ECR values.

Furthermore, a two-stage energy optimisation algorithm implemented on a sub-carrier level was presented to supplement the Time Domain Packet Scheduler. The energy optimisation algorithm is made up of a Lower Order Modulation Assignment stage and a Power Reduction stage. The Lower Order Modulation Assignment stage re-distributes the MCS assignment per sub-carrier with a bias towards lower order MCSs while ensuring that the users' QoS is not compromised. The Power Reduction stage reduces the transmit power to the lowest permissible transmit power that can support the assigned MCS.

Finally, the study showed that the new composite energy aware packet scheduling criteria produced Radio Head Energy Reduction Gains of 20% compared to the established throughput based proportional fair scheduler with uniform power allocation, without compromising the spectral efficiency performance and user QoS performance.

CHAPTER 6 **: ENERGY EFFICIENT CO-ORDINATED INTER CELL INTERFERENCE AVOIDANCE: A TWO PLAYER SEQUENTIAL GAME MODELLING FOR THE LTE DOWNLINK**

Chapter 5 explored the potential of producing energy efficiency improvements in a radio access network when the channel quality cannot be improved and demonstrated that energy aware packet scheduling metrics alone produced marginal energy reduction gains. From an energy efficient radio resource management perspective, this highlights the positive correlation between improvements in the user channel quality and energy efficiency of the radio access network developed in chapters 3 and 4.

The user channel quality is degraded by several factors such as, path loss, multipath distortion, noise and Inter-Cell Interference (ICI). In a multi-cell multi-user radio access network (RAN), ICI is a key limiting factor to the user channel quality and hence radio frequency (RF) energy performance. The channel quality of the cell edge users is greatly impaired by ICI owing to the fact that cell edge users are furthest away from their serving base stations (BSs) and closest to the interfering BSs. Consequently, the BS is compelled to allocate more PRBs to the cell edge users in order to meet their Quality of Service (QoS) targets.

Traditionally ICI management was carried out to improve the cell edge throughput performance while neglecting the potential energy efficiency attributes inherent to ICI mitigation techniques particularly under low to median loading conditions. As previously noted in chapter 2, the 3GPP LTE employs Orthogonal Frequency Division Multiple Access (OFDMA) as the multiple access scheme for down link transmissions [65]. From an interference management point of view the granularity of resource allocation in OFDMA makes it possible to estimate ICI thus providing opportunities to mitigate ICI on a sub-carrier basis.

This chapter introduces a novel Inter-Cell Interference (ICI) management technique that mitigates the effects of ICI through a sequential game play between cells in the E-UTRAN[13] based on the instantaneous cell offered load. The proposed technique was shown to produce greater user channel quality improvements of 4dBs greater than the state of the art ICI management techniques. The channel quality improvements derived there from result in a utilisation of less physical resource blocks (PRB[14]s), RF and radio head energy which translate to energy reduction gains of 34% and 45% at low and high offered loads respectively. In addition, the proposed scheme does not require a central processing entity such as a radio network controller (RNC) and can be implemented in unplanned self-organising networks.

The chapter is structured as follows; Section 6.1 discusses the research contribution. Section 6.2 presents a review of the State-of-the-Art interference avoidance techniques. Section 6.3 describes the Sequential Game Coordinated Radio Resource Management (SGC/RRM) algorithm. Section 6.4 describes the system model and the Layer 2 packet-scheduling model considered. Section 6.5 defines the performance metrics utilised. Section 6.6 presents the performance results and analysis. Section 6.7 concludes the chapter with a summary of the key results.

6.1. Research Contribution

The third generation partnership project (3GPP) standard for LTE [66] defines an X2 interface to facilitate communication between evolved NodeBs[15] (eNBs). The 3GPP standard provides the framework for the exchange of load information among the eNBs with the objective of interference coordination and load balancing, however the standard doesn't explicitly detail how the exchanged load information can be utilised to mitigate ICI. This

[13] E-UTRAN: Evolved Universal Mobile Telecommunications Systems (UMTS) terrestrial radio access network (UTRAN)

[14] In LTE a physical resource block (PRB) spans 12 sub-carriers each with a bandwidth of 15KHz over a 0.5 ms time slot

[15] evolved NodeB is the LTE terminology for a base station.

chapter presents a novel Sequential Game Coordinated Radio Resource Management (SGC/RRM) algorithm that employs the principles of game theory to dynamically mitigate the effects of ICI in the E-UTRAN.

In recent years, a number of game theory based solutions have been proposed to solve numerous problems associated with communication networks. The authors in [67] presented a game theoretical overview of dynamic spectrum sharing, in [68] coalition game theory was shown to improve user throughput, in [69] network formation games were shown to decrease the number of relay transmission hops, in [70] the game theoretic concept of Nash Bargaining Solutions (NBS) was proposed as a solution to the sub-carrier allocation problem, in [71] role game theory was applied to uplink power control, and in [72] a game theoretic analysis for load balancing was presented and shown to increase the capacity usage in a network.

Here, the SGC/RRM algorithm is implemented as a two player sequential game in which the game players (eNBs) communicate their instantaneous offered load information, via the X2 interface, and decide what transmission frequency band restrictions to adopt in order to mitigate ICI. The benefits of the proposed SGC/RRM algorithm include:

- Energy efficiency and cell site throughput improvement of the E-UTRAN as a result of channel quality improvements.
- The ability to mitigate ICI in unplanned or self-organising networks (SONs).
- Simplicity as no central processing entity, such as a RNC, is required to perform the ICI avoidance.

The SGC/RRM algorithm improves the user channel quality through an exchange of load information, via the X2 interface, between pairs of interfering eNBs and restricting transmission on particular frequency bands. The SGC/RRM improves the channel quality by 4dBs greater than the state-of-the-art ICI management techniques. The channel quality improvements produced energy reduction gains of 34% and 45% at low and high offered

loads respectively due to the fact that less PRBs and hence RF energy is required to transmit a given amount of data. Alternatively the channel quality improvements could be translated into throughput improvements e.g. in this study, at high offered loads, the SGC/RRM is shown to achieve a better cell site throughput performance when compared against Hard Frequency Reuse (HFR) factor 1. Since the LTE 3GPP standard supports self-configuration of the X2 interface, the SGC/RRM algorithm is able to mitigate ICI in unplanned SONs as it only requires an active X2 interface to implement transmission restrictions. Furthermore, the SGC/RRM algorithm does not require a central processing entity such as a RNC in order to perform the ICI avoidance since the transmission restrictions are imposed by the eNBs.

6.2. State-of-Art (SOA) Interference Avoidance Techniques

ICI mitigation techniques can be broadly categorised as follows; power control Techniques [73], Interference regeneration and cancellation techniques [74], multiple antenna techniques [75] and interference avoidance techniques. The focus of this study was interference avoidance as detailed below. Interference avoidance techniques can be grouped into three categories namely static ICI avoidance, semi static ICI avoidance and dynamic ICI avoidance.

6.2.1. Static ICI Avoidance Techniques

Static ICI avoidance techniques impose transmission restrictions that are fixed over a long period of time i.e. hours or days.

6.2.1.1. Hard Frequency Reuse

Traditionally, ICI avoidance has been implemented by dividing the available usable spectrum into sub sets of frequency bands and imposing the restriction that these frequency bands may

only be reused in cells that have a sufficiently large distance between them [13]. This frequency partitioning scheme results in a single reuse factor of say 1, 1/3 etc. Hard frequency reuse (HFR) improves the performance of the cell edge users at the expense of the total cell spectral efficiency since less of the available usable bandwidth is utilised for transmission. Figures 6.1 (f) and 6.1 (h) depict HFR factors of 1/3 and 1 respectively. Figure 6.1 (b) describes the colour mapping for a single cell site and is used to interpret the ICI avoidance diagrams in Figures 6.1 (c) to 6.1 (j). Considering Figure 6.1 (c) as an example, the transmission restrictions are as follows; cell 1 (blue) can only transmit on frequency bands F3, F4, F5, F6, F7 & F8, cell 2 (red) can only transmit on frequency bands F1, F2, F5, F6, F7 & F8, and cell 3 (black) can only transmit on frequency bands F1, F2, F3, F4, F7 & F8, with a transmit power of 0.2 watts per resource block. In Figure 6.1, power/RB is the uniform power allocation per resource block.

6.2.1.2. Fractional Frequency Reuse

In order to overcome the spectral efficiency drawbacks of HFR, the authors in [76] proposed a reuse partitioning approach in which the available usable spectrum is divided into two or more sub sets of frequency bands with each set of frequency bands corresponding to a different reuse factor. Each cell can operate multiple reuse factors with users of good channel quality allocated the frequency bands with a high reuse factor e.g. reuse 1 while users with poor channel quality are allocated the frequency bands with low reuse factors e.g. 1/3, as shown in Figure 6.1 (e). In recent years, the reuse partitioning approach has been revisited and renamed “Fractional Frequency Reuse (FFR)” by the authors in [77], [78] and [79]. The authors in [80] propose two ICI avoidance techniques with effective reuse factors of 3/4 and 5/8, Figure 6.1 (c) and Figure 6.1 (d) respectively, that are variants of the FFR concept. The authors in [81] present a static inverted frequency reuse concept, which reverses the

frequency band allocation restrictions of any hard frequency reuse scheme. Upon closer inspection of the static inverse reuse principle, it was observed that it is yet another variant of FFR, Figure 6.1 (g). Despite the spectral efficiency improvements exhibited by FFR, and variations thereof, over HFR schemes, the spectral efficiency performance of FFR is still less than that of HFR factor 1 as shown in [82] and [83]. This is due to the fact that the system throughput reduction as a result of bandwidth restriction can't be compensated by the channel quality improvements resulting from ICI avoidance.

6.2.1.3. Soft Frequency Reuse

In order to overcome the limitations of FFR the authors in [84] and [85] propose a Soft Frequency Reuse (SFR) approach in which the entire available usable spectrum is utilised but with selected sets of frequency bands having higher transmit power than others. Consider two sets of frequency bands one transmitting at a high power and the other at a lower power level, the high transmit power level is $P_{High} = \alpha P_{Low}$, $\alpha > 1$, and the lower transmit power level is $P_{Low} = \frac{Z\lambda}{(\alpha-1)\mu+Z}$, where μ is the number of high power frequencies, Z is the total number of frequencies in the system, α is the power factor, and λ is the uniform transmit power per frequency in HFR reuse 1. Figure 6.1 (i) presents SFR with a power factor of 2.

6.2.2. Semi-Static ICI Avoidance Techniques

Unlike static ICI avoidance techniques semi-static ICI avoidance techniques are implemented by altering the frequency and/or power restrictions imposed on the available usable spectrum in response to load and interference conditions in neighbouring cells. Consequently, a BS can incorporate all the static ICI avoidance approaches in a semi-static fashion. The benefit of semi-static ICI avoidance techniques is the ability of the BS to adapt the ICI avoidance technique in order to efficiently mitigate ICI under the prevailing load and interference

conditions, for example in [81] the static inverted reuse approach was implemented in a semi-static manner based on the unbalanced load conditions. However, the drawback of semi-static ICI avoidance is the requirement of a homogeneous planned network (e.g. macro only). Thus, semi-static and static ICI avoidance techniques are unable to predict and hence limit interference in heterogeneous unplanned networks.

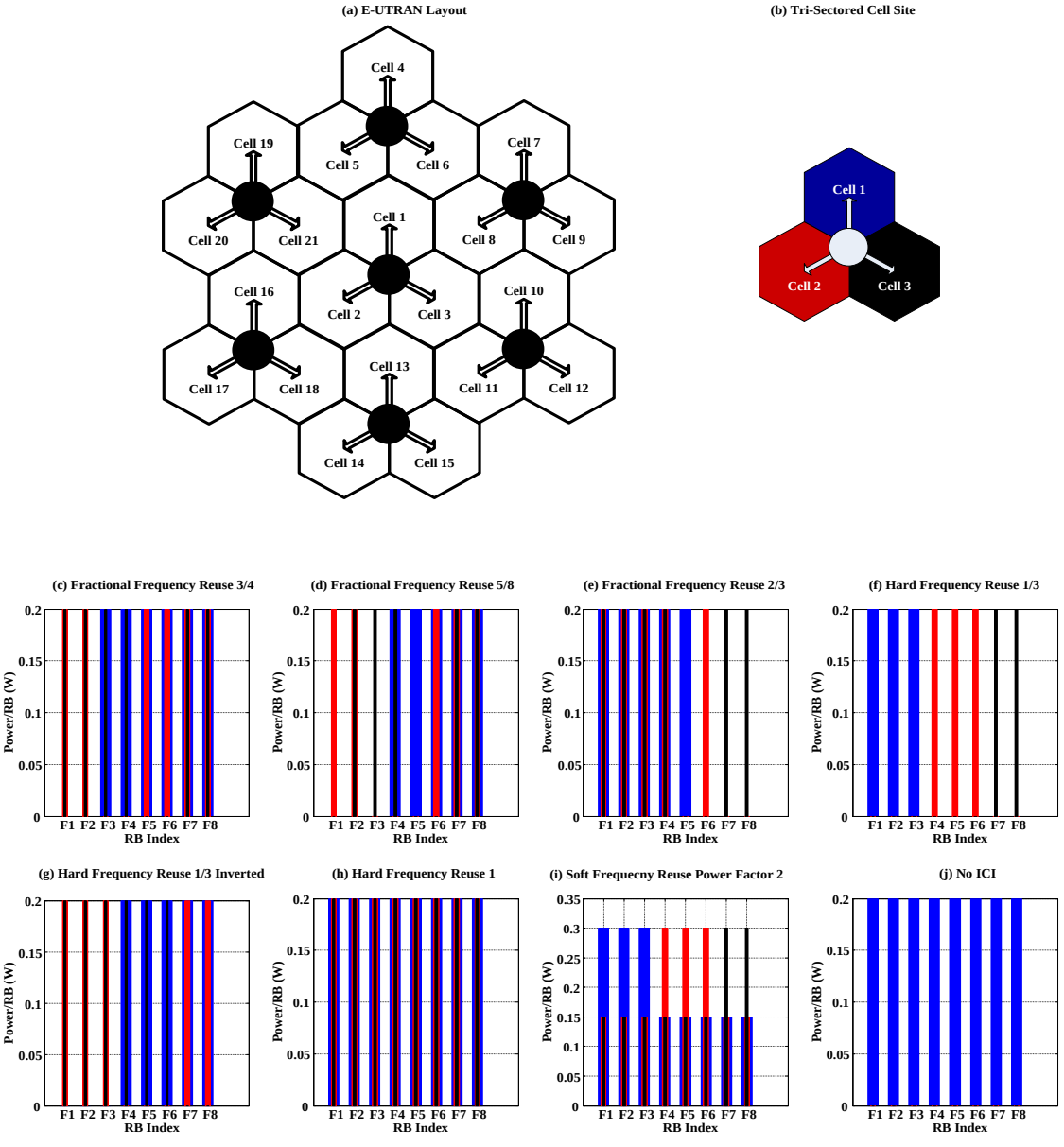

Figure 6. 1. E-UTRAN Layout and ICI Avoidance Techniques

6.2.3. Dynamic ICI Avoidance Techniques

Dynamic ICI avoidance approaches are not limited by frequency planning and can thus mitigate ICI as and when load and interference conditions vary in the E-UTRAN. The authors in [86], [87] and [88] proposed dynamic ICI avoidance approaches that generally involve users communicating their channel conditions, together with information about a group of dominant interferers, to their serving BSs. The serving BS computes the utility of each user and performs an initial resource assignment. This results in a conflict for resources by multiple users, therefore the BS forwards the initial resource assignments and the users' channel quality to a central processing entity/node connected to the BSs. The central processing entity/node performs conflict resolution and feeds back the resource allocations and restrictions to the BSs. The BSs in turn utilise this information to schedule their respective users. The dynamic ICI avoidance techniques proposed require a high level of signalling overhead and computational complexity. The computational complexity is implemented by a central processing entity/node, however, it should be noted that the E-UTRAN specification has no provision for a central processing entity/node such a Radio Network Controller (RNC). Dynamic ICI avoidance should therefore be implemented through an exchange of information between/among BSs without requiring a central processing entity/node.

6.3. Sequential Game Co-ordinated Radio Resource Management (SGC/RRM)

Game theory encompasses both simultaneous and sequential games and is widely used in the field of economics for strategic planning. Simultaneous games involve player(s) making strategic decisions independent of one another, while sequential games involve player(s) making decisions based on the decisions made by other player(s), in order to maximise or minimise some utility function. The motivation of the SGC/RRM algorithm is to exploit the communication between the eNBs, via the X2 interface, with a vision of exchanging instantaneous offered load information with the objective of reducing ICI thus reducing the required transmit power thereby reducing the energy consumption.

In this study, the SGC/RRM algorithm was defined as a dynamic radio resource allocation functionality modelled as a two player sequential game in which both players are independent cells. A two player sequential game generally involves the first player choosing a strategy and then the second player deciding what strategy to adopt based on the strategy of the first player. In a tri sectored E-UTRAN (Figure 6.1 (a)), each cell has primarily two dominant interferers, therefore imposing transmission restrictions on the dominant interferers will produce the most significant signal to interference noise ratio (SINR) improvements. It should, however, be noted that imposing transmission restrictions on both the dominant interfering cells could result in a compromise of the user service experience in those cells. In this study, the two player sequential game was played between a cell and one of its dominant interferers.

The E-UTRAN (Figure 6.1 (a)) was divided into cell pairs. The cells that could not be paired with a neighbouring interfering cell did not participate in the sequential game. Let N denote the set of all cells in the E-UTRAN, $N \in \{1,2,3,4,5,6,7,8,9,10,11,12,13,14,15,16,17,18,19,20,21\}$. The sets of cell pairs are; $\Phi_1 = \{1,8\}$ $\Phi_2 = \{2,21\}$ $\Phi_3 = \{3,13\}$ $\Phi_4 = \{5,19\}$ $\Phi_5 = \{6,7\}$ $\Phi_6 = \{9,10\}$ $\Phi_7 = \{11,15\}$

$\Phi_8 = \{14,18\}$ and $\Phi_9 = \{16,20\}$. The set of cells that didn't participate in the sequential game is; $\Phi_{10} = \{4,12,17\}$. In this study, the relevant performance statistics were taken from the centre cell site constituting cells 1, 2, and 3.

6.3.1. Player Status Assignment (PSA)

Consider a single pair of cells, PSA determines the principal player cell and the agent player cell. PSA was formulated as follows:

Maximise:

$$\sum_{k \in \Phi_j} L_k(1 - \beta_k), \tag{6.1}$$

subject to

$$\sum_{k \in \Phi_j} \beta_k \leq 1, \tag{6.2}$$

where k is the cell index, L_k is the offered load (Mbit/s) of cell k, Φ_j is a cell pair set and j is the cell pair index, since there are only nine cell pairs $j \in \{1,2,3,4,5,6,7,8,9\}$. β_k are binary values, $\beta_k \in \{0,1\}$, which represent the PSA. The value of β_k is 1 if cell k is the agent player and 0 if cell k is the principal player.

6.3.2. Game Strategy Definition

The game strategy of each player (principal or agent) defines the choice of transmission frequency bands and the associated maximum transmit power. The transmission frequency band strategy set (S^{Freq}) for both the principal player and the agent player was carefully chosen to adhere to the possible LTE bandwidth utilisation specifications i.e. 1.4, 3, 5, 10, 15 and 20 MHz. (S^{Freq}) is defined as;

$$S^{Freq} = \{Idle, VLow, Low, MediumL, MediumH, High, VHigh\}, \tag{6.3}$$

with an associated maximum transmission power strategy set of;

$$S^{Power} = \{0, 1.2, 3, 5, 10, 15, 20\}, watts \quad (6.4)$$

Considering a maximum LTE transmission bandwidth of 20MHz, Figure 6.2 (a) presents the SGC/RRM algorithm definition of the individual player/cell strategies. Players/cells that did not participate in the SGC/RRM algorithm were assumed to be transmitting with a very high transmission frequency strategy($S^{Freq} = VHigh$), i.e. utilising the whole 20 MHz bandwidth. Furthermore, the individual strategies of the principal player and the agent player were designed to avoid interference between the players.

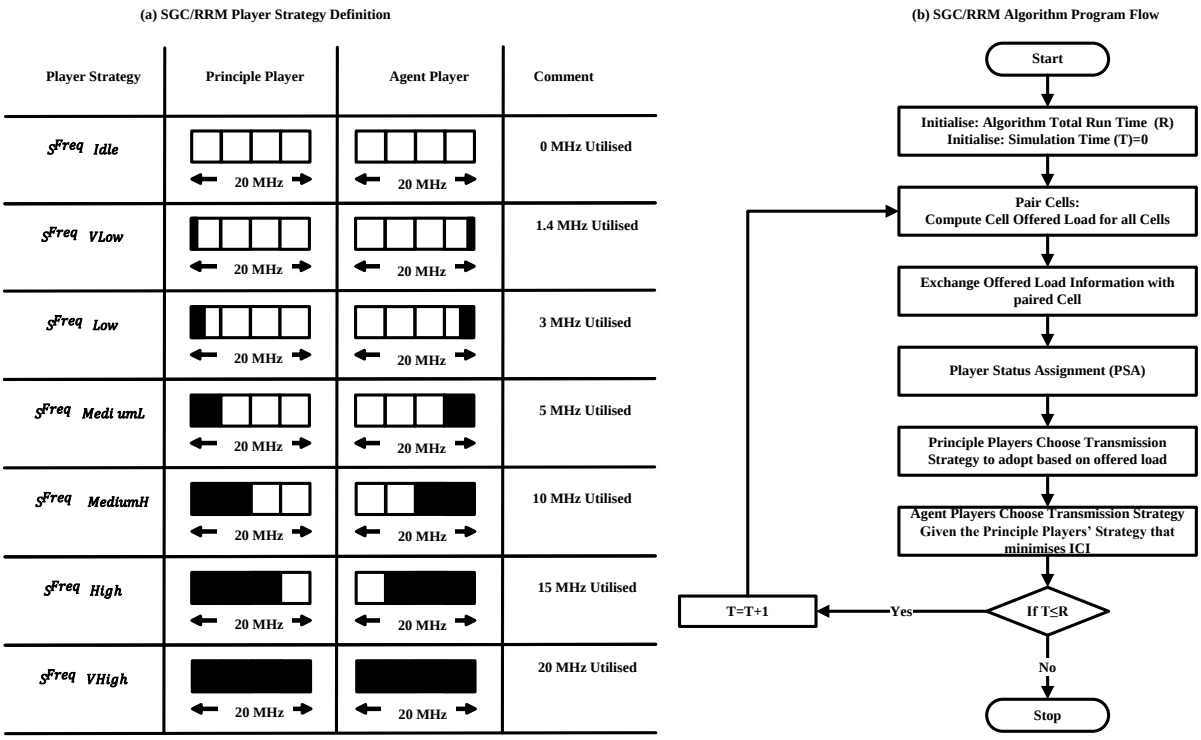

Figure 6. 2. SGC/RRM Algorithm (a) Player Strategy Definition and (b) Program Flow

6.3.3. Player Inter-Cell Interference (ICI) Rank Measurement

The player/cell ICI rank measurement (R_k) is a classification of the amount of interference to cell k due to the second paired player/cell participating in the SGC/RRM algorithm. Considering a couple of players/cells participating in the SGC/RRM algorithm, the ICI rank of each player is a function of the transmission frequency strategies adopted by both the principal ($S_{Principal}^{Freq}$) and agent (S_{Agent}^{Freq}) players.

$$R_k = f\left(S_{Principal}^{Freq}, S_{Agent}^{Freq}\right), k \in \{Principal, Agent\}, \quad (6.5)$$

$S_{Principal}^{Freq}$ and S_{Agent}^{Freq} are the transmission frequency strategies of principal and agent players respectively, defined in equation (6.3). Higher ICI rank values represent greater ICI between the players Thus the ICI rank R_k is proportional to the number of interfering frequency bands. In this study, the constant of proportionality was chosen as unity.

$$R_k = F, \quad k \in \{Principal, Agent\} \quad (6.6)$$

F is the number of interfering frequency bands in MHz.

Table 6.1 details the ICI rank payoff matrix for all possible transmission strategies by both the principal and agent player.

Table 6.1 ICI Rank Pay Off Matrix

Principal \ Agent	$S^{Freq}(Idle)$		$S^{Freq}(VLow)$		$S^{Freq}(Low)$		$S^{Freq}(MediumL)$		$S^{Freq}(MediumH)$		$S^{Freq}(High)$		$S^{Freq}(VHigh)$	
$S^{Freq}(Idle)$	0	0	0	0	0	0	0	0	0	0	0	0	0	0
$S^{Freq}(VLow)$	0	0	0	0	0	0	0	0	0	0	0	0	1.4	1.4
$S^{Freq}(Low)$	0	0	0	0	0	0	0	0	0	0	0	0	3	3
$S^{Freq}(MediumL)$	0	0	0	0	0	0	0	0	0	0	0	0	5	5
$S^{Freq}(MediumH)$	0	0	0	0	0	0	0	0	0	0	5	5	10	10
$S^{Freq}(High)$	0	0	0	0	0	0	0	0	5	5	10	10	15	15
$S^{Freq}(VHigh)$	0	0	1.4	1.4	3	3	5	5	10	10	15	15	20	20

6.3.4. Player Strategy Selection

First, the principal player decides what strategy to adopt based on the offered load presented, and then the agent player decides what strategy to adopt given the strategy of the principal player. The 2×2 SFBC MIMO capacities of the LTE Physical Downlink Shared Channel (PDSCCH) for 1.4, 3, 5, 10, 15 and 20 MHz are 4, 10, 16.9, 33.9, 50.9 and 67.9Mbit/s, respectively using the highest modulation and coding scheme (MCS) of Table A2. In order to achieve these capacity values, SINR values greater than 23dB are required. Since system users seldom experience such high SINR values, this study utilised a reduction factor of 0.5 from the capacity values in order to characterise the instantaneous offered load as shown in Table 6.2. e.g., offered loads between 0Mbit/s and 2Mbit/s are characterised as very low loads. Table 6.2 lists the instantaneous offered load characterisation alongside the principal player transmission frequency strategy choice. The agent player chooses a transmission strategy from the set of transmission frequency strategies that minimises its ICI rank with the

principal player given the transmission frequency strategy adopted by the principal player, defined by equation (6.7).

$$S_{Agent}^{Freq} = \min_{s \in S^{Freq}} \left(R_{Agent} | S_{Principal}^{Freq} \right), \quad (6.7)$$

The best response strategies are the strategies that result in an ICI rank measurement of zero. From the player ICI rank payoff matrix (Table 6.1), it is observed that there are multiple best responses[16] (roll back equilibriums) that the agent player can adopt given the strategy of the principal player. In situations where the agent player has multiple best response strategies to the strategy adopted by the principal player, the agent's best response strategy that utilises more of the transmission band is chosen as the agent player's strategy. The best response strategy sets for both players are given in Table 6.3. The SGC/RRM algorithm is repeated periodically to capture the dynamic characteristics of the instantaneous offered load and ensure that no single player/cell dominates the principal player status. Figure 6.2 (b) summaries the major stages during the program flow of the SGC/RRM algorithm.

Table 6.2. Offered Load Characterisation and Principal Player Strategy Choice

Offered Load Rating	Load (L) (Mbit/s)	Principal Player Strategy
Very Low	$L \leq 2$	VLow
Low	$2 < L \leq 5$	Low
Medium Low	$5 < L \leq 8.45$	MediumL
Medium High	$8.45 < L \leq 16.95$	MediumH
High	$16.95 < L \leq 25.45$	High
Very High	$L > 25.45$	VHigh

[16] In game theory, it is possible to have a number of strategies that yield the optimum payoff.

Table 6.3. Player Best Response Strategy Sets		
Principal Player Strategy	**Agent Player Strategy**	**(ICI) Rank**
$S^{Freq}(Idle)$	$S^{Freq}(Idle)$	(0,0)
$S^{Freq}(VLow)$	$S^{Freq}(High)$	(0,0)
$S^{Freq}(Low)$	$S^{Freq}(High)$	(0,0)
$S^{Freq}(MediumL)$	$S^{Freq}(High)$	(0,0)
$S^{Freq}(MediumH)$	$S^{Freq}(MediumH)$	(0,0)
$S^{Freq}(High)$	$S^{Freq}(MediumL)$	(0,0)
$S^{Freq}(VHigh)$	$S^{Freq}(Idle)$	(0,0)

The limitation of dynamic ICI avoidance techniques is the need for frequent channel state information and/or offered load information in order to update transmission restrictions on a timescale of one TTI. Therefore, latency of the required information is likely to degrade the transmission restriction decisions. Just as the dynamic ICI avoidance techniques proposed in [86], [87] and [88] are sensitive to the latency of channel state information, the SGC/RRM is sensitive to the latency of the offered load information. However, the rate of variation of average loads is expected to be sufficiently slow.

6.4. System Model and Simulation Assumptions

An LTE system level simulator was developed in MATLAB to evaluate the E-UTRAN downlink Radio Head Energy Consumption Ratio (RH-ECR), user SINR and cell site throughput for the various ICI avoidance techniques in a multi-cell, multi-user system model. Downlink transmission between the eNB and the user equipments (UEs) was based on the 2×2 Alamouti Space Frequency Block Coding (SFBC) Multiple Input Multiple Output (MIMO) principle. The location coordinates of the UEs were randomly assigned following a uniform distribution while the location coordinates of the eNBs were pre-assigned and fixed. In addition, each UE experienced ICI from all the neighbouring cells. The path loss and the multipath fading were computed from the WINNER II Urban Macro channel models [55].

The packet scheduler interacted with the Admission Control (AC), Channel Quality Indication (CQI) Manager, and Link Adaptation (LA). CQI specified the SINR of each UE on every sub-carrier. LA selected the modulation and coding scheme (MCS) based on the channel quality measurement, Table A2 presents the LA table for the 2X2 SFBC MIMO with WINNER II multipath and path loss channel models obtained from link level simulations at a Block Error Rate (BLER) of 10^{-1}[89]. AC selected the users to be passed to the packet scheduler. The main simulation parameters are detailed in Table 6.4.

Table 6.4. Simulation Parameters and Model Assumptions	
Parameter	Setting
System Bandwidth	20 MHz
Sub Carriers per PRB	12
Cellular Layout	Hexagonal grid, 21 Cells, Tri-Sectored
Inter-Site Distance (ISD)	1.5 Km
Maximum Transmit Power	20 W
Number of Users (UEs)	30 UEs per Cell Site
Downlink Transmission Band	2.11-2.17 GHz
Number of Resource Blocks	100
Path Loss Model	WINNER II Channel model (Urban Macro)
Multipath Fading Model	WINNER II Channel model (Urban Macro)
eNB Height	20m
eNB Antenna bore sight gain	17.6dB
eNB Antenna Down Tilt Angle	4^o
UE Height	1.5 m
UE Antenna Gain	0 dB
Channel Estimation	Perfect
CQI delay	1 ms
Modulation and coding schemes	QPSK 1/3, 1/2, 3/4 & 16QAM 1/3, 1/2, 3/4 & 64QAM 3/5, 3/4, 6/7
EPS[17] Bearer data amounts per TTI	1,2,3,4,5,6,7 Kbits
Antenna pattern	$min\left[12\left(\frac{\alpha}{\alpha_{3dB}}\right)^2, A_m\right]$ $\alpha_{3dB} = 70^{\circ}, A_m = 20dB$

[17] EPS Bearer is the LTE terminology for a data flow

6.4.1. Layer 2 Packet Scheduling Model

As discussed in chapter 2, layer 2 is an LTE radio interface protocol above the physical layer and consists of the following: Medium Access Control (MAC), Radio Link Control (RLC) and Packet Data Convergence Protocol (PDCP). The MAC is responsible for scheduling the data according to priorities and multiplexing data to the physical layer transport blocks. In order to benchmark the performance of the SGC/RRM algorithm against the state of the art ICI avoidance techniques, this study employed a common packet scheduler that maximises system throughput while ensuring fairness among the users. The packet scheduler is decoupled into three independent stages with the Time Domain Packet Scheduler (TD-PS) as the first stage, the Frequency Domain Packet Scheduler (FD-PS) as the second stage and a uniform power allocation as the third stage [36].

6.4.1.1. Time Domain Packet Scheduling

The TD-PS selects users to be scheduled in the next TTI and passes the candidate selection list (CSL) to the FD-PS. The CSL was obtained by sorting all the users according to the TD-PS policy. The study employed the Time Domain Proportional Fair (TD-PF) Scheduler with the metric defined by equation (3.2). It was assumed that each of the users constituting the CSL has full buffer data traffic

6.4.1.2. Frequency Domain Packet Scheduling

The FD-PS allocates PRBs to users in the CSL provided by the TD-PS. The PRB allocation was carried out based on the concept of localised resource allocation whereby an entire PRB was assigned to a single user. In order to fully exploit the good channels, this study considered the maximum SINR scheduler for the frequency domain defined by equation (6.9).

$$i' = \max_{i \in N}(SINR[i,n]), \tag{6.8}$$

where i' is the PRB allocation for user n, i is the PRB index, N is the total number of PRBs and $SINR[i,n]$ denotes the average SINR of user n on PRB i.

6.4.1.3. Uniform Power Allocation

This study employed a uniform power allocation scheme that scaled linearly with the number of utilised PRBs. $P_k(t) = \lambda \times RB_k(t)$, where $P_k(t)$ is the RF transmit power of cell k at time t, $RB_k(t)$ is the number of PRBs utilised by cell k at time t, and $\lambda = 0.2\ W$ is the uniform RF transmit power per PRB, i.e. maximum power of 20 W divided by the total number of PRB=100.

6.4.2. Energy Metrics

A framework for measuring the energy efficiency of a telecommunications network and equipment can be found in [34] where the average power consumption to effective throughput ratio was proposed as an energy consumption ratio (ECR) metric. The RH-ECR is defined as the radio head energy per delivered application bit (Joules/Bit). Equation (6.10), computes the RH-ECR for one cell in one TTI, where E is the energy required to deliver M application bits.

$$ECR_{Cell}^{RH} = \frac{E}{M} = \frac{P_{Cell}^{RF}(L) \times 10^{-3} / \mu_\varepsilon}{M} = \frac{\frac{\lambda \times 10^{-3}}{\mu_\varepsilon} \sum_{i=1}^{Q} k_i}{\sum_{i=1}^{Q} k_i f(SINR[n,i])}, \tag{6.9}$$

$P_{Cell}^{RF}(L)$ is the RF transmit power of a cell which is a function of the offered load. μ_ε is the aggregated efficiency of the radio head components. This study was carried out in an E-UTRAN deploying macro cells (inter site distance of 1.5 Km) with a maximum transmit power of 20 watts with a μ_ε value of 0.25 [30]. λ is the uniform transmit power per PRB of

0.2 W. k_i is the fraction of PRB i that is utilised. Q is the number of allocated resource blocks. $f(SINR[n,i])$ is the LA function given in Table A2 which determines the MCS and hence the number of bits that can be transmitted on PRB i by scheduled user n.

The percentage Radio Head Energy Reduction Gain (RH-ERG) is defined as;

$$ERG_{RH} = \frac{ECR_1^{RH} - ECR_2^{RH}}{ECR_1^{RH}} \times 100\%, \quad (6.10)$$

where ECR_1^{RH} and ECR_2^{RH} are the RH-ECR for the reference system and the systems under test, respectively.

6.4.3. Signal to Interference Noise Ratio (SINR)

The SINR for 2×2 Alamouti SFBC MIMO was computed for each UE on every sub carrier from equation (6.12).

$$SINR = \frac{\left[|h_{p\_11}|^2 + |h_{p\_12}|^2 + |h_{p\_21}|^2 + |h_{p\_22}|^2\right]^2 \times P_{r_{AVG}}}{\sum_{j=1}^{Z} \Psi(j) \times P_{j_{AVG}} + \left[|h_{p\_11}|^2 + |h_{p\_12}|^2 + |h_{p\_21}|^2 + |h_{p\_22}|^2\right] \times w}, \quad (6.11)$$

$$\Psi(j) = \left[\left(|h_{p\_11}|^2 + |h_{p\_12}|^2\right)\left(|h_{j\_11}|^2 + |h_{j\_12}|^2\right)\right] + \left[\left(|h_{p_{21}}|^2 + |h_{p_{22}}|^2\right)\left(|h_{j_{21}}|^2 + |h_{j_{22}}|^2\right)\right], \quad (6.12)$$

h_{p_11}, h_{p_12}, h_{p_21}, and h_{p_22} are the serving cell multi-path channel gains modelled as a circular symmetric Gaussian random variable of zero mean and a variance of 1 subject to the power delay profile of the WINNER II multipath urban macro channel model [55].

h_{j_11}, h_{j_12}, h_{j_21}, and h_{j_22} are the multi-path channel gains for interfering cell j, modelled as a circular symmetric Gaussian random variable of zero mean and a variance of 1 subject to the power delay profile of the WINNER II multipath urban macro channel model [55].

$P_{r_{AVG}}$ is the average received signal power, $P_{j_{AVG}}$ is the average received power from the j^{th} interfering cell and the noise power $w = KTB$, where K is the Boltzmann constant, T is the thermal temperature of 290K and B is the sub carrier bandwidth of 15 KHz.

6.5. Simulation Results and Analysis

The performance of the ICI avoidance techniques was evaluated in terms of the SINR performance, the RH-ECR performance, and the user and cell site throughput performance. The median SINR performance was used to quantify the expected channel quality experienced by a user measured in decibels (dBs). The RH-ECR performance was used to measure the energy efficiency of a cell site i.e. (joules/bit) while the cell site throughput performance was used to measure the achieved cell site data rate respectively, in Mbit/s.

6.5.1. SINR Performance

The SGC/RRM algorithm dynamically mitigates the effects of ICI based on the instantaneous offered load presented to the individual cells in the E-UTRAN. Figure 6.3, presents the median SINR performance of the various ICI avoidance techniques considered in this study.

The SGC/RRM algorithm produced a higher median SINR performance compared to the state of the art ICI avoidance techniques, e.g. 4dBs greater than HFR 1/3. The SINR performance improvement of the SGC/RRM is a result of two effects. First, a user in a particular cell will not experience interference from one of the dominant interfering cells due to the fact that the user's serving cell is engaged in the SGC/RRM algorithm with one of the dominant interfering cells. Second, a user in a particular cell will experience an additional interference avoidance due to the SGC/RRM algorithm being executed by other cell pairs in the E-UTRAN. An improvement in SINR translates to a utilisation of fewer resource blocks, for a given QoS target, thus reducing the required transmit power and radio head energy.

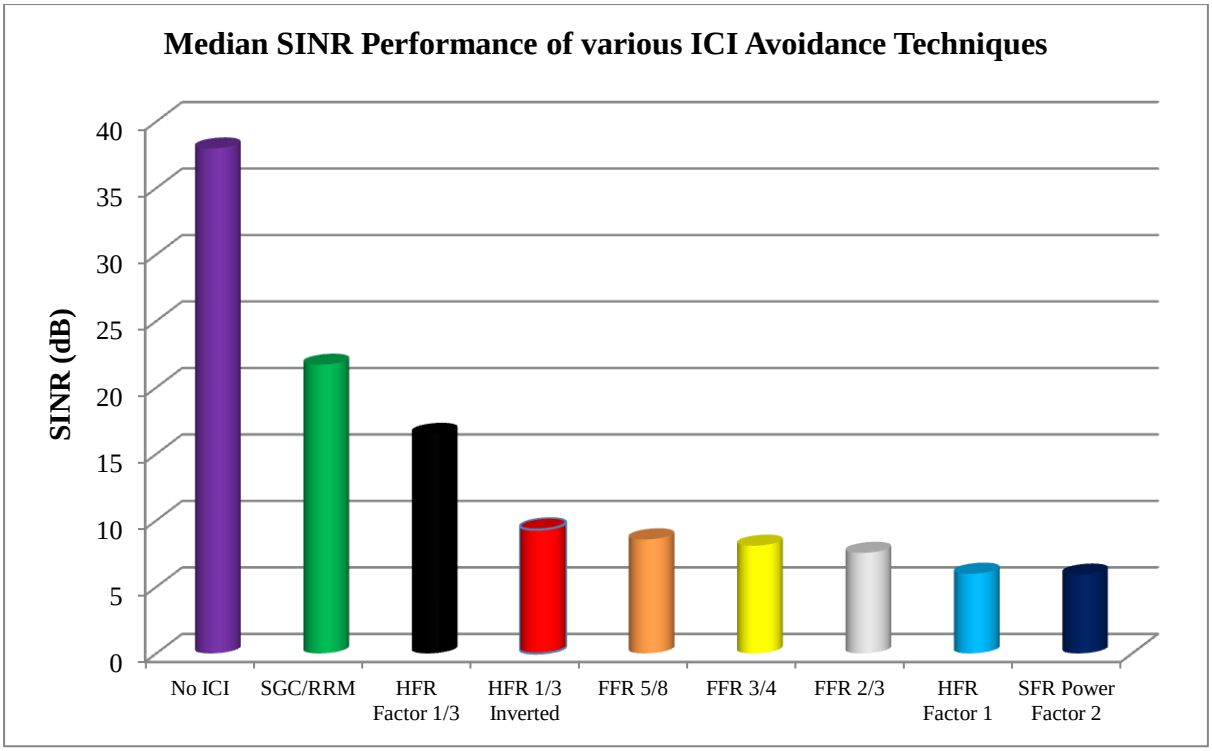

Figure 6. 3. Median SINR Performance of various ICI Avoidance Techniques

6.5.2. Radio Head (RH) Energy Performance

The radio head energy performance of the SGC/RRM algorithm was compared against that of the state of art ICI avoidance techniques both for a low and high offered load scenario. Figure 6.4 (a) and Figure 6.4 (b) present the radio head energy performance at a low offered load and a high offered load respectively, as measured by the ECR.

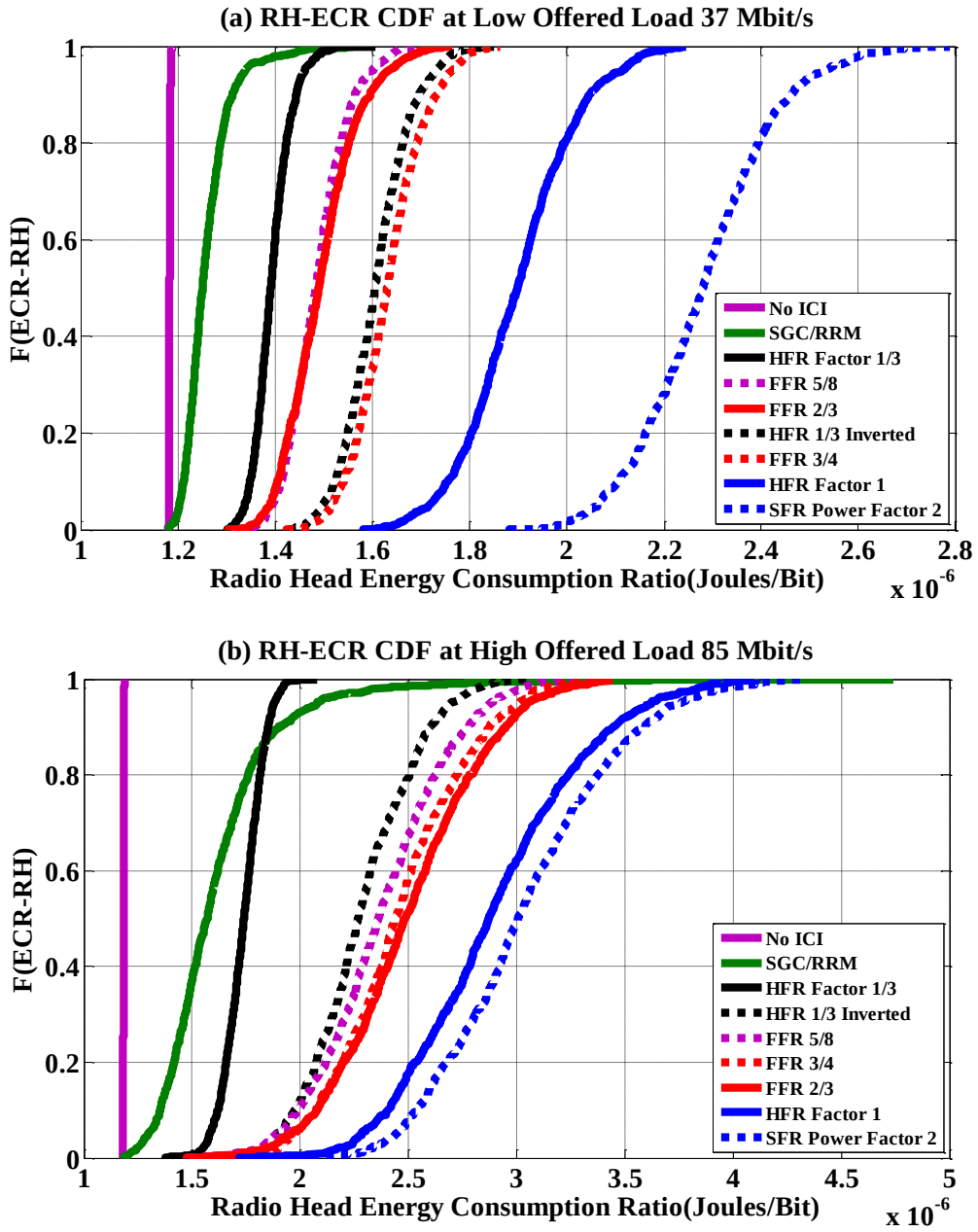

Figure 6. 4. Radio Head Energy Performance

Considering the HFR factor 1 as the benchmark, the median RH-ERGs at a low offered load are; 34%, 27%, 22%, 21%, 16%, 14% and -20% for SGC/RRM, HFR factor 1/3, FFR 5/8, FFR 2/3, HFR 1/3 inverted, FFR 3/4 and SFR power factor 2, respectively. At a high offered load the RH-ERGs are; 45%, 39%, 17%, 13%, 21% 15% and -5% for SGC/RRM, HFR factor 1/3, FFR 5/8, FFR 2/3, HFR 1/3 inverted, FFR 3/4 and SFR power factor 2, respectively.

6.5.3. Cell Throughput performance

Consider a cell pair in the E-UTRAN (Figure 6.1 (a)) participating in the SGC/RRM algorithm with N_{cell} cell sectors, and M_{total} users. The average number of users per cell is M_{total}/N_{cell}. At any instant, this value can be lower or higher, consequentially this can cause different game theoretic play-offs. The study assumes that each user demands a constant data rate D. Let M_{max} be the average maximum number of users that can be scheduled between the 2 cells within one TTI while avoiding interference. In each TTI, the game theory scenarios are:

- The number of users in a cell pairing ($M_{cell-pair}$) is equal to or less than M_{max}, then only 1 TTI is required to transmit the principal and the agent's data jointly. The throughput rate achieved is $R = M_{cell-pair}D$.
- The number of users in a cell pairing ($M_{cell-pair}$) exceeds M_{max}, then 2 TTIs are required to transmit the principal and the agent's data separately. The throughput rate achieved is $R = M_{cell-pair}D/2$.

Assuming a uniform distribution of users in the E-UTRAN, the probability of a user being in the cell-pair is $p=2/N_{cell}$. The probability of $M_{cell-pair}$ users being inside the cell-pair is a binomial distribution given by:

$$\mathrm{P}\left(\mathrm{M_{total}}, \mathrm{M_{cell-pair}}\right) = \frac{\mathrm{M_{total}!}}{\mathrm{M_{cell-pair}!(M_{total}-M_{cell-pair})!}} \mathrm{p}^{\mathrm{M_{cell-pair}}}(1-\mathrm{p})^{\mathrm{M_{total}-M_{cell-pair}}}, \quad (6.13)$$

Therefore, the achieved downlink rate for any number of users in a cell-pair is:

$$C\left(M_{total}, M_{cell-pair}\right) = P\left(M_{total}, M_{cell-pair}\right)R, \quad (6.14)$$

Thus, the average cell throughput is the sum of all probability scenarios and averaged over the 2 cells:

$$C_{cell}^{theory} = \frac{1}{2}\sum_{M_{cell-pair}=1}^{M_{total}} \binom{M_{total}}{M_{cell-pair}} p^{M_{cell-pair}}(1-p)^{M_{total}-M_{cell-pair}}R, \quad (6.15)$$

where R is the aforementioned cell-pair rate, given by:

$$R = \begin{cases} M_{cell-pair}D & M_{cell-pair} \leq M_{max} \\ M_{cell-pair}D/2 & M_{cell-pair} > M_{max} \end{cases}.$$

Note, because the value of R is conditional and contains the variable $M_{cell-pair}$, which changes for every cell-pair at every TTI, the theoretical expression is not a single continuous function. Equation (6.16) can be significantly simplified into a continuous function by making the assumption that on average the number of users in the principal and agent cells is equal. Therefore, the probability that the principal cell will have more than x additional users than the agent cell is:

$$P\left(M_{principle} - M_{agent} > x\right) = 2\sum_{M_{principle}=\frac{M_{cell-pair}}{2}+x}^{M_{cell-pair}} \binom{M_{cell-pair}}{M_{principle}} p^{M_{cell-pair}}, \quad (6.16)$$

For a small x and a large $M_{cell\text{-}pair}$, the probability expression in (6.16) is small. This approximation allows us to make the statement that $M_{cell-pair} = \frac{M_{total}}{N_{cell}}$. The theory can thus be approximated to (6.17) which is not dependent on the conditional variable R [90]:

$$C_{cell}^{Upper\ Bound} = \frac{M_{total}D}{4N_{cell}} \left[\begin{array}{c} 1 - \left(\frac{2}{N_{cell}}\right)^{M_{total}} + \\ \sum_{M_{cell-pair}=1}^{M_{max}} \binom{M_{total}}{M_{cell-pair}} p^{M_{cell-pair}} (1-p)^{M_{total}-M_{cell-pair}} \end{array} \right], \quad (6.17)$$

This approximation yields optimistic results, thus we can treat the simplification as an upper-bound.

Figure 6.5 presents the cell throughput for a variety of offered loads (varying M_{total}). It is worth noting that the theoretic analysis of the SGC/RRM algorithm supports the simulation results. Regarding the cell throughput results the following features of interest, arise:

- Under low loads, the cell throughput has a linear relationship with the offered load and is similar to that of HFR factor 1 (Linear Region 1). The SGC/RRM algorithm scenario is that all users within a cell-pair can be scheduled in 1 TTI. That is to say, the traffic demanded by each user is met.

• At medium loads, there is a transition by the SGC/RRM algorithm from utilising one TTI to two TTIs (Transition Region). Due to the fact that there is a large proportion of users who have marginally exceeded the first TTI threshold, there is therefore a reduction in cell throughput due to an inefficient usage of the second TTI. This is because the PRBs are largely empty in the second TTI.

• At high loads, most cell-pairs utilise the two TTIs efficiently. The linear gradient is half that of Linear Region 1 due to the 2 TTIs (Linear Region 2).

• At very high loads, the cell throughput saturates (Cell Saturation Region). It is worth noting that the SGC/RRM algorithm has a higher saturation point compared to HFR factor 1.

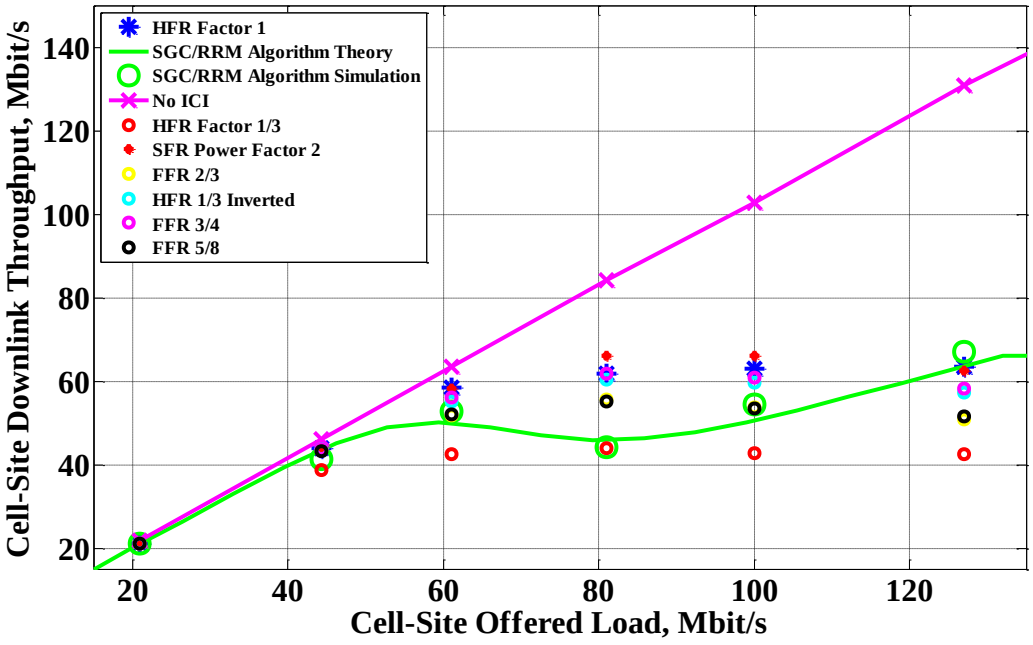

Figure 6. 5. Cell-Site Throughput Vs Offered Load

6.6. Summary of Results

This chapter presented a novel dynamic ICI avoidance technique that mitigates the effects of ICI through a sequential game play between cells in the E-UTRAN based on the offered load presented to the individual cells. The proposed SGC/RRM algorithm was shown to produce user SINR improvements of 4dBs greater than the state of the art ICI avoidance techniques.

It was shown that the SINR improvements derived from the SGC/RRM algorithm translated into significant radio head energy reduction gains of 34% and 45%, over HFR factor 1, at low and high offered loads respectively.

It was also shown that the SGC/RRM algorithm achieved the same cell site throughput performance as HFR factor 1 at low offered loads while at very high offered loads, the cell site throughput saturation level of the SGC/RRM algorithm exceeded that of HFR factor 1 with the theoretical analysis validating the simulation results.

In addition to the energy performance and channel quality improvements achieved by the proposed SGC/RRM algorithm, other benefits of the proposed technique include; the ability to mitigate ICI in unplanned self organising networks since LTE supports self-configuration of the X2 interface and simplicity as no central processing entity e.g. a RNC is required to perform ICI avoidance between the cells.

However, just as dynamic ICI avoidance techniques are sensitive to the latency of channel state information, the SGC/RRM algorithm is sensitive to the latency of the offered load information.

CHAPTER 7 **: CONCLUSIONS**

The research study conducted for this doctorial thesis was one of several projects under the Green Radio Core 5 Research Programme of the Virtual Centre for Excellence in Mobile and Personal Communications, Mobile VCE. The research study was aligned to the overall objectives of the Green Radio project with a vision of providing a 3-fold energy reduction contribution to the overall 100-fold energy reduction aspiration of the Green Radio project. This dissertation investigated the potential of utilising radio resource management techniques to improve the energy efficiency of the Third Generation Partnership Project (3GPP) Long Term Evolution (LTE) radio access network. The research study concentrated on the following specific areas of innovation.

- Investigating and modifying the existing packet scheduling algorithms with the objective of minimising the power/energy consumption while maintaining the user Quality of Service (QoS) guarantees. This objective was motivated by the multiuser diversity gain achievable in fast schedulers.
- Exploiting the collaboration, coordination and cooperation of the Evolved Node Bs (eNBs), in the 3GPP LTE radio access network, in order to mitigate and manage the interference and power/energy consumption. Interference is an important limiting factor to energy efficiency. If interference is increased by a given factor, the transmitted power level must be increased by that same factor in order to maintain the required performance, which of course has the effect of reducing energy efficiency for the system. Therefore, interference management is essential to energy efficiency performance.

The rest of the chapter is structured as follows: Section 7.1 highlights the research contributions and the major conclusions drawn. Section 7.2 concludes the chapter with a discussion of future work suggestions.

7.1. Research Contribution

7.1.1. Investigating existing packet schedulers

Chapter 3 presented a characterisation of the energy performance of common and well-known packet schedulers in a multi-cell multi-user 3GPP LTE system. This study highlighted the following observations.

- First, it was shown that the maximum SINR metric is more energy efficient than the round robin metric for both time and frequency domain packet scheduling, i.e. 2% to 18% and 16% to 49%, respectively.
- Second, it was shown that frequency domain packet scheduling had a greater impact on the energy efficiency of the system than time domain packet scheduling.
- However, the energy efficiency of the maximum SINR metric was achieved at the following costs: accurate channel quality measurements and fairness to users with low SINR channel quality measurements.

Chapter 4 presented a Radio Frequency (RF) energy efficiency, spectral efficiency and user QoS performance comparison between SISO and 2x2 Alamouti SFBC in an Urban Macro and an Urban Micro environment. This study highlighted the following observations.

- SFBC MIMO improved the RF energy efficiency performance of all the frequency domain packet schedulers both in the urban micro and urban macro scenarios i.e. Radio Frequency Energy Reduction Gains (RF-ERG) ranging from 14% to 49% The improved energy performance was attributed to the fact that SFBC MIMO improved the user SINR. Improved SINR values enable link adaptation to select higher order modulation and coding schemes hence more bits can be loaded onto the physical resource blocks. Since the ECR metric is inversely proportional to the number of transmitted bits, improved SINR values yield smaller ECR measurements.

- The RF energy efficiency performance improvements of SFBC MIMO over SISO were more pronounced in the urban macro cell environment. This was attributed to fact that users in a macro cell are more susceptible to experiencing poor channel conditions resulting from comparably larger propagation distances than those characteristic of micro cells. Consequently, the much needed channel quality improvements in a macro cell environment yield more transmission data rate improvements and hence more energy efficiency improvements than in a micro cell environment.
- SFBC MIMO improved the user QoS and spectral efficiency performance of all the frequency domain packet schedulers in both the urban micro and urban macro scenarios.
- However, the RF energy efficiency, user QoS and spectral efficiency performance improvements of SFBC MIMO are achieved at the cost of installing multiple antennas at both the eNB and the UE. Additionally MIMO introduces multiple radio chains, which in turn increase the overhead and operational energy consumption.

The research outputs emanating from this study were published in.

- C. Turyagyenda, T. O'Farrell, J. He, and P. Loskot, "SFBC MIMO Energy Efficiency Improvements of Common Packet Schedulers for the Long Term Evolution Downlink," in Proceedings of the IEEE Vehicular Technology Conference, pp. 1-5, May 2011.
- W. Guo, C. Turyagyenda, H. Hamdoun, S. Wang, P. Loskot, T. O'Farrell "Towards a Low Energy LTE Cellular Network: Architectures," EURASIP European Signal Processing Conference, pp. 879-883, Aug 2011.
- W. Guo, S. Wang, C. Turyagyenda, and T. O'Farrell, "Integrated cross-layer energy savings in a smart and flexible cellular network," in Proceedings of the IEEE International Conference on Communication in China, pp. 79-84, August 2012.

7.1.2. Modifying existing packet schedulers

Chapter 5 presented and evaluated a novel energy consumption aware Time Domain Packet Scheduler that incorporates the temporal dynamic user energy performance in its prioritisation metric. The proposed Proportional Fair Energy Consumption Ratio (PF-ECR) scheduler utilizes the users' cumulative past average ECR and/or the users' instantaneous ECR to assign different scheduling priorities to the users. The PF-ECR criteria schedules users such that on average each user exhibits the same ECR performance therefore the eNB RH-ECR will constitute RH-ECR values that are almost equal. This results in a low average eNB RH-ECR as there is no skew from high RH ECR values.

Furthermore, a two-stage energy optimisation algorithm implemented on a sub-carrier level was presented to supplement the Time Domain Packet Scheduler. The energy optimisation algorithm was made up of a Lower Order Modulation Assignment stage and a Power Reduction stage. The Lower Order Modulation Assignment stage re-distributes the MCS assignment per sub-carrier with a bias towards lower order MCSs while ensuring that the users' QoS is not compromised. The Power Reduction stage reduces the transmit power to the lowest permissible transmit power that can support the assigned MCS.

This study demonstrated that the new composite energy aware packet scheduling criteria produced Radio Head Energy Reduction Gains between 18% and 20% compared to the established throughput based proportional fair scheduler with uniform power allocation, without compromising the spectral efficiency performance and user QoS performance.

The research outputs emanating from this study were published in.

- C. Turyagyenda, T. O'Farrell, and W. Guo, "Long Term Evolution Downlink Packet Scheduling using A Novel Proportional-Fair-Energy Policy," in Proceedings of the IEEE Vehicular Technology Conference, pp. 1-5, May 2012.

7.1.3. Exploiting base station cooperation for energy efficiency

Chapter 6 presented a novel dynamic Inter-Cell Interference (ICI) avoidance technique that mitigated the effects of ICI through a sequential game play between cells in the 3GPP LTE radio access network based on the offered load presented to the individual cells. The proposed Sequential Game Coordinated Radio Resource Management (SGC/RRM) was shown to produce user SINR improvements of 4dBs greater than the state of the art ICI avoidance techniques.

It was shown that the SINR improvements derived from the SGC/RRM algorithm translated into significant radio head energy reduction gains of 34% and 45%, over HFR factor 1, at low and high offered loads respectively.

It was also shown that the SGC/RRM algorithm achieved the same cell site throughput performance as HFR factor 1 at low offered loads while at very high offered loads, the cell site throughput saturation level of the SGC/RRM algorithm exceeded that of HFR factor 1 with the theoretical analysis validating the simulation results.

In addition to the energy performance and channel quality improvements achieved by the proposed SGC/RRM algorithm, other benefits of the proposed technique include; the ability to mitigate ICI in unplanned self organising networks since LTE supports self-configuration of the X2 interface and simplicity as no central processing entity e.g. a RNC is required to perform ICI avoidance between the cells.

However, just as dynamic ICI avoidance techniques are sensitive to the latency of channel state information, the SGC/RRM algorithm is sensitive to the latency of the offered load information.

The research outputs emanating from this study were published in.

- C. Turyagyenda, T. O'Farrell, and W. Guo, "Energy efficient coordinated radio resource management: a two player sequential game modelling for the long-term evolution downlink," IET Journal on Communications, vol. 6, Iss. 14, pp. 2239-2249, November 2012.
- S. Wang, C. Turyagyenda, and T. O'Farrell, "Energy Efficiency and Spectral Efficiency Trade-Off of a Novel Interference Avoidance Approach for LTE-Femtocell Networks," in Proceedings of the IEEE Vehicular Technology Conference, pp. 1-5, May 2012.

7.1.4. Conclusions drawn

The major conclusion drawn from this research study are summarised below.

- There is a notable positive correlation between user channel quality improvements and energy efficiency of the radio access network. Channel quality aware packet scheduling is thus vital to energy reduction compared against channel quality ignorant packet schedulers.
- In a decoupled Time-Frequency packet-scheduling model, the frequency domain packet scheduler exhibits a significantly greater impact on the system energy efficiency than the time domain packet scheduler.
- User channel quality improvement techniques produced significantly more energy savings in large cell deployments such as a macro cells than in a small cell deployments such as a micro cells. This is of particular importance to radio access networks deployed in rural areas where access to an electric power grid maybe limited. In this scenario, energy savings would translate directly to base station fuel cost savings.
- Additionally channel quality improvement techniques also improve the spectral efficiency and user quality of service performance.
- Incorporating the instantaneous user energy consumption performance into the time domain prioritisation metric marginally improves the energy efficiency of the radio access network.

- Power control algorithms can be utilised to optimise and refine the energy efficiency performance of the rate adaptive frequency domain packet scheduling.
- The dynamic temporal and spatial traffic load characteristics, in the radio access network, present significant energy saving opportunities through collaborative and cooperative Inter-Cell Interference management among neighbouring base stations.

While this study demonstrated that radio resource management could be leveraged to achieve substantial energy efficiency improvements, a number of researchers have demonstrated energy efficiency improvements derived from sleep modes and radio access architectural modifications (i.e. small versus large cell deployments).

The optimum energy efficient "Green Radio" solution will ultimately constitute a mixture of sleep mode variants, architectural modifications and radio resource management solutions.

7.2. Future Work

The research study explored the potential of adapting radio resource management techniques to achieve improvements in the energy efficiency of radio access networks. However, radio resource management techniques can only impact the Radio Frequency (RF) transmit power and energy. Thus, one logical extension would be the overall system energy evaluation of the proposed techniques. The overall system energy measure would constitute both the Radio Head (RH) and Overhead energy consumption. The incorporation of the Overhead energy consumption is predicted to reduce the quoted energy efficiencies of the proposed techniques; particularly in radio access networks where the Overhead power in significantly greater than the Radio Head (RH) power.

Furthermore, the individual studies conducted for this thesis could be further investigated as follows.

- Extending the traffic agnostic energy performance study by considering differentiated traffic classes that often have varying QoS requirements. It is predicted that application proportional fairness may result into even more energy savings.
- Accounting for the energy consumption attributed to signalling and re-transmission overheads.
- Incorporating the user delay performance, particularly at high offered loads and in poor channel conditions.
- The correlation between user channel quality improvements and energy efficiency could further be explored by studying the energy efficiency of Forward Error Correction (FEC) techniques.
- The energy efficiency improvements derived from user channel quality improvements could be leveraged by increasing the inter site distance between base stations subsequently reducing the density of base stations in any given geographical area thus reducing the energy consumption of the RANs as a whole. For instance, it would be worthwhile to study the trade off between energy efficiency and the reduction of radio access network infrastructure, particularly in the case of MIMO.
- The proposed SGC/RRM Inter-Cell Interference management technique is susceptible to introducing additional user delays particularly at high offered loads. Future work could quantify and characterise the tradeoffs between the delay and energy efficiency performance of the SGC/RRM algorithm and interference management approaches in general. Furthermore, in order to improve the energy efficiencies derived from ICI mitigation, it would be beneficial to study energy efficiency of interference alignment techniques.

While this study focussed on the 3GPP LTE network, future radio access networks (5G and beyond) are envisioned to be heterogeneous networks constituting an amalgamation of radio

technologies working together seamlessly. It is therefore paramount that future energy efficiency studies place an emphasis on heterogeneous radio access networks.

REFERENCES

[1] A. Fehske, G. Fettweis, J. Malmodin, and G. Biczok, "The global footprint of mobile communications: The ecological and economic perspective," IEEE Communications Magazine, Vol.49, Iss. 8, pp. 52-62, August 2011

[2] Report on the FP 7 Consultation Meeting, "Future Mobile and Wireless Radio Systems: Challenges in European Research," February 2008

[3] J. Malmodin, Å. Moberg, D. Lunden, G. Finnveden and N. Lovehagen, "Greenhouse Gas Emissions and Operational Electricity Use in the ICT and Entertainment & Media Sectors," Journal of Industrial Ecology, Vol. 14, Iss. 5, pp. 770-790, October 2010

[4] G. Fettweis, and E. Zimmermann, "ICT Energy Consumption-Trends and Challenges," in Proceedings of the 11th International Symposium on Wireless Personal Multimedia Communications, Lapland, Finland, September 2008

[5] L. Bernstein et al, "Climate Change 2007: Synthesis Report," Fourth assessment report of the Intergovernmental Panel on Climate Change, Cambridge University Press, November 2007

[6] Mobile VCE Vision Group, "2020 Vision: Enabling the Digital Future," December 2007

[7] Mobile VCE Energy Focus Group, "Targeted Questions," May 2009

[8] M. A. Marsan, L. Chiaraviglio, D. Ciullo, and M. Meo, "Optimal Energy Savings in Cellular Access Networks," in proceedings of IEEE International Conference of Communication workshops, pp. 1-5, June 2009

[9] J. T. Louhi, "Energy Efficiency of Modern Cellular Base Stations," in proceedings of IEEE Telecommunications Energy Conference, pp. 475-476, October 2007

[10] Nobel Media AB 2013, "Guglielmo Marconi – Biographical," [online] Available at http://www.nobelprize.org/nobel_prizes/physics/laureates/1909/marconi-bio.html [Accessed 4 Jul 2013]

[11] Belrose, J.S, “Reginald Aubrey Fessenden and the birth of wireless telephony,” IEEE Antennas and Propagation Magazine Vol. 44, Iss. 2, pp. 38-47, April 2002

[12] E. Armstrong, “A Method of Reducing Disturbances in Radio Signalling by a System of Frequency Modulation,” in proceedings of the Institute of Radio Engineers, Vol. 24, Iss. 5, May 1936

[13] V. H. MacDonald, "The Cellular Concept," Bell Systems Technical Journal, Vol. 58, pp. 15-41, January 1979

[14] Sadahiko Kano, “Technical innovations, standardization and regional comparison - a case study in mobile communications,” Elsevier Telecommunications Policy Journal, Vol. 24, Iss. 4, pp. 305-321, May 2000

[15] Z. Zvonar, P. Jung and K. Kammerlander, “GSM Evolution Towards 3rd Generation Systems,” Kluwer Academic Publishers, 1st edition, 1998

[16] H. Holma and A. Toskala, “WCDMA for UMTS - Radio Access for Thrid Generation Mobile Communications,” John Wiley & Sons Ltd, 3rd edition, 2009

[17] H. Holma and A. Toskala, “LTE for UMTS-OFDMA and SC-FDMA Based Radio Access,” John Wiley & Sons Ltd, 1st edition, 2009

[18] 3rd Generation Partnership Project, “General Packet Radio Service (GPRS) enhancements for Evolved Universal Terrestrial Radio Access Network (E-UTRAN) access,” Release 12, 3GPP Technical Specification TS 23.401 V12.1.0, June 2013

[19] 3rd Generation Partnership Project, “Evolved Universal Terrestrial Radio Access (E-UTRA) and Evolved Universal Terrestrial Radio Access Network (E-UTRAN); Overall description,” Stage 2, Release 11, 3GPP Technical Specification TS 36.300 V11.6.0, June 2013

[20] 3rd Generation Partnership Project, “Policy and charging control architecture,” Release 12, 3GPP Technical Specification TS 23.203 V12.1.0, June 2013

[21] 3rd Generation Partnership Project, “Non-Access-Stratum (NAS) protocol for Evolved Packet System (EPS),” Stage 3, Release 12, 3GPP Technical Specification TS 24.301 V12.1.0, June 2013

[22] 3rd Generation Partnership Project, “Evolved Universal Terrestrial Radio Access (E-UTRA); Packet Data Convergence Protocol (PDCP) specification,” Release 11, 3GPP Technical Specification TS 36.323 V11.2.0, March 2013

[23] 3rd Generation Partnership Project, “Evolved Universal Terrestrial Radio Access (E-UTRA); Radio Link Control (RLC) protocol specification,” Release 11, 3GPP Technical Specification TS 36.322 V11.0.0, September 2012

[24] 3rd Generation Partnership Project, “Evolved Universal Terrestrial Radio Access (E-UTRA); Medium Access Control (MAC) protocol specification,” Release 11, 3GPP Technical Specification TS 36.321 V11.3.0, June 2013

[25] 3rd Generation Partnership Project, “Evolved Universal Terrestrial Radio Access (E-UTRA); LTE physical layer; General description,” Release 11, 3GPP Technical Specification TS 36.201 V11.1.0, December 2013

[26] K. Pedersen, T. E. Kolding, F. Frederiksen, I. Z. Kovács, D. Laselva, and P. E. Mogensen,“An Overview of Downlink Radio Resource Management for UTRAN Long-term Evolution,” IEEE Communications Magazine, vol. 47. Iss. 7. pp. 86-93, July 2009

[27] C. Han, T. Harrold, S. Armour, I. Krikidis, S. Videv, P. M. Grant, H. Haas, J. S. Thompson, I. Ku, C. Wang, T. A. Le, M. R. Nakhai, J. Zhang and L. Hanzo, “Green Radio: Radio Techniques to Enable Energy-Efficient Wireless Networks,” IEEE Communications Magazine Vol. 49, Iss. 6, pp. 46-54, June 2011

[28] Energy Aware and Radio neTwork tecHnologies Project, “Energy efficiency analysis of the reference systems, areas of improvements and target breakdown,” Deliverable D2.3, Version 2.0, December 2010

[29] G. Auer, V. Giannini, I. Godor, P. Skillermark, M. Olsson, M. A. Imran, D. Sabella, M. J. Gonzalez, C. Desset and O. Blume, “Cellular Energy Efficiency Evaluation Framework,” in Proceedings of the IEEE Vehicular Technology Conference, May 2011

[30] W. Guo, and T. O'Farrell, “Green Cellular Network: Deployment Solutions, Sensitivity and Tradeoffs,” in Proceedings of IEEE Wireless Advanced Conference, pp. 42-47, June 2011

[31] H. Jinling, “TD-SCDMA/TD-LTE Evolution-Go Green,” in proceedings of IEEE International Conference on Communication Systems, pp. 301-305, November 2010

[32] T. O'Farrell et al, “Mobile VCE Book of Assumptions,” version 1.6.0, September 2010

[33] B. Badic, T. O’Farrell, P. Loskot, and J. He, “Energy Efficient Radio Access Architectures for Green Radio: Large versus Small Cell Size Deployment,” in Proceedings of the IEEE Vehicular Technology Conference, September 2009

[34] ECR Initiative, “Network and Telecom Equipment – Energy and Performance Assessment, Metrics, Test Procedure and Measurement Methodology,” Draft 3.0.1, December 2010

[35] R. Rinaldi, G.M. Vecca, “The hydrogen for base stations,” in Proceedings of Telecoms Energy Conference (INTELEC’ 07) pp. 288-292, September 2007

[36] P. Kela, J. Puttonen, N. Kolehmainen, T. Ristaniemi, T. Honttonen, and M. Moisio, “Dynamic Packet Scheduling Performance in UTRA Long Term Evolution Downlink,” in Proceedings of the International Symposium on Wireless Pervasive Computing (ISWPC’08), May 2008

[37] A. Pokhariyal, T.E. Kolding and P.E. Mogensen, “Downlink Frequency Domain Packet Scheduling for the UTRAN Long Term Evolution,” in Proceedings of IEEE Personal Indoor and Mobile Radio Communications Conference (PIMRC’06), September 2006

[38] N. Wei, A. Pokhariyal, C. Rom, B. E. Priyanto, F. Fredriksen, C. Rosa, T. B. Sorensen, T. E. Kolding, and P. E. Mogensen, "Baseline E-UTRA Downlink Spectral Efficiency Evaluation," in Proceedings of the IEEE Vehicular Technology Conference (VTC'F06), September 2006

[39] K. Higuchi, T. Kawamura, Y. Kishiyama, Y. Ofuji, and M. Sawahashi, "System-Level Throughput Evaluations in Evolved UTRA," in Proceedings of the International Conference on Communication Systems, October 2006

[40] A. Pokhariyal, K. I. Pedersen, G. Monghal, I. Z. Kovacs, C. Rosa, T. E. Kolding, and P. E. Mogensen, "HARQ Aware Frequency Domain Packet Scheduler with Different Degrees of Fairness for the UTRAN Long Term Evolution," in Proceedings of the IEEE Vehicular Technology Conference (VTC'S07), April 2007

[41] G. Monghal, K. I. Pedersen, I. Z. Kovacs, and P. E. Mogensen, "QoS Oriented Time and Frequency Domain Packet Schedulers for the UTRAN Long Term Evolution," in Proceedings of the IEEE Vehicular Technology Conference (VTC'S08), May 2008

[42] A. Jalali, R. Padovani, R. Pankaj, "Data Throughput of CDMAHDR High Efficiency-High Data Rate Personal Communication Wireless System," in proceedings of IEEE Vehicular Technology Conference (VTC2000-Spring), May 2000

[43] COST Action 231, "Digital Mobile Radio Towards Future Generation Systems: Final Report," office for official publications of the European Committee, 1999

[44] International Telecommunication Union, "Guidelines for evaluation of Radio Transmission Technologies for IMT-2000," Recommendation ITU-R M.1225, 1999

[45] H. Asplund, K. Larsson, and P. Okvist, "How Typical is the "Typical Urban" Channel Model?," in proceedings of IEEE Vehicular Technology Conference (VTC Spring), pp. 340-343, May 2008

[46] H. Estroem, A. Furuskaer, J. Karlson, M. Meyer, S. Parkvall, J. Torsner, and M. Wahlqvist, "Technical Solutions for the 3G long-term evolution," IEEE Communications Magazine, Vol.44, Iss. 3, pp. 38-45, March 2006

[47] Y. Xiao, "IEEE 802.11n: Enhancements for higher throughput in wireless LANs," IEEE Communications, Vol.12, Iss. 5, pp. 82-91, December 2005

[48] R. T. Derryberry, S. D. Gray, D. M. Ionescu, G. Mandyam, and B. Raghothaman, "Transmit diversity in 3G CDMA systems," IEEE Communications Magazine, Vol.40, Iss. 4, pp. 68-75, April 2002

[49] E. Telatar, "Capacity of multi-antenna Gaussian channels," Europe Trans. Telecommun, Vol. 10, Iss. 6, pp. 585-595, December 1999

[50] G. J. Foschini and M. J. Gans, "On the limits of wireless communications in a fading environment when using multiple antennas," Kluwer Wireless Pers. Commun., Vol. 6, pp. 311-335

[51] G. J. Foschini, "Layered space-time architecture for wireless communication in a fading environment when using multiple antennas," Bell Systems Technical Journal, pp. 41-59, Autumn 1996

[52] S. M. Alamouti, "A simple transmit diversity technique for wireless communication," IEEE Journal Selected Areas Communication, Vol. 16, Iss. 8, pp. 1451-1458, October 1998

[53] V. Tarokh, N. Seshadri, and A. R. Calderbank, "Space-time codes for high data rate wireless communication: performance criterion and code construction," IEEE Transactions Information Theory, Vol. 44, Iss. 2, pp. 744-765

[54] J. Mietzner, R. Schober, L. Lutz, W. H. Gerstacker, and P. A. Hoeher, "Multiple-antenna techniques for wireless communications-A comprehensive literature survey," IEEE Communication Surveys and Tutorials, Vol. 11, Iss. 2, pp. 87-105, 2009

[55] P. Kyösti, et al., "WINNER II Channel Models," Version 1.1, September, 2007.

[56] Z. Li, C. Yin, G. Yue, “Delay-Bounded Power Efficient Packet Scheduling for Uplink Systems of LTE,” in proceedings of Wireless Communications Networking and Mobile Computing International Conference, pp. 1-4, October 2009

[57] D. Sabella, M. Caretti, R. Fantini, “Energy Efficiency Evaluation of State of the Art Packet Scheduling algorithms for LTE,” in proceedings of European Wireless Conference, pp. 1-4, April 2011

[58] C. Han, K. C. Beh, M. Nicolaou, S. Armour, A. Doufexi, “Power Efficient Dynamic Resource Scheduling Algorithms for LTE,” in Proceedings of the IEEE Vehicular Technology Conference, pp. 1-5, September 2010

[59] C.Turyagyenda, T.O’Farrell, J.He, P.Loskot, “SFBC MIMO Energy Efficiency Improvements of Common Packet Schedulers for the Long Term Evolution Downlink,” in Proceedings of the IEEE Vehicular Technology Conference, pp. 1-5, May 2011

[60] R. Wang, J. S. Thompson, H. Haas, P. M. Grant, “Sleep Mode Design for Green Base Stations,” IET Communications Journal, Vol. 5, Iss. 18, pp. 2606-2616, December 2011

[61] S. Mclaughlin, P. M. Grant, J. S. Thompson, H. Haas, D. I. Laurenson, C. Khirallah, Y. Hou, and R. Wang, “Techniques For Improving Cellular Radio Basestation Energy Efficiency,” IEEE Wireless Communications Magazine, Vol. 18, Iss. 5, pp. 10-17, October 2011

[62] M. A. Marsan, L. Chiaraviglio, D. Ciullo, M. Meo, “Optimal Energy Savings in Cellular Access Networks,” in Proceedings of the IEEE International Conference on Communication Systems, pp. 1-5, June 2009

[63] R. Wang, J.S. Thompson, H. Haas, “A novel time-domain sleep mode design for energy-efficient LTE,” in Proceedings of the IEEE International Symposium on Communication, Control and Signal Processing, pp. 1-4, March 2009

[64] S. Videv, H. Haas, “Energy-Efficient Scheduling and Bandwidth–Energy Efficiency Trade-Off with Low Load,” in Proceedings of the IEEE International Conference on Communication Systems, pp. 1-5, June 2011

[65] 3rd Generation Partnership Project, “E-UTRA and E-UTRAN Overall Description,” Stage 2, Release 10, 3GPP Technical Specification TS 36.300 V10.4.0, June 2011

[66] 3rd Generation Partnership Project, “E-UTRAN X2 Application Protocol,” Release 10, 3GPP Technical Specification TS 36.423 V10.2.0, June 2011

[67] Z. Ji, K. J. Ray Liu, “Dynamic Spectrum Sharing: A Game Theoretical Overview,” IEEE Communications Magazine, Vol.45, Iss. 5, pp. 88-94, May 2007

[68] A. Attar, V. Krishnamurthy, O.N. Gharehshiran, “Interference management using cognitive base-stations for UMTS LTE,” IEEE Communications Magazine, Vol.49, Iss. 8, pp. 152-159, August 2011

[69] S. Walid, H. Zhu, B. Tamer, D. Merouane, H. Are, “Network Formation Games Among Relay Stations in Next Generation Wireless Networks,” IEEE Transactions on Communications, Vol. 59, Iss. 9, pp. 2528-2542, September 2011

[70] S. Vatsikas, S. Armour, M. De Vos, T. Lewis, “A Fast and Fair Algorithm for Distributed Sub-Carrier Allocation Using Coalitions and the Nash Bargaining Solution,” in proceedings of 2011 IEEE Vehicular Technology Conference (VTC Fall), pp. 1-5, September 2011

[71] V. Poulkov, P. Koleva, O. Asenov, G. Iliev, “Combined Power and Inter-Cell Interference Control for LTE Based on Role Game Approach,” in proceedings of 34th International Conference on Telecommunications and Signal Processing (TSP), pp. 213-217, August 2011

[72] A. Awada, B. Wegmann, I. Viering, A. Klein, “A Game-Theoretic Approach to Load Balancing in Cellular Radio Networks,” in proceedings of 21st IEEE Symposium on Personal Indoor and Mobile Radio Communications (PIMRC), pp. 1184-1189, September 2010

[73] N. Himayat, S. Talwar, A. Rao, R. Soni, “Interference Management for 4G Cellular Standards,” IEEE Communications Magazine, Vol. 48, Iss. 8, pp. 86-92, August 2010

[74] G. Boudreau, J. Panicker, N. Guo, R. Chang, N. Wang, S. Vrzic, “Interference Coordination and Cancellation for 4G Networks,” IEEE Communications Magazine, Vol. 47, Iss. 4, pp. 74-81, April 2009

[75] J. Andrews, W. Choi, R. Heath Jr, “Overcoming Interference in Spatial Multiplexing MIMO Cellular Networks,” IEEE Wireless Communication, Vol. 14, Iss. 6, pp. 95-104, December 2007

[76] S. W. Halpern, “Reuse Partitioning in Cellular Systems,” in proceedings of 33rd IEEE Vehicular Technology Conference, Vol. 33, pp. 322-327, May 1983

[77] 3rd Generation Partnership Project, “Evolved UTRA Uplink Scheduling and Frequency Reuse,” Siemens, RAN WG1 #41, R1-050476, Athens, Greece, May 2005

[78] 3rd Generation Partnership Project, “Interference Mitigation-Considerations and Results on Frequency Reuse,” Siemens, RAN WG1 #42, R1-050738, London, UK, September 2005

[79] 3rd Generation Partnership Project, “Interference Mitigation by Partial Frequency Reuse,” Siemens, RAN WG, R1-060135, Helsinki, Finland, January 2006

[80] M. M. Wang, T. Ji, “Dynamic Resource Allocation for Interference Management in Orthogonal Frequency Division Multiple Access Cellular Communications,” IET Communications Journal, Vol. 4, Iss. 6, pp. 675-682, April 2010

[81] C. G. Gerlach, I. Karla, A. Weber, L. Ewe, H. Bakker, E. Kuehn, and A. Rao, “ICIC in DL and UL with Network Distributed and Self-Organising Resource Assignment Algorithms in LTE,” Bell Labs Technical Journal, Vol. 15, Iss. 3, pp. 43-62, November 2010

[82] 3rd Generation Partnership Project, “Downlink Inter-Cell Interference Co-ordination/Avoidance-Evaluation of Frequency Reuse,” Ericsson, RAN WG1 #45, R1-061374, Shanghai, China, May 2006

[83] A. Simonsson, “Frequency Reuse and Intercell Interference Co-ordination in E-UTRA,” in proceedings of 65th IEEE Vehicular Technology Conference, pp. 3091-3095, April 2007

[84] 3rd Generation Partnership Project, “Soft Frequency Reuse Scheme for UTRAN LTE,” Huawei, RAN WG1 #41, R1-050507, Athens, Greece, May 2005

[85] 3rd Generation Partnership Project, “OFDMA Downlink Inter-cell Interference Mitigation,” Nokia, RAN WG1 #44, R1-060291, Denver, Colorado, February 2006

[86] M. Rahman, H. Yanikomeroglu, “Enhancing Cell-Edge Performance: A Downlink Dynamic Interference Avoidance Scheme with Inter-Cell Coordination,” IEEE Transactions on Wireless Communication, Vol. 9, Iss. 4, pp. 1414-1425, April 2010

[87] R. Madan, J. Borran, A. Sampath, N. Bhushan, A. Khandekar, T. Ji, “Cell Association and Interference Coordination in Heterogeneous LTE-A Cellular Networks,” IEEE Journal on Selected Areas in Communications, Vol. 28, Iss. 9, pp. 1479-1489, December 2010

[88] S. H. Ali, V. C. M. Leung, “Dynamic Frequency Allocation in Fractional Frequency Reused OFDMA Networks,” IEEE Transactions on Wireless Communication, Vol. 8, Iss. 8, pp. 4286-4295, August 2009

[89] C. Han, S. Armour, "Energy Efficient Radio Resource Management Strategies for Green Radio," IET Communications Journal-Special Issue: Green Technologies for Wireless Communications and Mobile Computing, Vol. 5, Iss. 18, pp. 2629-2639, December 2011

[90] C. Turyagyenda, T. O’Farrell, and W. Guo, “Energy efficient coordinated radio resource management: a two player sequential game modelling for the long-term evolution downlink,” IET Journal on Communications, vol. 6, Iss. 14, pp. 2239-2249, November 2012

APPENDIX A:

Table A1. Modulation and Coding Lookup Table 20 MHz (Urban Macro SISO)		
MCS Level	SINR values	Rate (Mbit/s)
QPSK, 1/3	-4.06	0.35
	-2.06	1.98
	-0.06	5.60
	1.94	9.21
	3.70	10.81
QPSK, 1/2	4.70	13.00
	5.70	15.10
16QAM, 1/3	6.95	18.70
	8.95	21.63
16QAM, 1/2	10.71	29.06
	12.71	32.71
	13.65	33.10
16QAM, 3/4	14.47	33.88
	15.07	41.20
64QAM, 3/5	15.26	43.09
	17.26	55.70
	19.26	59.84
	20.10	60.40
64QAM, 3/4	22.23	71.82
	24.23	74.66
	26.23	75.60
	27.60	75.60
64QAM, 6/7	28.81	79.49
	30.81	83.33
	32.81	85.23
	34.81	85.67
	36.81	86.40

Table A2. Modulation and Coding Lookup Table 20 MHz (Urban Macro 2x2 SFBC MIMO)		
MCS Level	SINR values	Rate (Mbit/s)
QPSK, 1/3	-6.06	0.40
	-4.06	5.73
	-2.06	10.80
	-0.90	11.00
QPSK, 1/2	-0.30	15.02
	1.70	16.77
16QAM, 1/3	2.95	21.88
	3.25	22.40
QPSK, 3/4	3.46	23.35
	4.27	24.10
16QAM, 1/2	4.71	28.70
	6.71	33.45
	7.94	33.60
16QAM, 3/4	8.47	41.27
	10.47	49.76
	10.80	50.00
64QAM, 3/5	11.26	57.00
	13.26	60.37
	13.75	60.40
64QAM, 3/4	14.23	69.51
	16.23	75.28
	17.88	75.50
64QAM, 6/7	18.81	83.66
	20.81	86.16
	22.81	86.40

Table A3. Modulation and Coding Lookup Table 20 MHz (Urban Micro SISO)		
MCS Level	SINR	Rate (Mbit/s)
QPSK, 1/3	-4.06	0.62
	-2.06	2.42
	-0.06	5.54
	1.94	8.36
	3.20	9.5
QPSK, 1/2	3.70	10.78
	5.70	14.14
	5.90	14.34
16QAM, 1/3	6.95	17.32
	8.75	20.4
16QAM, 1/2	10.71	27.78
	12.71	31.5
	13.50	32
16QAM, 3/4	14.47	37.68
	15.00	39.6
64QAM, 3/5	15.26	41.8
	17.26	53.08
	20.13	58.7
64QAM, 3/4	20.23	59.58
	22.23	69.44
	24.23	73.34
	26.23	75
	27.80	75.3
64QAM, 6/7	28.81	78.92
	30.81	81.96
	32.81	83.8
	34.81	85.28
	36.81	86.14
	38.81	86.4

Table A4. Modulation and Coding Lookup Table 20 MHz (Urban Micro 2x2 SFBC MIMO)		
MCS Level	SINR	Rate (Mbit/s)
QPSK, 1/3	-6.06	0.8
	-4.06	5.6
	-2.06	10.28
	-1.03	10.74
QPSK, 1/2	-0.30	13.84
	1.70	16.62
16QAM, 1/3	2.95	21.2
	3.32	21.5
QPSK, 3/4	3.46	22.24
	4.32	23.5
16QAM, 1/2	4.71	26.86
	6.71	33.16
	7.97	33.5
16QAM, 3/4	8.47	39.64
	10.47	49.32
	10.88	49.6
64QAM, 3/5	11.26	54.68
	13.26	60
	13.85	60.2
64QAM, 3/4	14.23	66.32
	16.23	75.02
	17.84	75.5
64QAM, 6/7	18.81	83.38
	20.81	85.96
	22.81	86.4